THE EFFECTS OF WINDBREAKS ON THE

EFFECTIVENESS OF SPRINKLER IRRIGATION

SYSTEMS

A thesis submitted in partial fulfilment of the

requirements for the Degree in

Master of Water Resource Management

By Eric Kisambuli Kilaka

Waterways Centre for Freshwater Management

University of Canterbury
Christchurch, New Zealand
2015

ACKNOWLEDGEMENT

Discussion and interaction with my postgraduate colleagues (both in HydroEco research group and the WCFM) were very helpful and productive in my research. Special thanks to my friend, Phil Clunies-Ross at WCFM for his help, support and encouragement during the period of my data collection, particularly with fieldwork during cold weather.

Finally, thanks and praises to the almighty God for His guidance and protection throughout the study period. It is my believe that He has aided me beyond my own natural ability, and has opened doors which no man would have opened. To God be glory for the great things he has done in my life.

I would like to dedicate this thesis to the following people:

My parents Josephine Kavunye and John Kilaka who have taught me more about hard work in life than anyone else and who will be thrilled beyond words to see their son submit this research work for his master's degree.

My wife Anne, and my daughter Shanice Ndanu, and my nephew Philip Mutisya, who have painfully endured my long absence at a very young age. I love you very much and I will take care of you to the best of my ability.

ABSTRACT

In the Canterbury region, New Zealand, water is a contentious issue when irrigation and dairy farming are involved. The Canterbury region accounts for 70% of the total irrigated land area in New Zealand and is one of the most productive agricultural regions. Traditionally, water has been seen as an abundant resource, but growing water demands are now outstripping the supply of water, hence threatening the sustainability of agricultural productivity. In the long term, this problem may worsen as a result of climate change, which is predicted to increase water demands and reduce supply in many parts of Canterbury.

In the recent and on-going expansion of irrigation systems, modern sprinkler irrigation methods, namely centre pivot and lateral spray irrigation technology, have replaced the old border-dyke systems. This has been due to the need to increase irrigation flexibility and efficiency to guarantee pasture growth for dairy production in dry periods. This conversion has resulted in a reduction of windbreaks to 2 m heights or sometimes led to 100% removal of windbreaks so as to accommodate centre pivot or linear move irrigation systems. Removal of windbreaks or reduction of windbreak height may increase wind speed across a field. Both spray evaporation loss and evapotranspiration are a function of wind speed. Hence, any increase in wind speed may lead to an increase in irrigation requirements. There is little information currently available on outlining how reduction of windbreak height or the complete removal of windbreaks affects efficiency in water application. Thus, this research was done to quantify the effects of windbreaks on water savings under sprinkler irrigation systems in the Canterbury region under various climatic conditions.

The research was done in three major steps: (1) spray evaporation loss (SEL) was measured under various climatic conditions for two typical spray nozzles (Nelson Irrigation Corporation Rotator R3000 and Spinner S3000 nozzles) to develop SEL prediction models; (2) wind speed reduction behind windbreaks was quantified for fields under various wind conditions; and (3) the effects of wind speed reduction by windbreaks was modelled for evapotranspiration, spray evaporation loss and irrigation. The results showed that an increase of wind speed, due to the removal of windbreaks or a reduction of height of windbreaks, leads to an increase in

evapotranspiration and spray evaporation losses in irrigated agriculture. For the size of the fields considered in this study which are 80 m by 80 m (Site 1 with medium porosity windbreaks) and 120 m by 120 m (Site 2 with low porosity windbreaks), extra irrigation water of up to 14% is needed in one growing season when windbreaks are reduced to 2 m in height. When windbreaks are completely removed from the field, extra irrigation water of up to 38 % and 64% is needed when irrigating using the Rotator R3000 nozzle and the Spinner S3000 nozzle, respectively. Thus, reduction of water resource use can be achieved in irrigated agriculture if irrigation systems can be designed to operate under existing windbreaks. Other savings can follow, from reduced requirements for pumping, fuel and labour costs. Lastly, with future climate change projections showing that the Canterbury region will get windier and hotter, windbreaks can help mitigate water losses associated with sprinkler irrigation.

LIST OF ABBREVIATIONS

$\overline{O}$	Mean of the observed values
u_*^R	Friction velocity at the field
u_*^{WS}	Friction velocity at the weather station
z_o^R	Roughness height t the field
z_o^{WS}	Roughness height at the weather station
a, b, c and *d*	Constants
ACSEL	Above canopy spray evaporation loss
As	Apparent specific gravity
C_d	Denominator constant that changes with reference crop type and calculation time step
Cn	Numerator constant dependent on reference crop type and calculation time step
CU	Coefficient of uniformity
e_a	Actual vapour pressure
EC	Electrical conductivity
EC_c	Electrical conductivity of water in the catch can
EC_s	Electrical conductivity of the source water
e_s	Saturation vapour pressure
e_s	Saturation vapour pressure at
ET	Evapotranspiration
ET_c	Actual crop evapotranspiration
ET_o	crop reference evapotranspiration
ET_{os}	short reference crop evapotranspiration
ET_{rs}	tall reference crop evapotranspiration
ET_{sz}	Standardized reference crop evapotranspiration
FC_v	Field capacity (by volume)
FSPS	Fixed spray plate sprinklers
f_{xh}	Friction velocity reduction;
G	Soil heat flux density at the soil surface

GIR	Gross irrigation requirement
h	Windbreak tree height
I	Solar radiation
k	von Kármán constant
K_c	Crop factor
MAD	Maximum allowable depletion
ME	Modelling Efficiency
NIR	Net irrigation requirement
NIWA	National Institute of Water and Atmospheric Research
O_i	Observed value for the i_{th} pair
op	Optical porosity
PET	Potential evapotranspiration
P_i	Predicted value for the i_{th} pair
PWP_s	Permanent wilting point (by volume)
RH	Relative humidity
R_n	Calculated net radiation at the crop surface
RRMSE	Relative Root Mean Square Error
RSPS	Rotating spray plate sprinklers
SEL	Spray evaporation Loss
T_a	Air temperature
u	Wind velocity at any wind logger station
u(z)	Average wind speed
u*	Wind friction velocity
u_0	The approach wind speed in the zone unobstructed by windbreaks (- 5
h	height of windbreak
u_2	Wind speed measured at 2 m above ground surface
u_z	Measured wind speed at z_w m above ground surface
VPD	Vapour pressure deficit
w	Width of windbreak
WaSim	Water Simulation Model
WDEL	wind drift and evaporation loss

WEPS	Wind Erosion Prediction System
x	Independent variable
xh	Distance from the windbreak in terms of windbreak
y1, y2, y3, y4, y5	Empirical coefficients in multiple regression analysis
z	Height of instrument
z_o	Roughness height
z_w	Height of wind measurement above ground surface
α	Aerodynamic porosity
γ	Psychrometric constant
Δ	Slope of the saturation vapour pressure-temperature curve
θ	Windbreak porosity
σ	Standard deviation

TABLE OF CONTENTS

LIST OF FIGURES

LIST OF TABLES

CHAPTER 1: INTRODUCTION

1.1. Statement of the problem

The Canterbury region lies on the east coast of the South Island of New Zealand. It accounts for 17% or 4.53 M ha of New Zealand's total area with 800 km of coastline as the eastern boundary (Tapper & Sturman, 2006). The Canterbury region is considered one of New Zealand's most productive agricultural regions. The climate of Canterbury is the principal factor governing irrigation water use. It is dominated by high- and low-pressure depressions that approach from the west across the Tasman Sea (Tapper & Sturman, 2006). The Southern Alps have a major influence on the impact of these depressions, including the amount and location of consequent precipitation (Salinger, 1979). The high-pressure depressions bring settled weather conditions with periods of strong, drying, northwest wind conditions and mean summer time potential evapotranspiration (PET) rates of 4 - 6 mm/day. Near the coast and inland from Banks Peninsula, northeast winds prevail (Tapper & Sturman, 2006). Low-pressure depressions that move across from the west bring rain, sleet and snow, with snow settling at sea level to the east in winter months. Rainfall ranges from 300 - 800 mm and annual evapotranspiration (ET) ranges from about 900 - 1000 mm. Typical summer daytime temperatures range from 15 - 25º C, and winter temperatures range from 5 - 15º C (Salinger, 1979). Moderate temperatures mean that virtually all precipitation during the irrigation season is in the form of rainfall rather than snow. Rainfall is evenly distributed in most locations throughout the year, on average, but the eastern area of Canterbury is well short of PET demand (Goulter, 2010). As a result, there are regular summer soil moisture deficits, and irrigation is necessary to compensate for soil moisture deficits from the middle of September to the end of March. During this irrigation period, warm, dry, and high wind speeds, and high solar radiation are common. These conditions are the key factors affecting crop ET and spray evaporation loss (SEL) during sprinkler irrigation.

Irrigation has led to increased agricultural production in New Zealand. Sheep and beef grazing has been converted to pastoral dairy farming, made possible by the higher stock carrying capacity of the irrigated land (Thorrold et al., 2007). The Canterbury region accounts for 70% of the total irrigated land area in New Zealand, with 550,000 hectares currently consented for irrigation (Goulter, 2010). Currently, irrigation is the major use of freshwater in New Zealand, accounting for 80% of all allocated water (Thorrold et al., 2007). While the Canterbury region is considered as one of New Zealand's most productive agricultural regions, water is a contentious issue when irrigation and dairy farming are involved. Irrigation water is sourced from limited groundwater and surface water supplies, and irrigation demand far exceeds surface water supplies (Thorrold et al., 2007). The area of irrigated land has doubled in the last two decades and ongoing irrigation development continues to increase the demand for water abstraction (Thorrold et al., 2007).

In the recent and on-going expansion of irrigation systems in the Canterbury region, modern sprinkler irrigation methods, namely centre pivot and lateral spray irrigation technology, have replaced the old border-dyke systems. This has been due to the need to increase irrigation flexibility and efficiency to guarantee pasture growth for dairy production in dry periods. However, this conversion has required windbreak height to be reduced to 2 m or sometimes windbreaks to be removed completely to accommodate centre pivot or linear move irrigation systems. Removal of windbreaks removes their sheltering effect, and therefore increases wind speed across a farm. These windbreaks were first implemented as a soil conservation strategy to reduce wind erosion of agricultural land. Soil erosion due to wind is no longer a major concern because of permanent pasture cover. However, both ET and SEL can potentially increase with an increase in wind speed; thus, more irrigation water is required. The effect of wind on irrigation losses due to increased SEL and ET is of significant concern because water is sourced from limited supplies of ground and surface water.

Sprinkler irrigation is often considered more efficient than border-dyke systems, but significant water losses due to increased ET and SEL can occur when windbreaks are reduced or removed allowing an increase in wind speed across fields. Wind is a dominant feature of

the Canterbury landscape (Price, 1993) and, with the use of windbreaks, one of the few weather variables over which a farmer can exert some control.

Taking measures to improve water conservation is of particular importance in the Canterbury region because the on-going demand for irrigation water has led to an increase in pressure on both surface and ground water sources. Further, climate change predictions suggest that in the future the Canterbury region will become warmer, windier, and drier with an increased frequency of drought and storms (O'Donnell, 2007). As these changes occur, the demand for water resources is also likely to increase. Therefore, increased efficiency of water use and general farming practices will be necessary to maintain and increase agricultural production. The most significant effects which may result if irrigation efficiency is increased (Wolters, 1992) are:

a) a larger area can be irrigated with the same volume of water;
b) the competition between water users can be reduced;
c) energy used for pumping can be reduced; and
d) in-stream flows, after withdrawals, will be larger, thereby benefitting aquatic life, recreation, and water quality.

No systematic study on the influence of windbreak removal on both ET and SEL has been conducted in the Canterbury region or abroad. In this respect, it is essential to quantify the effects of windbreak removal in terms of water resource use. SEL in Canterbury needs to be evaluated in order to quantify the efficiency of sprinkler irrigation for different weather conditions and windbreak characteristics (porosity and height). Calculation of crop ET is needed to quantify irrigation requirement as influenced by windbreak characteristics during an irrigation event. Quantifying evaporation losses for different windbreak characteristics and weather conditions will give information outlining how the presence, removal, or reduction of windbreaks will affect SEL. This information can be used in farm management to take advantage of low evaporation loss conditions; and avoid high evaporation loss conditions to conserve valuable water resources. It is important for farm management to know how much irrigation water is lost by evaporation and hence unavailable to plants, and therefore what additional amount of water needs to be applied to cater for losses. It is, however, beyond the

scope of this research to quantify the effect of windbreak species, distribution, and the effects of windbreaks on wind erosion, or its impacts on human and animal wellbeing.

1.2. Research aim and objectives

The aim of this research was to quantify the effects of windbreaks on water savings under sprinkler irrigation systems in the Canterbury region. The results of the research aimed to answer the research question: "How effective are windbreaks in reducing water use under sprinkler irrigation in the Canterbury Region under varying climatic conditions?" To answer this research question effectively, the following were the main objectives:

1) to develop a statistical spray evaporation loss model for a range of climatic conditions in the Canterbury region;
2) to determine wind speed reduction for fields protected by multiple windbreaks;
3) to simulate and compare scenarios of spray evaporation losses with irrigation requirements for different weather conditions and windbreak characteristics; and
4) to quantify the benefits of windbreaks in terms of water resource use.

1.3. Organization of Thesis

The thesis consists of six chapters, comprising an introduction, literature review, methodology, results, discussion of results; and conclusions and recommendations. After the introduction in Chapter 1, Chapter 2 provides a review of the scientific literature related to this research, starting with an overview of evaporation losses in sprinkler irrigation and the factors affecting spray evaporation losses. A review of the electrical conductivity method as a suitable method to separate spray evaporation loss and drift loss is presented. Evapotranspiration is discussed with an emphasis on its impact on irrigation, factors that influence it in the Canterbury region and how it is measured. This chapter also reviews the available literature on the potential effects of a single windbreak on wind speed, and how this compares with windbreaks in the Canterbury region. Past studies where windbreaks proved to be effective in saving irrigation water are also discussed.

Chapter 3 describes the methods and materials used to quantify changes in SEL and ET as influenced by the reduction in wind speeds afforded by windbreaks. The first section describes the spray irrigation experiments, which were conducted to provide data for developing spray evaporation loss prediction models. The second section gives a description of the experiments used to calculate wind speed reduction by windbreaks. The methodology of how the data obtained in the experiments were used to develop and validate a windbreak model to determine the effect of multiple windbreaks on wind speed is given. In the third section, methods used for developing the windbreak model to quantify the effect of wind speed reduction on ET, SEL and irrigation requirements are presented.

In Chapter 4, results are presented graphically or in tabular form and explained while, Chapter 5 follows with a discussion and detailed interpretation of the results. The effects of windbreak removal or reduction to a 2 m height with respect to increase in water resource use are also discussed. Finally, Chapter 6 provides a summary of the thesis, the main conclusions, and a number of recommendations for future research on the effects of windbreaks on irrigation in the Canterbury region.

CHAPTER 2: LITERATURE REVIEW

2.1. Introduction

The major aim of this research is to quantify the effects of windbreaks on water savings under sprinkler irrigation systems in the Canterbury region. Therefore, a comprehensive review of the literature has been undertaken:

- to understand water balance during sprinkler irrigation;
- to understand the state of knowledge of spray evaporation losses and the factors that affect it;
- to find an appropriate measurement technique for spray evaporation loss;
- to understand evapotranspiration rates, how it is measured and how it is affected by wind speed;
- to understand the state of knowledge on how wind speed is influenced by a single windbreak; and
- to review existing case studies investigating how windbreaks have helped to save water resource use in irrigated agriculture .

2.2. Water balance in sprinkler irrigation

During sprinkler irrigation, water is distributed over the irrigated area by spraying it through the air. When a stream of water is discharged from the sprinkler nozzle into the air at high velocity, friction between the air and the water stream causes the stream to break apart into water droplets that fall to the surface, in the same way as rainfall. Water loss under sprinkler irrigation occurs in three ways: through the air, from the canopy and from the ground. Water loss in the air can occur as *spray evaporation loss (SEL)* (before it reaches the crop canopy or soil surface), and as *drift loss* from the irrigation area (McLean et al., 2000). Drift losses that occur as a result of wind are not considered a loss as long as the spray drift falls within the boundaries of the cultivated area; as only the uniformity of water application is affected (McLean et al., 2000). The remainder of the water enters the canopy as *precipitation*. This portion of the water is partitioned between *canopy interception* and direct *through-fall* to the

6

soil. Interception can be further divided into the portion of water remaining on the leaves and the remainder either dripping onto the lower leaves or the soil or running down the stem to the soil. The water remaining on the leaves (*intercepted water)*, is then evaporated to meet the atmospheric demand and is called *canopy evaporation* (Wang et al., 2006). The water which reaches the soil surface by direct through-fall is also partitioned into four components:

a) *soil evaporation,* which is the portion of the water which evaporates from the surface through evaporation;

b) the portion of the water which is lost through *direct run off*;

c) the portion of water which is available in the root zone for plant uptake; and

d) the portion of water which is lost by *deep percolation*.

The portion of water that is available in the root zone enters the plant via the roots, and then passes to the foliage where it is vaporized and then lost to the atmosphere through tiny pores in the leaves known as stomata. This process is called *transpiration*. In contrast, water lost through soil evaporation passes directly from the soil to the atmosphere. The combined loss of water through transpiration and soil evaporation is called *evapotranspiration (ET)*, and is a major source of water loss in agriculture.

However, direct run off and deep percolation losses are usually considered negligible in sprinkler irrigation (Thompson, 1986); therefore, ET and SEL are the major ways in which water is lost in sprinkler irrigation. The influence of windbreaks on wind velocity, which in turn affects SEL and ET, will be fully discussed according to the scope of this research.

2.3. Spray evaporation losses during sprinkler irrigation

The efficiency of sprinkler irrigation depends on the various losses that take place from the sprinkler nozzle to the point where water reaches the root zone. Since a negligible amount of water is lost in the conveyance of sprinkler irrigation systems, the major losses are SEL (Clark & Finley, 1975; Kincaid & Longley, 1989; Steiner et al., 1983). Evaporation losses during sprinkler irrigation are still a vital issue to the irrigation community all over the world. Previous experimental results have shown that sprinkler irrigation losses may vary from 0 to

45% of the applied water and that a large proportion of the loss is droplet evaporation in the atmosphere (Uddin et al., 2010). As a result, sprinkler irrigation efficiency is significantly influenced by the amount of spray losses.

Irrigation efficiency is an essential component of sprinkler irrigation system management due to its relationship with water resources, energy and labour requirements. When SEL is high, extra water is required from the source to compensate for the volume of water lost to the atmosphere. Increases in the amount of water required on the farm also lead to an increase in energy requirements because extra power is needed to pump the additional water to cater for the amount lost due to SEL. Additionally, SEL not only reduces the volume of water reaching the ground, but also increases the salinity of the remaining water (Hermsmier, 1973).

2.3.1. Physical processes of evaporation losses during sprinkler irrigation

Evaporation losses from sprinkler irrigation sprays take place through the exchange of energy between the water droplets and the atmosphere above the canopy or soil surface (Thompson, 1986). The composite theory of droplet evaporation in still air is presented in detail by Ranz & Marshall (1952) and Hardy (1947). In the process of evaporation, the heat required for evaporation is transferred by conduction and convection from the environment to the surface of the droplet, from which vapour is transferred by diffusion and convection back into the atmosphere. When liquid is sprayed (i.e. discharged from the sprinkler nozzle) into the air (which has a different temperature), the temperature of the droplets will change depending upon the rate at which the heat is transferred to, or from, the air both by convection and evaporation (Hardy, 1947). The exchange by radiation is so small that it can be neglected, except in cases where combustion is involved. The rate of mass transfer per unit area of interface is a function of air temperature, vapour pressure deficit, and the diameter and temperature of the droplets (Ranz & Marshall, 1952).

2.3.2. Factors that affect spray evaporation losses

The amount of water which evaporates from droplets during sprinkler irrigation depends mostly on climatic factors (i.e. air temperature, air friction, relative humidity, solar radiation, vapour pressure deficit and wind velocity) and equipment-related factors (including nozzle size, nozzle angle, operating pressure and sprinkler height). In addition, the travel time to reach the crop or soil surface determines the time available for evaporation to occur; hence this is also an important factor. These factors are discussed in detail below.

a) Climatic factors

The amount of water that evaporates from water droplets is closely related to the evaporative demand of the atmosphere, which is mainly influenced by climatic factors. The evaporative demand is a measure of the energy available for evaporation and the capacity of the air to store and transmit water vapour. The evaporation process requires 2.42 kilojoules of energy to convert one gram of water from liquid to vapour form (Zazueta, 2011). Therefore, sufficient energy must be available from the environment surrounding the sprinkler for evaporation to take place during irrigation.

The climatic variables affecting wind drift and evaporation losses (WDEL) are wind speed, air temperature, relative humidity, and vapour pressure deficit. Among these, wind speed has often been recognized as being the most vital factor affecting WDEL (Playán et al., 2005). Wind increases evaporation by transporting warmer or drier air from the surrounding areas to displace the moist, cool air above an irrigated surface. It also increases the evaporation rates by transporting water vapour away from the irrigated surface. Therefore, there is an increase in the renewal of air surrounding the flying drops with unsaturated air. Solar radiation and temperature provide energy required for evaporation (Smajstrla & Zazueta, 2003). As a result, during high levels of solar radiation and air temperature, energy is readily available. Conversely, low temperatures and low levels of solar radiation provide less energy for evaporation. Relative humidity ranges from 0 to 100%, with low values indicating dry air and high values indicating moist air. Since dry air has a greater capacity for moisture, evaporation will occur more rapidly when the air is dry than when it is moist. The vapour pressure deficit

(VPD) is the difference between the amount of moisture in the air and how much moisture the air can hold when it is saturated. Under high VPD conditions, small drops are subjected to large evaporation losses.

A close linear relationship between evaporation losses and wind velocity and VPD was reported by Frost & Schwalen (1955) while Ortega et al., (2000) estimated that evaporation losses were a function of vapour pressure deficit to the power of 0.5 and wind speed. They also reported that losses were inversely proportional to the relative humidity. Abo-Ghobar (1992) reported that evaporation losses increased with decreasing relative humidity and increased with air temperature and wind velocity. Studies by both Bavi et al. (2009) and Yazar (1984) showed that wind speed and vapour pressure deficit were the predominant factors significantly affecting evaporation losses during sprinkler irrigation. They concluded that these losses are exponentially correlated with wind speed and vapour pressure deficit. Hermsmier (1973) suggested that air temperature and rate of application were more important factors affecting evaporation losses than wind velocity or relative humidity.

b) Equipment-related factors

Equipment-related factors that affect evaporation losses from irrigation sprays in a sprinkler irrigation system are nozzle size and droplet diameter. The equipment variables that affect droplet diameter are the nozzle size, geometry, and operating pressure. Larger nozzle size produces larger droplet diameters, while smaller nozzle diameters break irrigation sprays into fine droplets (Dadiao & Wallender, 1985; Frost & Schwalen, 1955; Kohl et al., 1987; Solomon et al., 1985). Smaller droplets are produced at a higher operating pressure than at a lower operating pressure for the same nozzle (Dadiao & Wallender, 1985). Larger droplets are more resistant to drift and present less area surface area per unit mass for evaporation to occur than smaller droplets (Kohl et al., 1987). Since evaporation occurs from the surface of the water droplets, the total surface area of water droplets greatly affects the amount of evaporation loss. The total surface area of the water droplet depends on the droplet diameter. For a unit volume of water, the surface area doubles as the droplet diameter decreases by half (Smajstrla & Zazueta, 2003) . For this reason, evaporation rate increases as droplet size decreases if other factors remain constant, and the factors that cause droplet size to decrease will cause evaporation loss to increase.

Kohl et al. (1987) reported that for low-pressure agricultural sprinklers the geometry of the spray plate surface, rather than the nozzle size and operating pressure, was the dominant parameter that influenced drop size distribution. Edling (1985) found that, drift and evaporation losses were inversely proportional to droplet diameter, whereas Lorenzini (2004) and De Wrachien & Lorenzini (2006) proposed that evaporation losses were directly proportional to the droplet diameter. Frost & Schwalen (1955) found that a 25% increase in nozzle operating pressure increased evaporation losses by 25%. They found smaller nozzle diameters tended to break up fine droplets leading to greater evaporation losses.

The time available for droplet evaporation begins when a water droplet leaves the nozzle until it falls on the ground or crop surface. When this time is extended long enough due to the suspension of drops by wind, small droplets evaporate before they fall to the ground (Smajstrla & Zazueta, 2003). In addition, when water is sprayed from greater heights and over greater distances, the time available for evaporation to occur is increased (Yazar, 1984). Thus, for the same sprinkler operated at the same pressure, more evaporation would be expected to occur if the sprinkler operated on a taller riser than if it was installed on a shorter one. This is due to the longer trajectory and increased wind exposure, since wind profile over a canopy is logarithmic (Playán et al., 2005). In addition, wind speeds are higher at greater heights above the ground surface, where there are fewer obstacles to air movement. Thus, evaporation loss from sprinklers mounted on taller risers is also increased because of these higher wind speeds.

2.3.3. *Studies of methods for estimating spray evaporation losses during sprinkler irrigation*

Literature review shows that methods are available for modelling and measuring water losses that occur to the atmosphere by evaporation while water is travelling from the sprinkler nozzle to the ground surface or crop canopy (spray evaporation losses). These methods include field tests, analytic studies, laboratory tests and physical-mathematical modelling. The use of field tests to determine SEL during sprinkler irrigation will be discussed according to

the scope of this research, while detailed discussions of the other methods have been presented by Uddin et al. (2010).

Experimental field tests

Field studies reported in the literature show estimates of evaporation losses in sprinkler irrigation ranging from near zero to 45% (Abo-Ghobar, 1992; Bavi et al., 2009; Chawla & Singh, 1975; Clark & Finley, 1975; Frost & Schwalen, 1955; George, 1957; Hermsmier, 1973; Kohl et al., 1987; Yazar, 1984) and it is commonly assumed that the losses are significant. In some of the field studies, researchers have combined losses due to evaporation (spray evaporation) and spray drift together, into "spray losses", largely due to difficulties with the measurement techniques necessary to separate the two (Kincaid & Longley, 1989). The combined "spray losses" are traditionally determined in the field using the catch can method with volumetric or gravimetric measurements of water collected in catch cans. In this method, the water reaching the crop canopy or soil surface is determined from the amount of water caught in the catchment devices (funnels and containers), and the difference in water applied and the depth of water received in the catch cans represents the losses (Kohl et al., 1987). The use of this method is labour intensive and prone to errors because accurate measurement of water that reaches the ground or crop canopy is very difficult, especially in windy conditions which increase the sampling area due to drift. As a result, spray evaporation losses are included with the wind drift losses.

For the same nozzle height, drop size and exit pressure; wind drift losses are affected only by wind speed and direction, while spray evaporation losses are affected by both wind speed and other weather variables such as ambient temperature, vapour pressure deficit, relative humidity and solar radiation (McLean et al., 2000). Since this research was specifically focussed on measurement of spray evaporation losses, it was desirable to separate the wind drift loss component from the spray evaporation loss component. To separate losses due to evaporation from those due to drift, the electrical conductivity (EC) method combined with the catch can method has been used in field tests in different parts of the world.

2.3.4. *Spray evaporation loss measurement using the electrical conductivity method*

The EC method is based on the fact that any loss or gain of water by a droplet travelling through the air will lead to a corresponding change in its solute concentration, hence its EC (George, 1957). Generally, as spray droplets evaporate, the solute concentration increases, and this raises the EC of the applied water. This method of determining spray evaporation loss assumes that all salts remains in the water during the evaporation process. The EC method does not depend on sample size and does not measure drift losses.

By measuring the EC of the source water and the EC of the water caught in individual collectors positioned above the soil surface, the SEL can be calculated using Equation (2-1) below.

$$\text{SEL (\%)} = \frac{EC_c - EC_s}{EC_c}(100) \qquad\qquad (2\text{-}1)$$

Where,

- EC_c = electrical conductivity of water in the collector (mhos/cm); and
- EC_s = electrical conductivity of the source water (mhos/cm).

Additionally, experimental data obtained from such tests under different climatic and operating conditions can be used to develop a statistical regression model. Such a model can be used to determine SEL if climatic and operating conditions are known for a given irrigation event in a particular region.

George (1957) used EC to estimate the spray evaporation loss component from lateral impact sprinklers. He found that the losses ranged from 2% at a relative humidity of 48% with wind velocity 1.79 m/s, to 15% at a relative humidity of 14% and wind speed of 9.95 m/s. He found a good correlation between the losses and the relative humidity of the air. However, he found no relationship with vapour pressure deficit. He also found that spray evaporation losses were greater near the sprinkler and near the periphery of the application diameter. These results

were attributed to the fact that spray droplets landing closest to the nozzle are the smallest and hence evaporate more. Also, the droplets travelling to the outer limits of the spray pattern travel the greatest distance in the air and, therefore, evaporate more.

Using the EC method, Kraus (1966) estimated losses that ranged from 3.4 to 17% after adjusting for catch can evaporation. To reduce evaporation from the metallic catch cans, cans were painted white and filled with paraffin to a depth of 6.4 mm. He also reported that evaporation and total loss were approximately proportional to the vapour pressure deficit, but had no apparent relationship with wind velocity.

Hermsmier (1973) carried out an experiment in the Imperial Valley of California using the EC method and placed oil in the catch cans to reduce evaporation from the catch container. He determined that evaporation was reduced by 17.2% from that measured without oil and reported that evaporation from sprinklers could range from 0 to 50% over short periods. He also found that air temperature and the rate of application were better factors for estimating sprinkler evaporation, than wind speed or relative humidity.

In Punjab Agricultural University, Ludhiana, India, Chawla & Singh (1975) studied the effects of climatic and operating conditions on sprinkler irrigation losses. The EC method combined with the catch can method was used to determine the amount of evaporation, wind drift and interception losses under different conditions of temperature; vapour pressure deficit; wind speed and direction; nozzle size and pressure. The results on spray evaporation pattern around a single sprinkler showed that evaporation losses were more nearer to and at the periphery of the sprinkler while they were less in the intermediate zone of the sprinkler pattern. These findings had also been observed by George (1957). Tests on spray evaporation as a function of vapour pressure deficit showed a linear relationship beyond a deficit of 39.2 mbar under low wind conditions.

In Nebraska, Yazar (1984) reported losses of 1.5 – 16.8% of the total volume of applied water from impact sprinklers. He found that both wind velocity and vapour pressure deficit were the major determinants of spray evaporation which increased exponentially. He used the

experimental data to develop a prediction equation (Yazar's model) for the SEL (Equation (2-2), with wind and vapour pressure deficit as the independent variables.

$$SEL = 0.389 \exp(0.18u)(e_s - e_o)^{0.7} \qquad (2\text{-}2)$$

Where,

- SEL is the percentage of discharged flow lost to evaporation;
- u is the wind speed measured at 2 m (in m/s); and
- ($e_s - e_o$) is the vapour pressure deficit (mbar).

Different expressions are available for calculations of vapour pressure deficit (Allen et al., 2005). Considering the wind as the only factor affecting evaporation losses in a test with a sprinkler lateral, SEL was expressed by Equation (2-3)

$$SEL = 1.68 \exp(0.28u) \qquad (2\text{-}3)$$

In Iran, Bavi et al. (2009) determined spray evaporation losses using a hand move irrigation system fitted with impact sprinklers under different climatic and operating conditions. They found that wind velocity and vapour pressure deficit were the most important factors affecting evaporation from sprinkler sprays. They reported that losses varied from 4.4% to 8.9% of applied water. Using multiple regressions, they developed a statistical model (Equation (2-4) - Bavi's model) which can be used to estimate losses given climatic conditions. The conditions for which this model was developed are temperature of $19.8 - 45.4°C$, a wind speed of $3 - 9.50$ m/s and a vapour pressure deficit $0.70 - 8.90$ mbar.

$$SEL = 4.337\exp(0.077u)(e_s - e_a)^{-0.098} \qquad (2\text{-}4)$$

McLean et al. (2000) used the EC method to determine the above canopy spray evaporation loss (ACSEL) from different types of sprinkler irrigation systems calculated at increasing distances from the sprinkler nozzles. For the centre pivot irrigation system, the ACSEL was

found to be uniform for any rotation angle of the pivot. He concluded that that EC method was appropriate to measure ACSEL in the field with a precision of ±0.5%.

In Canterbury, New Zealand, spray evaporation losses have been estimated using both Bavi's and Yazar's models (Edmondson, 2012). Daily evaporation rates of up to 9% were predicted for northwester conditions for Winchmore, Canterbury. However, the prediction of evaporation losses was done by extrapolation rather than interpolation. Extrapolation to predict outside the range to which the models were established is not recommended statistically, as it is prone to errors.

2.3.5. *Summary and conclusion*

The literature review presented above has shown that spray evaporation during sprinkler irrigation is a significant loss in sprinkler irrigation that affects irrigation efficiency. It has also shown that spray evaporation processes are mainly governed by droplet diameter, as determined by nozzle geometry and climatic conditions (such as wind velocity, air temperature, vapour pressure deficit, and relative humidity) operating at any given time; with wind speed being cited as the most influential factor. The EC method can be used to separate spray drift from evaporation loss, and experimental data can be used to develop statistical models for spray loss determination given any conditions.

However, the previous models developed using this method do not take into account nozzle diameter and newer nozzle designs which are currently in use in the Canterbury region. Furthermore, the models were derived from conditions far different from Canterbury conditions, with different data ranges of wind speed and vapour pressure deficit. As a result, calculation of SEL would require extrapolation outside the range of conditions for which the models were developed. To solve this problem, the electrical conductivity method can be used to develop a statistical model for Canterbury conditions using newer nozzle designs.

2.4. Evapotranspiration

Knowledge of ET is important because it can provide accurate estimates of daily water use of crops and thus assist irrigation managers with the important decisions of when to apply water and how much to apply. ET is defined as the loss of water from both the evaporation of the soil surface and by transpiration from the leaves of the plants growing on it (Brown, 1974). It represents the evaporative processes; the difference between the two rests in the path by which water moves from the soil to the atmosphere. Water lost by transpiration must enter the plant via the roots, then pass to the foliage where it is vaporized and lost to the atmosphere. In contrast, water lost through soil evaporation passes directly from the soil to the atmosphere. Evapotranspiration data are usually presented as a depth of water loss over a particular time.

ET determines the water requirement for a given crop over a specific period of time in a given field. When ET is high, soil water potential must be maintained at a higher level so that the soil can supply water fast enough to meet the plants' demands without placing them under water stress. An increase in ET causes an increase in the irrigation water requirement of a field during an irrigation period. Similar to SEL, increases in ET also cause increases in energy costs because extra water must be pumped to cater for the increased irrigation requirements.

2.4.1. Factors affecting evapotranspiration

The rate of ET for a given environment (vegetation) is a function of four critical factors: solar radiation, air temperature, vapour pressure and wind speed. Among these, wind speed and solar radiation are the most influential factors affecting ET in the Canterbury region (de Vries et al., 2010). The wind has two major roles; Firstly, it transports heat that builds up on adjacent surfaces such as dry desert or asphalt to vegetation, which accelerates evaporation (a process referred to as advection). Secondly, wind accelerates evaporation by enhancing turbulent transfer of water vapor from moist vegetation to the dry atmosphere. In this case, the wind is constantly replacing the moist air located within and just above the plant canopy with

dry air from above i.e. increases in wind speed lowers aerodynamic resistance. Solar radiation provides the radiant energy necessary for evaporation to take place. However, other factors such as available water, crop type and irrigation type also affect agricultural water management (Irmak et al., 2006). In general, when crops transpire water, the immediate surrounding environment of the crop canopy will be moist. In dry climates, the wind flow is most likely to replace this moist air with dry air, which causes an increase in ET. Increase in ET causes an increase in demand for agricultural water.

2.4.2. Determination of evapotranspiration

Accurate estimations of crop water requirements are necessary to ensure efficient use of water resources (Estévez et al., 2009). One way of determining the crop water requirements is by the crop reference evapotranspiration (ET_0). Crop reference evapotranspiration (ET_0) is an important variable in agro-hydrological systems; it models the evapotranspiration of an ideal and well-watered grass surface. The direct measurement of ET_0 is not easy and involves considerable time and cost (Zhang et al., 2010). Therefore, in most situations, ET_0 is estimated from meteorological parameters. A number of equations are available for estimating ET_0: e.g. Penman (1948); Blaney & Criddle (1952); Hargreaves & Samani (1985); FAO-56 Penman-Monteith (1998), ASCE Standardized Reference Evapotranspiration Equation (Allen et al., 2005). Among these equations, the ASCE Standardized Reference Evapotranspiration Equation that incorporates both energy balance and aerodynamic theory, is considered to be the most appropriate model to predict ET_0 (Zhang et al., 2010). The equation is discussed in more detail under Section 3.4.7. Actual crop evapotranspiration can then be derived from ET_0 by means of proper crop and water stress coefficients (Jensen et al., 1990).

2.4.3. Summary and conclusion

Evapotranspiration is major source of water loss in agriculture. Among the key factors that affect ET, wind speed and solar radiation are the most influential factors affecting ET in the Canterbury region. Furthermore, wind speed can be controlled by use of windbreaks in a farm. The review of literature has also shown that ET of a crop can be determined by using

the ASCE Standardized Reference Evapotranspiration Equation if the meteorological variables are known.

2.5. Windbreaks

Windbreaks have been used for centuries to modify wind profiles and defend against the damaging effects of wind. They are used to control snow and sand accumulation and pesticide drift. They have also been reported to increase crop yield, protect animals and buildings, reduce soil erosion and noise, and improve aesthetics (Guan et al., 2003; Heisler & Dewalle, 1988; Ucar & Hall, 2001; Vigiak et al., 2003). Aerodynamically, windbreaks function as wind momentum sinks as they can protect surrounding zones from wind damage. Reduction of wind velocity by windbreaks is presumed to be beneficial in irrigation systems in the following ways:

a) increasing the efficiency of sprinkler irrigation. By reducing wind speed, the atmospheric evaporative demand in the protected zone is also reduced. In turn, the evaporation loss of droplets between the nozzle and the ground is reduced, thus minimizing SEL. Consequently, the amount of irrigation water used per unit of crop produced is reduced, which results in increased water use efficiency;

b) protecting irrigation equipment e.g. the centre pivot equipment is protected from damage by windstorms;

c) reducing evapotranspiration. Wind is a key factor that determines the ET of a farm. It determines ET as described earlier in Section 2.4.1. In windy areas, such as the Canterbury region, reduction of wind speed by windbreaks lowers crop ET and hence irrigation requirements;

d) if irrigation requirements are reduced as a result of wind protection, energy costs associated with the application of water like pumping are also reduced.

2.5.1. Windbreaks in New Zealand

The recognition of wind effects and the need for wind protection, in order to improve crop growth, livestock productivity, and human welfare dates back to the 1840's in New Zealand. In the Canterbury region of New Zealand, there are over 300,000 km of windbreaks which

were first implemented as a soil conservation strategy to reduce wind erosion of prime agricultural land. The windbreaks are characterised by single or multiple rows of Monterey Pine (Pinus Radiata) and Monterey Cypress (Cupressus Macrocarpa) (Price, 1993). The windbreaks are typically spaced between 100 – 200 m, but can be 500 - 1000 m apart. Their heights range from 5 m to 15 m and tend to be somewhat lower and more closed at the bottom.

To understand more about windbreaks, the basic concepts of windbreaks are presented first, followed by a review of the literature of wind speed reduction by single windbreaks; and comparison with windbreaks in New Zealand. Then the research methods on windbreaks and reported studies of windbreak benefits, with respect to irrigation practice, are presented.

2.5.2. Basic concepts of windbreaks

A windbreak is generally defined as any barrier that reduces wind velocity (Price, 1993), and is commonly associated with a natural vegetative barrier. The basic function of windbreaks is to reduce wind velocity and change its direction. A windbreak can be a planting of single or multiple rows of trees or shrubs; that through their presence in the airflow reduces the effect of wind velocity not only at the windbreak itself but also at a certain windward and leeward distance. Several words are synonymous with windbreaks: shelterbelt, vegetative barrier, wind barrier, hedge, and hedgerow (Caborn, 1965; Ucar & Hall, 2001).

Windbreak porosity can be described by optical porosity (op) and aerodynamic porosity (α). Optical porosity is the ratio or percentage of pore space to the space occupied by the tree trunks, branches, twigs and leaves and affects the degree of wind speed reduction as well as the shelter extent behind the windbreak (Brandle et al., 2004; Cleugh, 1998; Wang et al., 2001). Aerodynamic porosity (α) is defined as the ratio of mean wind speed (bleed wind speed) immediately leeward from the bottom to the top of the windbreak to that upwind before windbreak interference. Guan et al. (2003) suggested the following relationship between the optical and aerodynamic porosities.

$$\alpha = \text{(op)}^{0.4} \qquad\qquad\qquad (2\text{-}5)$$

Thus, aerodynamic porosity is larger than optical porosity.

Optical porosity can be determined by using digitizing techniques to analyse windbreak photographs. The method requires digitized black and white photographic silhouettes, and optical porosity is expressed as the ratio of white cells to black cells. Unfortunately, it is impossible to measure the aerodynamic porosity of a natural tree windbreak. For wide, natural windbreaks, optical porosity is not always the appropriate parameter for expressing the optimal condition because optical porosity shows only the two-dimensional gap (the ratio between open area and total area) rather than the three-dimensional spaces (volumetric porosity) through which the wind flows across the width of the windbreak. Nevertheless, optical porosity has frequently served as the descriptor of natural windbreaks for lack of a practical alternative (Heisler & Dewalle, 1988).

Horizontal distances from windbreaks are usually expressed in terms of windbreak height (h) while wind speed are usually expressed and approach (open) wind speed. The open or approach wind speed is the wind speed measured from the farthest point not influenced by the windbreak on the windward side. The zone of windbreak protection (also known as the shelter extent) is the distance to which a significant reduction in wind speed extends. It is often represented by the distance (in multiples of the windbreak height) which reduces wind speed by a given significant percentage and by the minimum wind speed (maximum wind reduction) and its location. Windbreaks are normally rectangular and usually the higher the windbreak, the larger the protected zone. They are more efficient when oriented perpendicular to the prevailing winds. (Caborn, 1957; Kenney, 1987).

2.5.3. *Influence of windbreaks on wind speed*

Windbreaks work by adsorption of momentum from the wind flow which results in a decrease of wind velocity and turbulence in the protected field (Vigiak et al., 2003). The wind speed

reduction patterns for different windbreak characteristics have been summarised by Vigiak et al. (2003) according to Figure 2-1. Windbreak influence extends from approximately -5 h (windward) to 35 h (leeward). This means that the distance between windbreaks is often less than 35 times the height of the windbreaks on a typical field in the Canterbury region, and the subsequent windbreak falls within the zone of protection of the upstream windbreak. As a result, wind velocity in one field is not only affected by one barrier but by several others close to it. As shown in Figure 2-1, wind speeds can be reduced by up to 90% for low porosity windbreaks, which may have a considerable influence on crops growing in the influence of the windbreak.

The minimum wind speed occurs in the near lee, at distances of 4 - 6 h. Further leeward, at about 20 h, wind speed recovers to 80% of the approaching wind speed. For very dense windbreaks, the wind profile shows a lower minimum wind speed but a faster wind speed recovery near the lee (between 0 h and 10 h), compared to a porous windbreak (Heisler & Dewalle, 1988; Ucar & Hall, 2001; Vigiak et al., 2003).
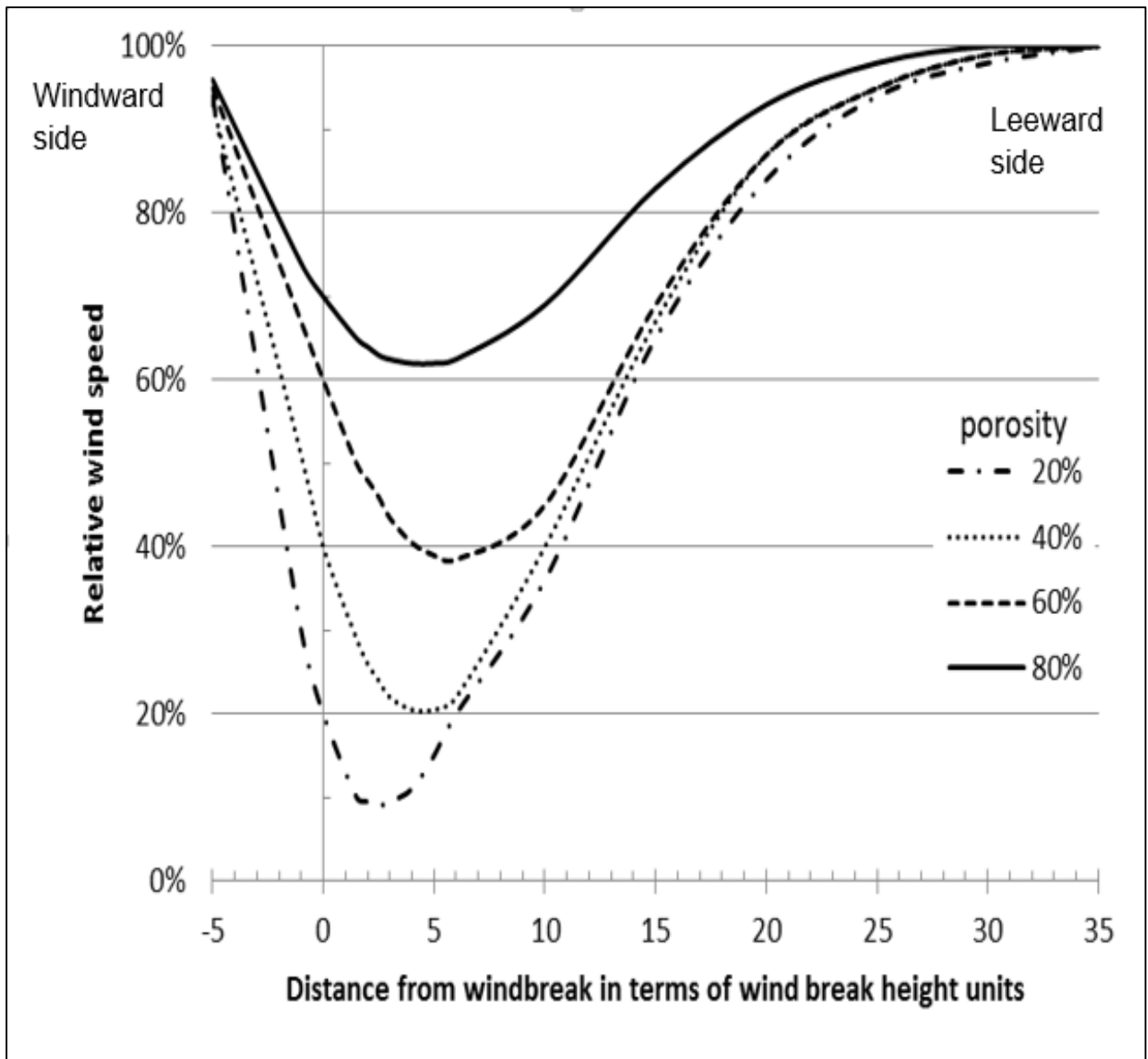
Figure 2-1. Reduction in wind speed behind windbreaks of different porosities (Vigiak et al., 2003).

The efficiency of wind speed reduction depends mainly on height and porosity. The distance affected by a windbreak is increased proportionately by increasing the windbreak height (Heisler & Dewalle, 1988; Vigiak et al., 2003); thus, the height of a windbreak is important in considering the horizontal extent of sheltered area. The porosity of the windbreak determines the extent to which a windbreak obstructs airflow or reduces the kinetic energy of the wind by filtering it (maximum wind reductions). A very low porosity windbreak (less than 20%)

creates more turbulence downwind than a medium porosity windbreak (40 - 50%) (Vigiak et al., 2003). As a result, the recovery of mean wind speed to open wind speed occurs at a closer distance to a low porosity windbreak (up to 10 h) than for a medium porosity windbreak (up to 20 h), thus resulting in a shorter protected distance. Other factors that influence wind speed reduction are the approach flow characteristics: wind speed, wind direction, turbulence intensity and atmospheric stability conditions; as well as windbreak shape, orientation, width and length (Heisler & Dewalle, 1988; Vigiak et al., 2003).

2.5.4. Past studies on the application of windbreaks on irrigation systems

Studies from various parts of the world have shown that windbreaks have potential benefits if integrated into irrigation system. The benefits are related to the ability of windbreaks to reduce speed, and hence lower SEL and ET. In turn, irrigation water is saved. Specifically, water use for crops protected by a windbreak tends to be lower due to reduced evapotranspiration while spray evaporation losses during sprinkler irrigation are minimized if wind velocity is reduced by the use of windbreaks.

In Sudan, Bayoumi (1976) (cited in Sturrock,1988), estimated that shelterbelts would save 10 percent of water, enabling an additional 34 000 ha of cotton to be irrigated. In the Russian steppes, shelter from windbreaks was found to reduce irrigation requirements by 20 - 23 mm of water per year (Vasil'ev 1980 as cited in Sturrock, (1988). Other savings would follow from reduced requirements for pumping and fuel, and in the case of overhead irrigation, moving irrigators.

In the United States, Flemer (1974) (as cited in Sturrock, 1988), reported that under constant winds and clear skies, an irrigated field of 1-year-old peach trees required twice the volume of pumped water to maintain some growth than a comparable field protected by a cypress shelterbelt. Despite the more lavish use of water on the exposed site, the trees were only half the height of those in shelter and in addition to a doubling of the cost of pumping and pipe moving, the exposed crop was one-third less in value at the time of sale. In the United States,

evaporation and drift losses as high as 42% have been measured in fields without windbreaks (Kraus, 1966). Also in the United States, Dickey (1988) showed that in areas of high ET demand (10 mm/day), a windbreak could improve irrigation application efficiency of fine spray by 10% by reducing the wind velocity from 4.5 to 1.8 m/s. He also reported that a greater reduction in wind velocity would result in greater irrigation efficiencies, especially at higher ET rates. In North America, shelter that reduced the speed of hot dry summer winds across a lucerne crop by 40% resulted in a 10% saving of irrigation water (Kort, 1988) (as cited in Bird, 1998). here was no difference in crop yield between the exposed and sheltered sites when irrigation was applied to compensate for the difference in water usage. For dry land crops in the same trial, shelter was responsible for a 9% increase in yield, soil moisture being consistently higher beneath the sheltered crops.

In New Zealand, studies have also shown that windbreaks can have great benefits in terms of saving water resource use in agriculture. de Vries et al. (2010) studied the influence of windbreaks on ET and irrigation requirement on a typical field in the Canterbury region which was protected by a single windbreak using a modelling approach. Irrigation water requirements were estimated by calculating actual ET for a pasture crop at various horizontal distances from a windbreak. Results showed that windbreak shading can reduce solar radiation by 90% on a full sunshine day and, if combined with reduction in wind speed, ET can be reduced to zero percent for dense wind breaks. The findings also showed that windbreaks can reduce on-farm water requirement by 10 - 20% and still maintain ideal farm yield. They also showed that for a typical field in Canterbury with a total length of 300 m, the total reduction from just shade is 3% at mid-day and 9% in the afternoon.

2.5.5. Summary and Conclusion

Reviewing the literature shows that the length of fields protected by windbreaks is largely determined by the height of the windbreaks, while the degree of protection at any distance from windbreak is influenced by the porosity of the windbreaks. The distance protected by a windbreak on the leeward side increases with an increase in the height of the windbreak.

Porosity determines the position of minimum wind speed and the rate of recovery of wind speed.

The literature also shows that a single windbreak has an effect extending up to 35 times the windbreak height on the leeward side and up to 5 times the height on the windward side. Therefore, for a typical field on the Canterbury region where windbreaks are spaced as close as 10 times their heights apart, this assumption cannot be simply held. Hence, there is a need for physical experiments to quantify the wind speed reduction for multiple windbreaks in field.

.

CHAPTER 3: METHODS AND MATERIALS

3.1. Introduction

This chapter describes the materials and methods used to complete the research in this thesis.

i.   In the first section (Section 3.2), the methods and materials used to quantify spray evaporation losses are presented. It describes the spray evaporation experiments which were done and the methods used in the development of spray evaporation loss predictive models;

ii. Section 3.3 describes the materials and methods used to collect wind data. Wind data were collected from two farms to quantify wind speed reductions in fields protected by multiple windbreaks;

iii. Section 3.4 describes the modelling approach used to model the effects of windbreaks on irrigation efficiency. Wind data were used to calibrate and validate a windbreak model. The validated windbreak model was used to calculate reduction in wind speed for different scenarios from which ET was calculated for different scenarios. Lastly, a hydrological model (WaSim) was used to simulate irrigation requirements for pasture crop and SEL was calculated for the corresponding irrigation events. Statistical analysis was performed using a two-sample t-test assuming equal variances to test if the change from one scenario to another was significant.

3.2. Determination of spray evaporation losses

The literature review (Chapter 2) demonstrated that the EC method could be used to separate wind drift losses from spray evaporation losses. The data obtained from such experiments can be used to develop a statistical model, which can be used to predict spray evaporation losses for the conditions in which it was developed. Hence, to develop a spray evaporation prediction model under Canterbury conditions, spray evaporation loss experiments were conducted using an experimental irrigation rig under different weather conditions using two commonly used centre pivot sprinkler nozzles. Spray loss was determined from the change of electrical conductivity between the source water and the water in the catch can. The data

obtained from spray evaporation losses were used to develop statistical models that were used to estimate SEL for any conditions in the Canterbury region. Droplet size distributions were determined using a laser optical disydrometer, and the results used to explain the losses between the two sprinkler nozzles studied.

3.2.1. The study site

The spray evaporation loss experiments were conducted in an open field at the University of Canterbury. The site had flat open ground: - it was free from any obstacles, dust and had very short mown grass. The geographic location of the site is 43º31'26"S, 172º35'13"E. The site is surrounded by few a buildings to the north and west as shown in Figure 3-1.
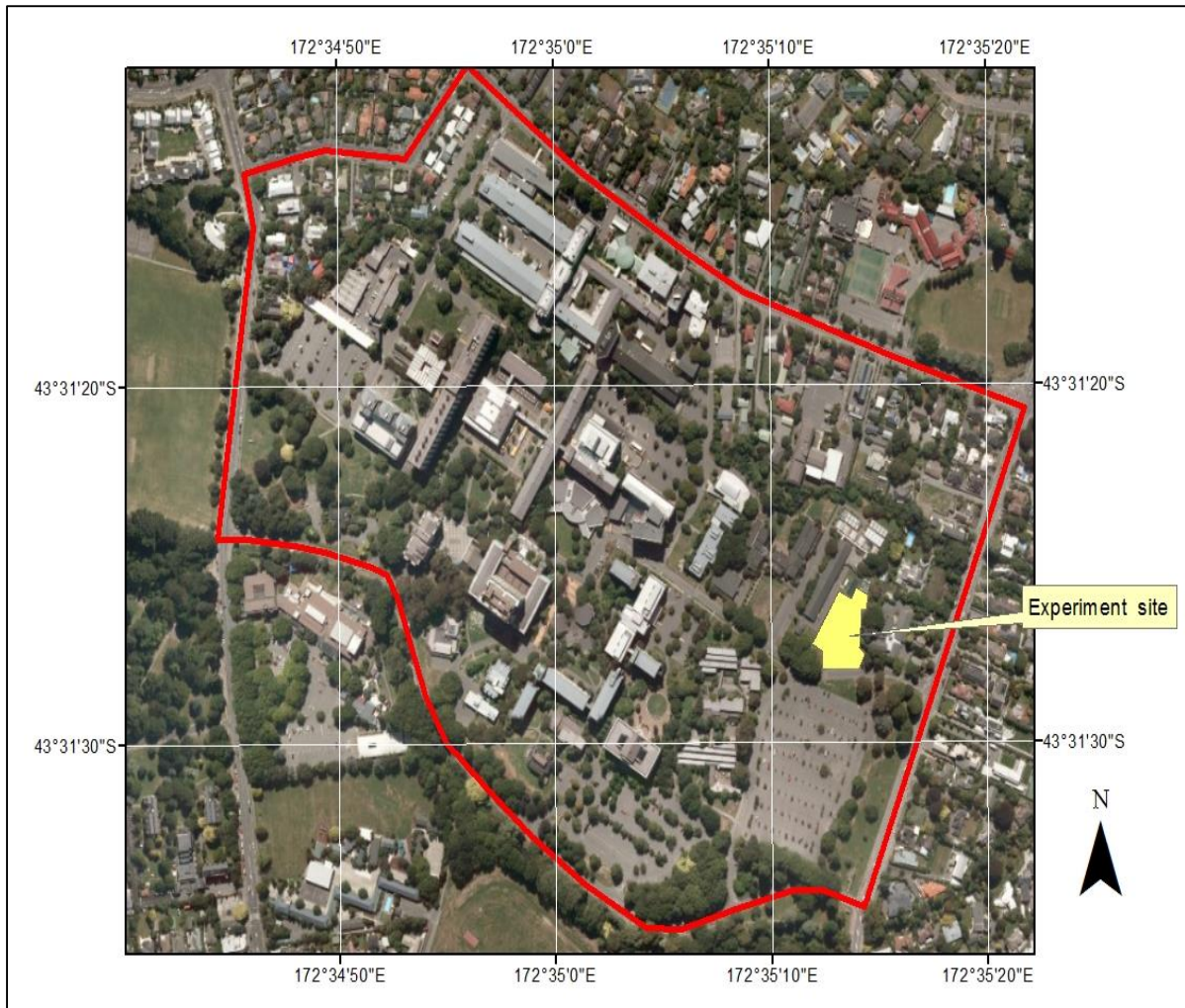
Figure 3-1. Map of the University of Canterbury main campus showing the location of the spray evaporation experiment site.

3.2.2. Description of the experimental system

An experimental irrigation machine with a stable base was fabricated to simulate irrigation spray from a single sprinkler nozzle as shown in Figure 3-2. The sprinkler nozzle was connected to the mains water supply source through a one bar pressure regulator, a flexible rubber hose, a water flow meter to measure the water flow and a T- connection to sample water for analysis. The area around the sprinkler was divided into equal squares and a catch can placed at the centre of each square to represent the precipitation falling on that area. The

catch cans were located around the sprinkler at a spacing of 3 m on a grid of 18 m by 18 m for the Rotator R3000 sprinkler nozzle and a spacing of 1.5 m on a grid of 9 m by 9 m for the Spinner S3000 sprinkler nozzle, as shown in Figure 3-2.
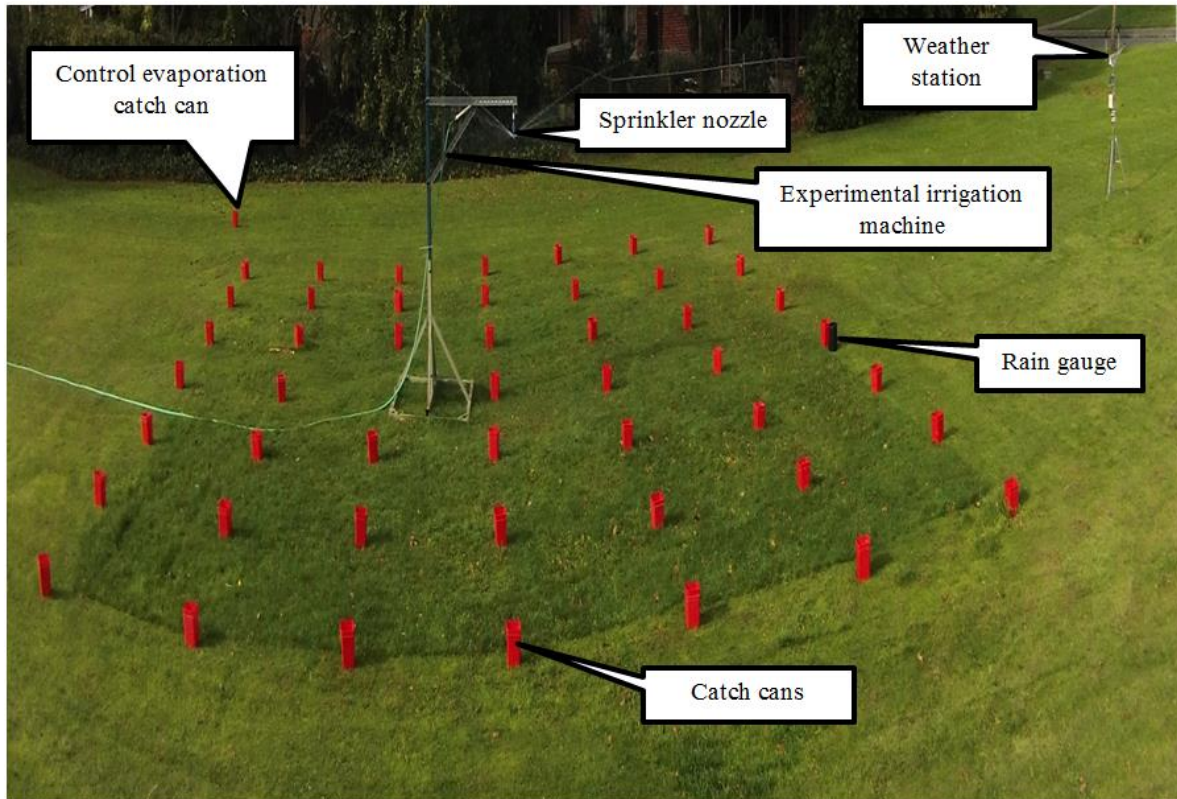
Figure 3-2. Experimental set up for determination of spray evaporation.

Catch cans

Identical plastic catch cans were used to collect irrigation spray during the irrigation. A total of 49 catch cans were placed around the sprinkler nozzle to collect sprinkled water during the irrigation event. While procuring catch cans, identical red plastic catch cans were found, which were considered suitable because they were cheap and met the minimum requirements for catch cans as set out by the ASAE (2001), test procedure for determining the uniformity of water distribution of centre pivot and lateral move irrigation machines equipped with spray nozzles. The ASAE standards 2001 states that catch cans should be identical, with a minimum height of 120 mm, and, a minimum opening diameter of 60 mm. The dimensions of the chosen catch cans were 175 mm and 160 mm for height and opening, respectively. To prevent

tipping or blowing of the catch cans during the tests, one catch can holding sand and gravel was used to stabilise the other catch can receiving the sprinkled water during irrigation, as shown in Figure 3-3 below.
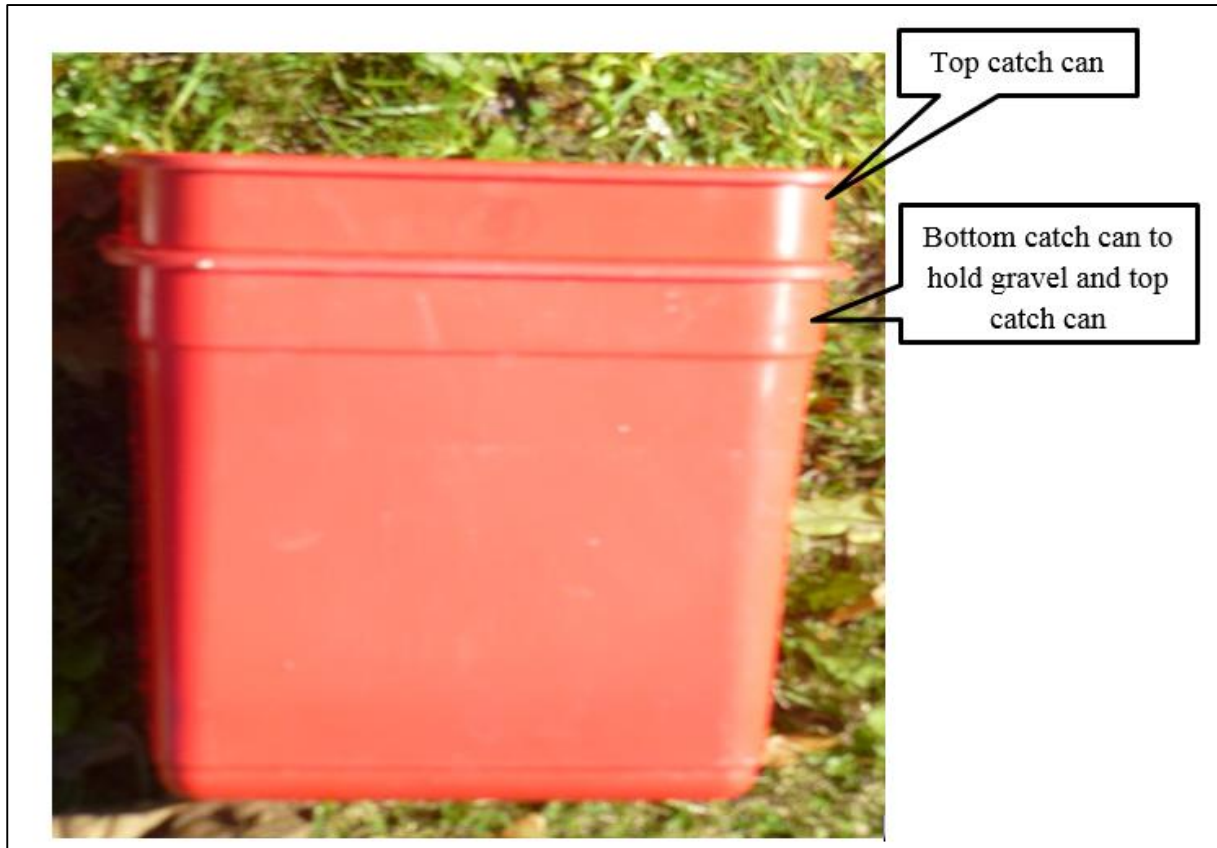
Figure 3-3. Photograph of catch cans as used in the study.

Sprinkler nozzles

The experimental irrigation machine was fabricated with a provision to hold sprinkler nozzles one at a time during the test. Two different types of commercial sprinkler nozzles used in centre pivot and lateral move irrigation equipment in Canterbury region were selected for study. The nozzles are widely available in the markets and the current trend is to shift into their use in centre pivots in the Canterbury region. The selected sprinkler nozzles are the R3000 Rotator® and the S3000 Spinner® from the Nelson Irrigation Corporation. Throughout this thesis, the R3000 Rotator® and the S3000 Spinner® will be referred to as the

Rotator R3000 and Spinner S3000 respectively. These two types of nozzles are classified as rotating spray plate sprinklers (RSPS). Rotating spray plate sprinklers differ from fixed spray plate sprinklers (FSPS) in that in RSPS the grooved plate rotates under the effect of the water jet while FSPS are based on the impact of the water jet on a fixed grooved plate. The main difference between the Spinner S3000 and the Rotator R3000 is that the Rotator R3000 uses a slowly rotating plate while the Spinner S3000 uses the spinning action of the rotor plate to produce a desirable canopy of droplets. The Spinner S3000 is suited for use on sensitive crops and soils that do well under a more gentle application of water. A sprinkler nozzle No.28 was used for Rotator R3000 and No. 18 was used for the Spinner S3000 (coded blue and grey respectively). A 8-grooved deflector plate was used during the test. Figure 3-4 and Figure 3-5 show the types of sprinkler nozzles and spray plate configurations used in the study. The performance data for the Rotator R3000 and the Spinner S3000 nozzles under no wind conditions are shown in Table 3-1. From the performance data, it can be seen that, for the same operating pressure and nozzle height above the ground surface, the Rotator R3000 gives a larger throw diameter than the Spinner S3000.
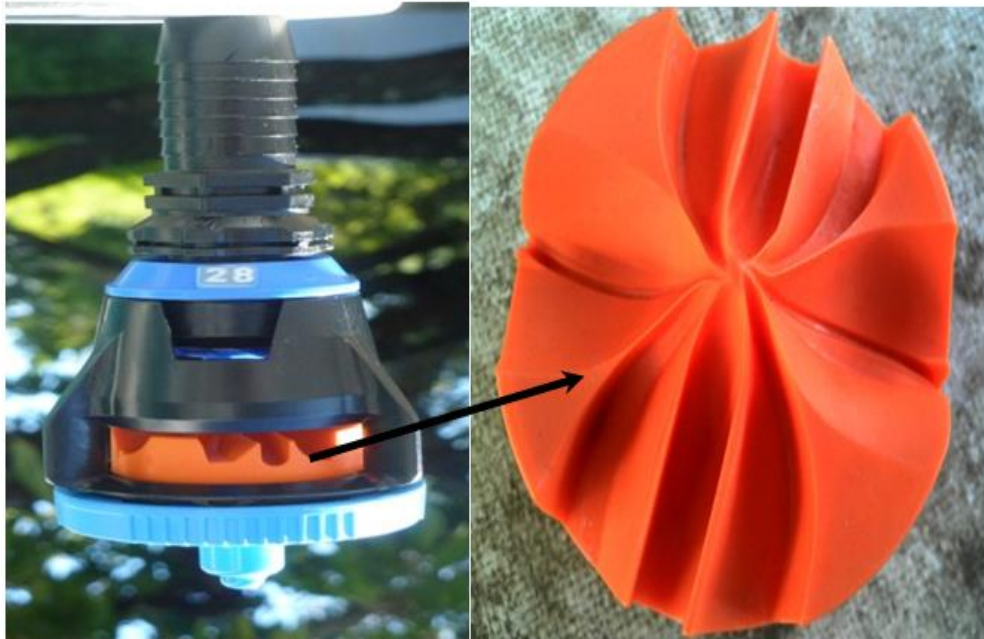
Figure 3-4. Photograph showing Rotator R3000 sprinkler nozzle and spray plate used in the experiment.
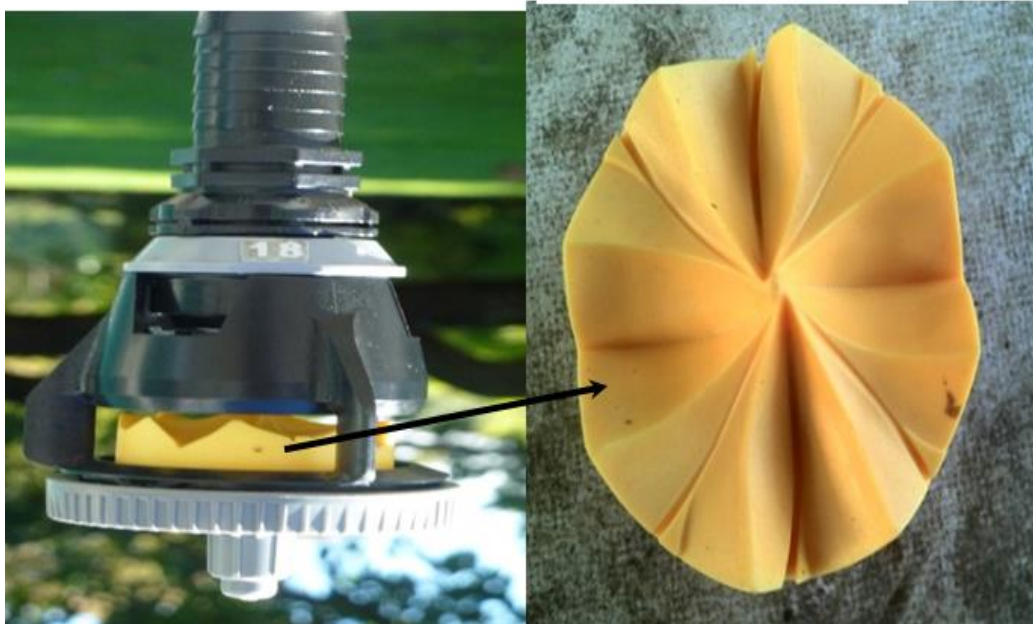
Figure 3-5. Photograph showing Spinner S3000 sprinkler nozzle and spray plate used in the experiment.

Table 3-1. Performance data for the Rotator R3000 sprinkler nozzles under no wind conditions.

Nozzle type	R3000 with orange multi-trajectory plate			
Nozzle orifice diameter	6.35 mm			
Operating pressure (bar)	Throw diameters (m) and CU at mounting height of			
	0.3 m	0.9 m	1.8 m	2.7 m
1.0	15 (n/a)	16 (85)	18 (90)	19 (n/a)
0.9	16 (n/a)	17 (85)	18 (90)	20 (n/a)
1.8	17 (n/a)	18 (90)	19 (90)	21 (n/a)
2.7	17 (n/a)	18 (90)	19 (95)	21 (n/a)

Source: www.nelsonirrigation.com

Table 3-2. Performance data for the Spinner S3000 sprinkler nozzles under no wind conditions.

Nozzle type	S3000 with orange multi-trajectory plate	
Nozzle orifice diameter	6.35 mm	
Operating pressure (bar)	Throw diameters (m) and CU at mounting height of	
	0.9 m	1.8 m
0.7	9 (85)	11(85)
1.0	10 (85)	12(85)
1.4	11(90)	13(90)

Source: www.nelsonirrigation.com

Values in brackets terms represent the Coefficient of Uniformity (CU) of the nozzles.

3.2.3. Data collection

Preliminary laboratory tests

In order to confirm that the EC method would work in the field, preliminary EC tests were carried out using a digital handheld YSI Model 30 EC meter in the laboratory, to calibrate the meter and ensure that the meter was reliable and sensitive to small changes in solute concentration. The specifications for the EC meter used in this study are shown in Table 3-3.

Table 3-3: Measurement ranges for the YSI Model 30 EC meter.

Measurement	Range	Resolution	Accuracy
Conductivity	0 to 499.9 μS/cm	0.1 μS/cm	±0.5%
	0 to 4999 μS/cm	1.0 μS/cm	±0.5%
	0 to 49.99 mS/cm	0.01 mS/cm	±0.5%
	0 to 200.0 mS/cm	0.1 mS/cm	±0.5%
Temperature	-5 to 95° C	0.1° C	±0.1° C

Source: http://www.coleparmer.com/Assets/manual_pdfs/19750-00,-10.pdf.

These tests were done by evaporating a 1000 ml sample of the water to be used in the experiment in an oven and therefore protected from pollution by dust. Specific conductance, which is temperature compensated electrical conductivity, was measured to determine the EC of the water before and after evaporation. The decrease in mass of the evaporated water and the corresponding increase of EC (EC %) were graphically compared as shown in Figure 3-6.
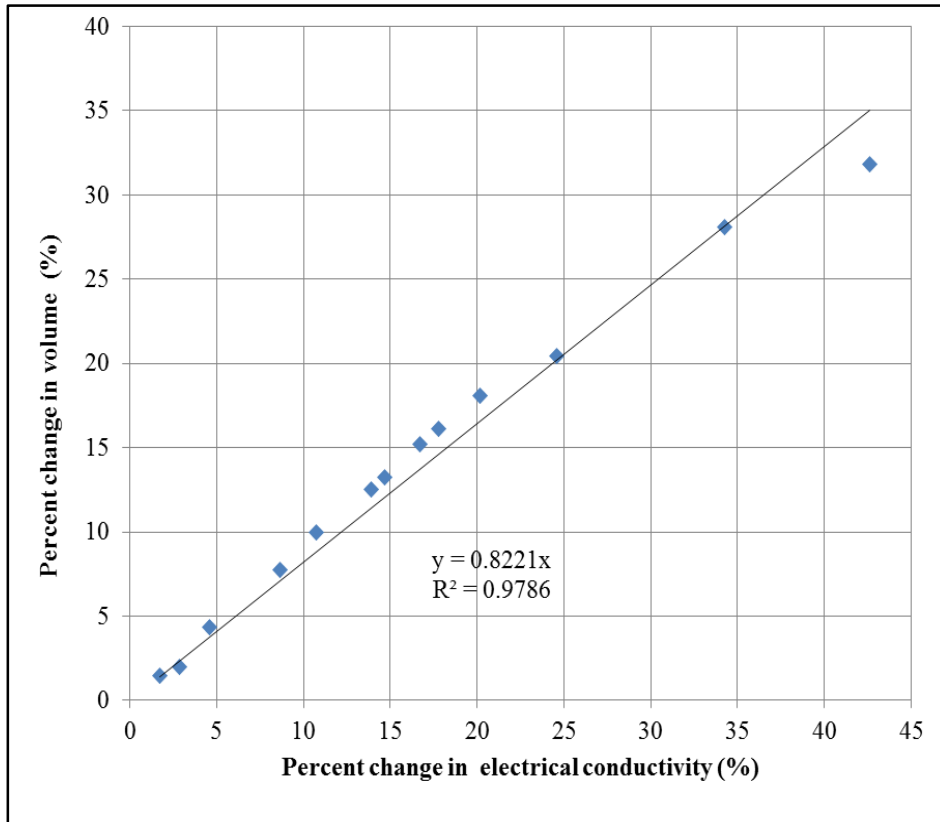
Figure 3-6. Relationship between percentage changes in electrical conductivity with percentage change in volume of water due to evaporation.

The results showed an excellent linear correlation (R^2 = 0.98) between the percentage evaporation and percentage change in electrical conductivity of the sample after evaporation. Therefore, it could be assumed that the percentage increase in EC gives the percentage loss in irrigation water due to evaporation. To determine the reproducibility of the measurements from the EC meter, tests were done on a solution to check whether individual readings from the same solution did not vary for more than 10% of the average conductivity readings. It was therefore justified that the method would work well under field conditions.

Field tests

Irrigation test runs were done using the improvised irrigation simulator at different hours of the day to represent wide-ranging weather conditions. Each test was run for a duration of one hour at a pressure level of one bar and with the sprinkler nozzle height at 2 m from the catch can opening, which is the approximate height at which sprinklers commonly operate in the Canterbury region. Weather parameters at the experiment site were recorded at 2 m height at intervals of 1 minute by a portable HOBO weather station (see Figure 3-7), placed at approximately 30 m from the experimental site. These weather parameters are solar radiation, wind direction, wind speed, dew point temperature, relative humidity and air temperature.
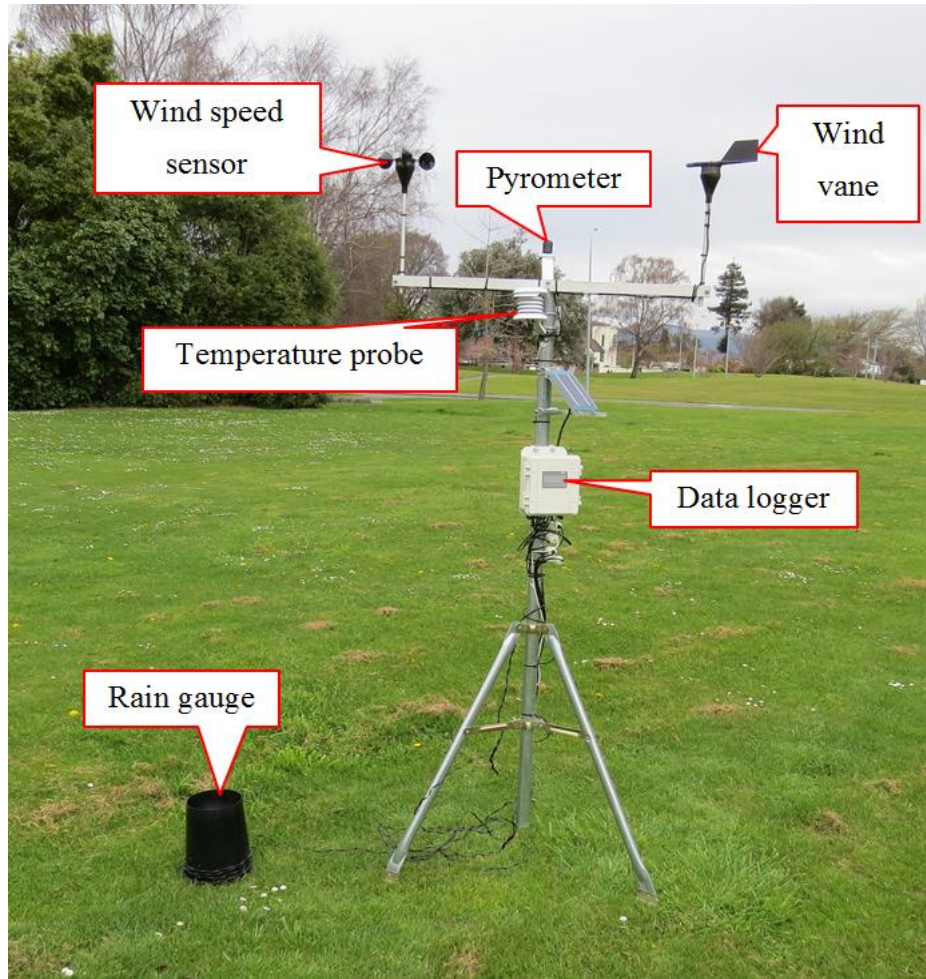
Figure 3-7. Photograph of the portable weather station used in this study.

The sprinkler's flow discharge was read three times during the test at intervals of 15 minutes from the flow meter attached to the mains. Water samples from the main flow line were taken every 15 minutes for determination of electrical conductivity (EC).

At the end of each test, the catch cans were immediately capped to reduce the chances of evaporation while waiting for EC measurements to be taken. A sample from each catch can was poured into a 100 ml beaker for EC measurement determination. The samples were marked with the number of the test run and its relative position from the sprinkler nozzle. Then, three EC measurements were made from the same solution in the beaker and the sample was discarded after each measurement. The EC meter's probe was rinsed with deionized water prior to any EC measurements being taken to minimize errors that might arise from

adsorption of ions to the walls of the conductivity probe. If any large amount of variance (by more than 10%) existed in the three readings, additional readings were made to until more consistent values were obtained. The average of the three values was then reported as the EC for that particular catch can.

Catch can evaporation experiment

The evaporation of water which occurs in the water caught in a catch can during a test is difficult to control. To quantify this, a separate experiment was done following the approach proposed by Tarjuelo et al. (2000). A known amount of water was put in a typical catch can outside the sprinkled area during the test. EC of the water was determined at the beginning and the end of each test. The difference in EC was assumed to be due to catch can evaporation under conditions similar to those in the test site. Assuming that the rate of catch can evaporation was uniform over the test site, corrections were made to account for evaporation losses which occurred after the water reached the catch cans. Such experimental conditions have been reported to be more extreme than when the sprinkler nozzle is operated in an irrigated area and the results should be therefore be regarded as an upper boundary for catch can evaporation during irrigation (Playán et al., 2005).

Estimation of droplet size distribution

Sprinkler nozzles deliver droplets of many sizes depending on the nozzle geometry and the size distribution varies with the distance from the sprinkler nozzle. An accurate knowledge of droplet size distribution as a function of the nozzle is essential to explain the difference between the SEL from the two nozzles. Therefore, droplet size distributions along the sprinkler radius for each experiment were measured using a laser optical disydrometer (see Figure 3-8) at the ground at 1 m radial distance increments for both sprinklers, as shown in Figure 3-9. This device is based on the attenuation of an infra-red beam as drops pass through an optical window. The drop size measuring process uses a flat beam of laser light, directed by mirrors to a horizontal array of photo-sensitive diodes. As each drop passes through the optical window, it crosses the beam, casting a shadow and thus causing an attenuation of the signal. The attenuation of the signal from each drop is then related to the drop diameter and

time of passage. The specifications for the laser optical disydrometer used are given in Table 3-4.

Figure 3-8. Photograph of the optical laser disydrometer used in the study.

Figure 3-9. The optical laser disydrometer set-up.

Table 3-4: Technical specifications for the laser optical disydrometer used in this study.

Parameter	Specification
Measuring area	180 x 30 mm (54 cm^2)
Particle size (Liquid precipitation)	0.2 to 5 mm
Particle velocity	0.2 to 20 m/s
Precipitation intensity	0.001 to 1200 mm/h
Accuracy of precipitation amount	± 5%
Precipitation measurement	- 32 size - 32 velocity classes
Measurement accuracy (precipitation measurement)	± 1 size class (0.2 to 2mm) ± 0.5 size class (> 2 mm)
Types of precipitation	Drizzle, drizzle/rain, rain, mixed rain/snow, snow, snow grains, sleet, hail)
Environmental conditions	- - 40 to +70°C - 0 to 100 % relative humidity

3.2.4. Statistical data analysis of spray evaporation data

Spray evaporation loss was determined from the Equation (2-1). Since the electrical conductivity was measured as a specific conductance of the water (temperature compensated electrical conductivity), no temperature corrections were made for the measured values. The average spray evaporation loss for a particular test was calculated as the average of losses from all catch cans in the irrigated area. In compiling the results, the average of the losses from all catch cans is reported as the evaporation loss for that particular test run.

Statistical analysis using R program

The experimental values of spray evaporation losses were related to meteorological variables recorded during the experiments: with wind speed, air temperature, relative humidity, solar radiation, and vapour pressure deficit as independent variables. The results obtained were used to develop a statistical model relating spray evaporation losses as a function of the different measured climatic data. Multiple regression analysis was performed using the R program for each sprinkler nozzle test in order to obtain the simplest model that best estimated spray evaporation loss.

The R program is software written with an environment for data manipulation, calculation and graphical displays. Among other things, it has:

- an effective data handling and storage facility;
- a suite of operators for calculations on arrays, in particular matrices;
- a large, coherent, integrated collection of intermediate tools for data analysis;
- graphical facilities for data analysis and display either directly at the computer or on hardcopy, and
- a well-developed, simple and effective programming language which includes conditionals, loops, user defined recursive functions and input and output facilities.

Data from each experiment were organized in two different ways. In the first case, spray evaporation loss was expressed as a function of the directly measured variables: solar radiation, wind speed, air temperature, and relative humidity. In the second case, the spray evaporation loss was expressed as a function of wind speed, solar radiation, and vapour pressure deficit. The vapour pressure deficit was calculated from air temperature and relative humidity from the equations below:

$$e_a = \frac{RH}{100} e^0(T_a) \qquad\qquad (3\text{-}1)$$

$$e_s = e^0(T_a) = 6.108 * e^{\left(\frac{17.27 T_a}{T_a + 237.3}\right)} \qquad\qquad (3\text{-}2)$$

$$\text{Vapour pressure deficit (VPD)} = e_s - e_a \qquad\qquad (3\text{-}3)$$

Where,

- e_a is the actual vapour pressure representing the humidity of the air at the weather station site (mbar);
- e_s is the saturation vapour pressure representing the capacity of the air to hold water vapour (mbar);
- T_a is the mean air temperature during the hourly period (^{0}C);
- $e^0(T_a)$ is the saturation vapour pressure function; and
- RH is the mean relative humidity for the hourly period (%).

Many other expressions exist for calculating vapour pressure deficit depending on the data availability (Allen et al., 2005). Equations (3-1), (3-2) and (3-3) were chosen to calculate vapour pressure deficit because the wind logger used was able to measure relative humidity and air temperature directly, and thus such data was considered to have integrity and represent the actual environmental conditions.

Statistical analyses were done by writing and executing mathematical scripts; and then making a conclusion of the output. The R mathematical script used in developing the models

is shown in Appendix A. The detailed statistical modelling process in R program is described in detail by Crawley (2013).

For each experiment, a general spray loss predictive model using all variables was first obtained using the models of the logarithmic form of the equation below.

$$\log_e SEL = \ y1 \log_e u + y2 \log_e I + y3 \log_e T_a + y4 \log_e RH$$

(3-4)

$$\log_e SEL = \ y1 \log_e u + y2 \log_e I + y5 \log_e(e_s - \ e_a)$$

(3-5)

The results of Equations (3-4) and (3-5) were then expressed in the general form given in Equations (3-6) and (3-7) respectively; where each independent variable x was considered in the mathematical form x^y (Bavi et al., 2009 and Yazar, 1984).

$$SEL = \ u^{y1}I^{y2}T_a^{y3}RH^{y4}$$

(3-6)

$$SEL = \ u^{y1}I^{y2} \ (e_s - e_a)^{y5}$$

(3-7)

Where,

- I is the solar radiation (MJ/m^2);
- $(e_s - e_a)$ is the vapour pressure deficit (VPD); and
- y1, y2, y3, y4, y5 are empirical coefficients to be determined using multiple regression analysis.

Then, each independent variable x was considered in the mathematical forms; x, log(x), 1/x and e^X (Playán et al., 2005). Equations were then developed using different combinations of mathematical forms of the independent variables. Backward elimination of variable(s) was used to get an improved model in each model. In backward elimination, a general equation using all variables is first developed (as above), then testing of the variable(s) is done to check if its deletion or inclusion improves the model using R^2 (coefficient of determination) criterion and the process is repeated until no further improvement is possible. R^2 provides a measure of how well observed outcomes are replicated by the model, as the proportion of

43

total variation of outcomes explained by the model (Crawley, 2013). Values of R^2 range from 0 to 1: a R^2 of 1 indicates that the regression line perfectly fits the data. This led to a variety of regression models with different numbers of independent variables and their mathematical forms.

For each model developed, model diagnostic diagrams were plotted in order to determine whether the models could be trusted. The first step was to examine residuals: residuals are estimates of experimental error obtained by subtracting the observed responses from the predicted responses. Examining residuals is a key part of all statistical modelling which helps to show whether assumptions made are reasonable and if the choice of model is appropriate (Crawley, 2013). This examination was done by plotting the residuals versus corresponding predicted values: plotting residuals versus the value of a fitted response should produce a distribution of points scattered randomly about zero, regardless of the size of the fitted value (Crawley, 2013). This was done to check for increasing residuals as size of fitted value increases. If the model fit to the data is correct, the residuals approximate the random errors that make the relationship between the explanatory variables and the response variable a statistical relationship (Crawley, 2013). Therefore, if the residuals appear to behave randomly, it suggests that the model fits the data well. On the other hand, if a non-random structure is evident in the residuals, it is a clear sign that the model fits the data poorly (Crawley, 2013).

The second plot was a normal probability plot used to assess whether or not a dataset is approximately normally distributed or what the nature of departure from normality exists (data skewed, shorter than expected trails, or longer than expected trails). The data were plotted against a theoretical normal distribution in such a way that the points should form an approximate straight line. Departures from this straight line indicate departures from normality: a nearly linear pattern indicates that the normal distribution is a good model for that particular data set (Crawley, 2013).

A procedure following Playán et al. (2005) was developed to select the best suited, most simple predictive equations for each experiment:

- the equations were classified into two groups: those expressing SEL as function of wind speed, relative humidity, air temperature and solar radiation, and those expressing SEL as function of wind speed, solar radiation and vapour pressure deficit;

- in a given group, the equation was discarded if presenting a coefficient of determination (R^2) less than 0.6;

- if inclusion or deletion of a variable or its mathematical form led to a low R^2, then the variable or its form was rejected as part of the best model desired;

- equations involving fewer independent variables were only accepted if their R^2 was better than that of complex equations;

- R^2 is not enough to tell if a model fits the data, and therefore a high R^2 value does not guarantee that the model fits the data well (Crawley, 2013). Use of a model that does not fit the data well cannot provide good answers to the underlying engineering or scientific questions under investigation. The models whose residuals increased with an increase in fitted values were rejected; also, the models whose residuals decreased with an increase in fitted value were rejected. Therefore, only models whose residuals appeared to behave randomly were selected. From the normal probability plot, models which showed a nearly linear pattern were selected, which indicated that the normal distribution was a good model for the data set; and

- Statistical comparison of the two forms of models from each experiment was then done to pick the most suitable one (models expressing SEL as a function of air temperature, wind speed, relative humidity; and vapour pressure deficit and wind speed). The comparison was done by using modelling efficiency (ME) and relative root mean square error (RRMSE). Both ME and RRMSE are discussed in detail in Section 3.4.3 below.

The spray evaporation models selected were then used in further studies in this research to determine the magnitude of SEL under various weather conditions. Scenarios were developed to determine how SEL is affected by changes of wind speed for different windbreak characteristics.

3.3. Wind speed reduction through wind breaks

Literature review showed both ET and SEL depend on wind speed, and that wind speed is the predominant factor in the Canterbury landscape which the farmer can control by the use of windbreaks. Although the effect of a single windbreak extends to around 35 times the windbreak height, the windbreaks in Canterbury fields are spaced as close as 10 times their heights apart (100 m – 200 m). Thus in many situations, the next windbreak falls within the zone of protection of the upstream windbreak. For this reason, two different sites with different windbreak characteristics were selected to quantify wind reduction for a field protected by two parallel windbreaks. The data were used to calibrate and validate a model, which was used to model the effect of wind speed changes (as affected by different windbreaks) on SEL, ET and then calculate irrigation requirements.

3.3.1. Description of the study sites

This study has two main sites for the measurement of wind speed reduction: the sites are at geographical coordinates (43°33'31"S, 172°24'03"E) and (43°31'45"S, 172°21'49"E) for Site 1 and Site 2, respectively. Both sites are located on farms in the Canterbury region in the Selwyn District, about 30 km apart as shown in Figure 3-10.
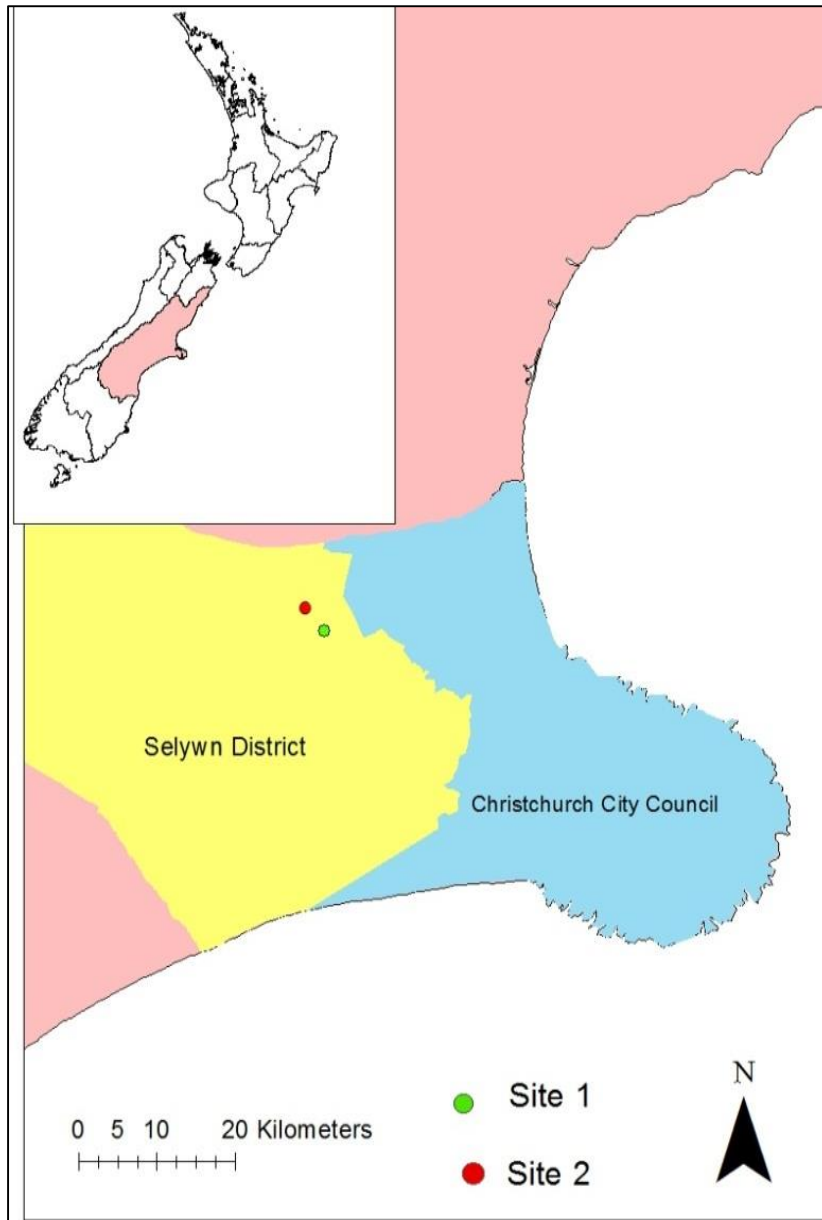
Figure 3-10.Map showing the location of the study sites in the Canterbury region.

In both sites, the land is flat with short pasture and there are other windbreaks on neighbouring farms. Site 1 has uniform Leyland Cypress windbreaks, 5.5 m tall while Site 2 is bounded by both Radiata Pine and Leyland Cypress windbreaks, both 8 m tall. In both sites, the windbreaks are similar to those of typical properties reported by de Vries et al. (2010). The land in both sites is flat and the major crop is pasture grass. Figure 3-11 and Figure 3-12 show the windbreaks at Sites 1 and 2, respectively.

47
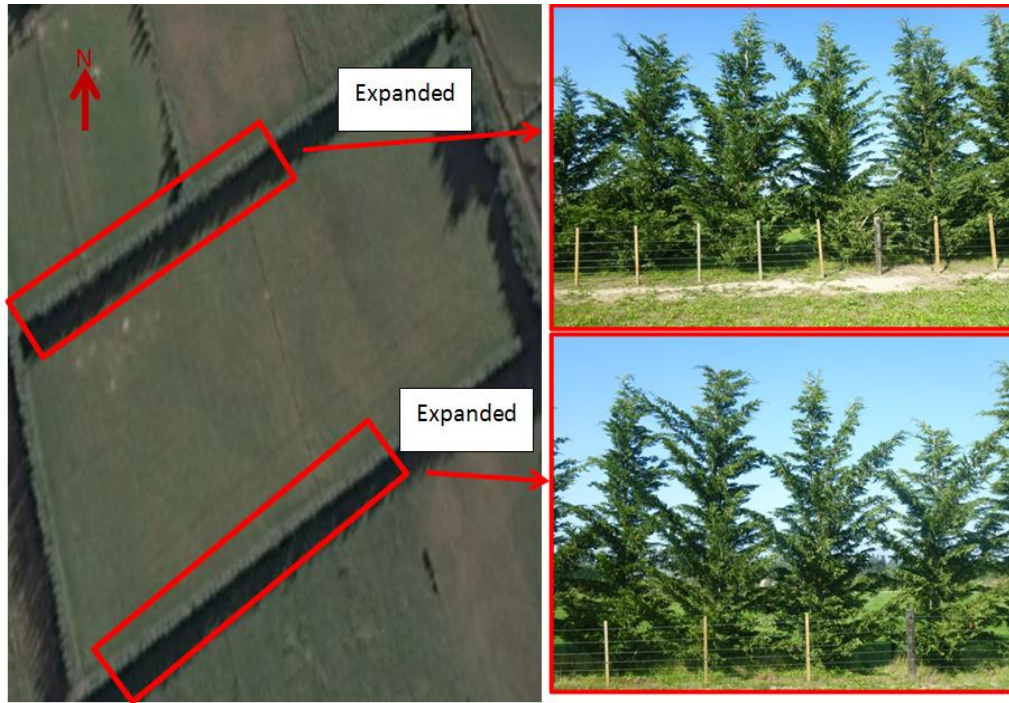
Figure 3-11. Photograph showing the windbreaks studied at Site 1.

Figure 3-12. Photograph showing the windbreaks studied at Site 2.

3.3.2. Experimental set up

For each site selected, wind loggers were installed perpendicular to the windbreak length to record wind direction and speed, as shown in Figure 3-13, Figure 3-14, and Figure 3-15 at Site 1; and Figure 3-16, Figure 3-17, and Figure 3-18 at Site 2. All wind loggers were set to log average wind speeds at intervals of 15 minutes. The wind loggers used were the automatic Windlog® wind loggers from RainWise Inc. and their performance specifications are shown in Table 3-5. The calibration of the wind loggers was performed in an open area by installing all of them 1.5 m apart and then checking whether they registered the same values. An alternative method, such as the use of a wind tunnel, would have been more accurate but was not used due to logistical reasons.

Table 3-5. Specifications of Windlog® wind loggers.

	PARAMETER	
	Speed	Direction
Range	0 – 67 m/s	$360^{°}$ – no dead band
Accuracy	+/- 2%	$+/-22.5^{0}$
Threshold	0.45 m/s	0.9 m/s at a $10^{°}$ deflection
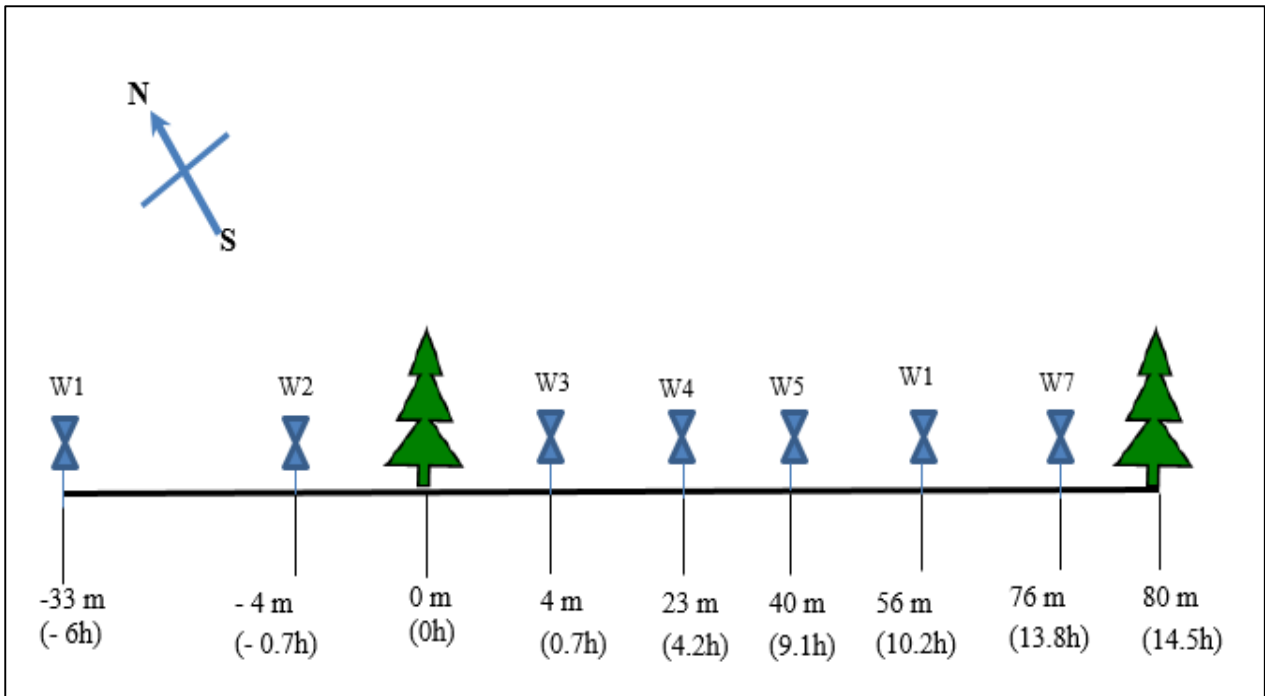
Figure 3-13. Schematic representation of wind logger settings at Site 1. The wind loggers are in a NW-SE direction. Bracketed values represent distances from the windbreak in multiples of windbreak height. Blue figures show wind loggers while green figures show windbreaks (not drawn to scale).

At Site 1, the wind loggers installed as above represented the horizontal wind speed profile perpendicular to both windbreaks. As shown in Figure 3-13, the horizontal profile extends from − 6 h to 14.5 h (with reference from the northwest).

Where,

- h is the average windbreak height; and
- Windward is negative and leeward positive.

Figure 3-14. Photograph showing wind logger settings perpendicular to both windbreaks when viewed from the south (red circles represent the wind loggers).

Figure 3-15. Photograph showing wind logger settings perpendicular to the northwest windbreak when viewed from the southeast at Site 1.
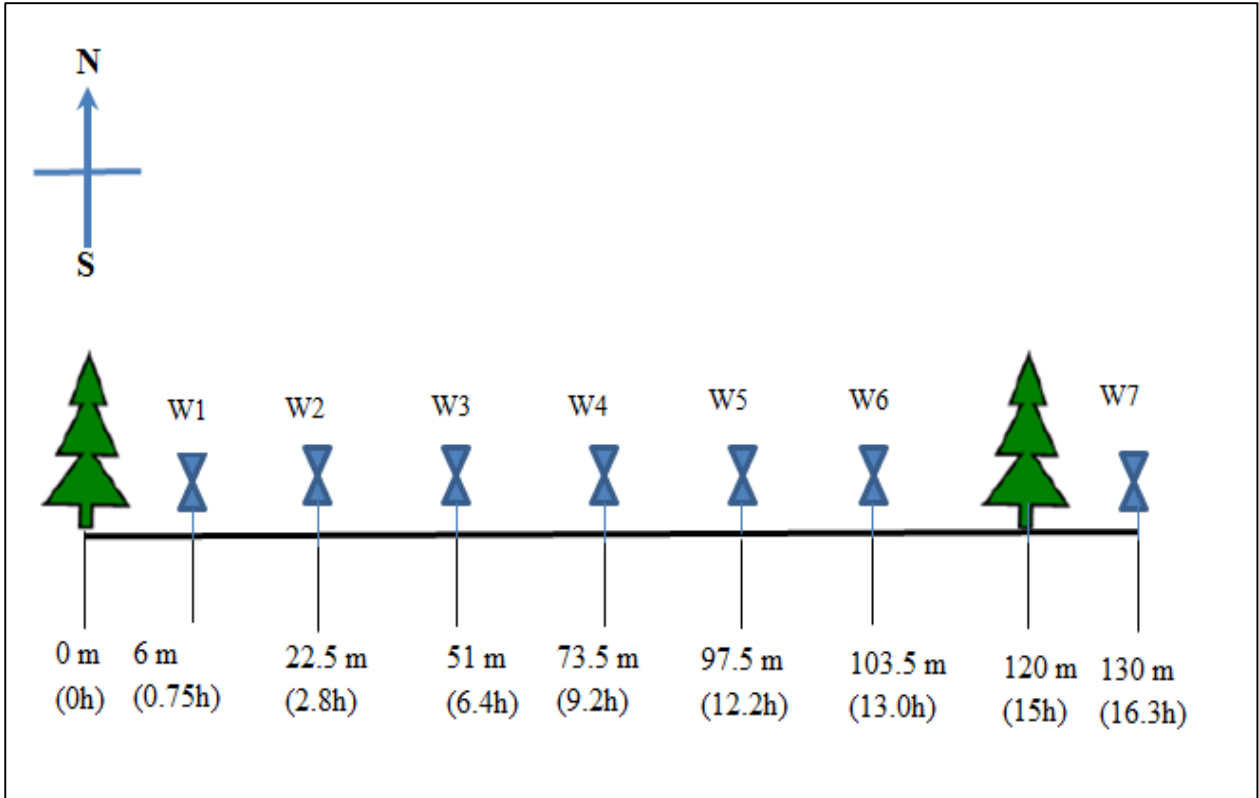
Figure 3-16. **Schematic representation of wind logger settings at Site 2. The wind loggers are in a W-E direction. Bracketed values represent distances from the windbreak in multiples of windbreak height. Blue figures show wind loggers while green figures show windbreaks (not drawn to scale)**

The wind loggers at Site 2 (Figure 3-16) above show the horizontal wind profile that extends from 0 h to 16.3 h (with reference from the west).

Figure 3-17. Photo showing the set-up of wind loggers perpendicular to the eastern windbreaks at Site 2 when viewed from the west.

Figure 3-18. Photo showing the set-up of wind loggers perpendicular to the western windbreak at Site 2 when viewed from the east. Red circles indicate the wind loggers.

3.3.3. *Data collection*

3.3.3.1.   *Wind speed and direction*

The wind data from Site 1 were collected during the period February 24, 2014 to May 15, 2014, and for the nearby Site 2 from June 8, 2014 to August 1, 2014, using the same wind loggers. Wind speed and direction were recorded at a height of 2 m at different distances in multiples of windbreak height upwind and downwind of the windbreaks each site.

3.3.3.2.   *Determination of windbreak porosity*

In addition to windbreak tree height, windbreak porosity is an important factor that controls the effectiveness of windbreaks. Knowledge of windbreak porosity is important because it determines the reduction in wind speed in the protected area. It is not possible to physically measure the aerodynamic porosity of a natural windbreak. An alternative has been to measure the optical porosity, although it does not take into account the three-dimensional nature of the pores in windbreaks through which wind flows. The porosity of the windbreaks was used in calibration of the windbreak model and also to explain the difference in the wind reduction in the two sites.

Ten digital photographs were taken using a digital camera as close as possible to each windbreak, ensuring that all but the smallest pores or branches were visible for optical porosity determination. The photographs were taken perpendicular to the windbreak, keeping the sun far out to the side of the photographer to limit unwanted leaf reflection. If the sun is behind the photographer when photographing, excessive reflection from the foliage appears as pores leading to an overestimation of porosity. The height and width of the windbreaks were estimated using a tape measure at the time of the first visit.

3.3.4. Data analysis

a) Optical porosity estimation

Full height optical porosity of the windbreaks was determined from photographs using the method proposed by Kenney (1987). The full windbreak height defined according to Loeffler et al. (1992), is the distance from the ground to the top of the trees in the in the depicted windbreak segment, disregarding the fine, small branches at the top of the tallest trees, so as to remove the effects of large gaps due to variation in tree height in the upper part of the windbreaks. Optical porosity was estimated by converting image grids into white and black cells using ArcGIS 10.2. In this technique, optical porosity was determined as the ratio of white (empty spaces) to the total pixels of the converted black and white cells. This technique has been reported to estimate optical porosity with 2% error (Kenney, 1987). Up to five different photographs were used for porosity determination for each windbreak. Porosity was determined separately for each image, and then average values for each windbreak were computed. All photos from all windbreaks at each site were analysed in the same method.

b) Relative wind speed

The relative wind velocity was calculated for each wind logger for every 15 minute interval when wind direction was perpendicular within $\pm$ 22.5° to the windbreak in each site as shown in Table 3-6. The wind direction was considered perpendicular within $\pm$22.5° because this was the accuracy level of the instruments given by the manufacturer.

Table 3-6. Wind direction considered in the data analysis.

Wind direction	Site 1	Site 2
West – East		$270\pm22.5°$
East - West		$90\pm22.5°$
Northwest to Southeast	$315\pm22.5°$	
Southeast to Northwest	$135\pm22.5°$	

To calculate relative wind speed, the values recorded at each wind logger station were divided by the corresponding value of the farthest wind logger station (- 5 h), which was assumed to be beyond the influence of the windbreak in the windward direction. For instance, the relative wind speed value at 1200 hr for Site 1, Station 4, when wind was blowing west to east, was

obtained by the absolute value recorded at this time and station divided by the absolute value at Station 1 (- 27.5 m) at 1200 hr.

$$\text{Relative wind speed (\%)} = \frac{u}{u_0}(100)$$ (3-8)

Where,

- u is wind velocity at any wind logger station ; and
- u_0 is the approach wind speed in the zone unobstructed by windbreaks (- 5 h).

This approach to expressing the absolute values in terms of relative values reduces the impact of other factors that are beyond the influence of the windbreak (Kenney, 1987). The effective wind speed reduction can therefore be expressed in percentage as:

$$\text{Effective wind speed reduction} = 100\left(1 - \frac{u}{u_0}\right)$$ (3-9)

Relative wind speeds that were perpendicular to a windbreak within ± 22.5° were then sorted and averaged for each wind logger station for the study period. The velocity of the approaching airflow was not considered to affect the relative wind speed reduction behind a windbreak, except when very high wind speeds caused the porosity of the windbreak to change due to leaf and branch movement (Loeffler et al., 1992). All data for each site in the considered wind direction were plotted to produce wind reduction profiles which describe the effect of the wind on the ground to both the windward and the leeward side of the windbreaks. The plotted wind speed profiles were then used to calibrate a windbreak model for use in modelling as detailed in the next section.

3.4. Modelling the effects of windbreaks on the efficiency of sprinkler irrigation

3.4.1. Introduction

The modelling process for the effects of windbreaks on sprinkler irrigation was done in several steps, as shown in Figure 3-19. First, wind data were used to calibrate and validate wind equations in the Wind Erosion Prediction System (WEPS) model. Calibration was done by adjusting parameters in the wind equations to fit within the means first half of measured data. Secondly, validation was carried out by comparing results of calibrated windbreak models to the second half of the measured data. Percentage wind reduction factors were then determined at several distances from the windbreak for all the scenarios considered. Thirdly, using past climate data for the growing season July 1, 2010 to June 30, 2011 from Winchmore, Canterbury, average wind velocities were determined for all the scenarios at each site. Fourthly, assuming pasture crop, crop ET was determined for the entire growing season considered. In the fifth step, soil water balance simulation was done to schedule the net irrigation required for periods when rainfall was not adequate to meet the crop ET. In the sixth step, it was assumed that the net irrigation required was to be applied using a sprinkler irrigation machine fitted with nozzles considered in this study. Then SEL was determined using the SEL models developed for each nozzle, based on the corresponding weather conditions at the time of irrigation. Lastly, the gross irrigation requirement was calculated as sum of ET and net irrigation requirements (NIR). A t-test statistical analysis was the done to determine the significance of removal of windbreaks or reducing windbreak height to 2 m.
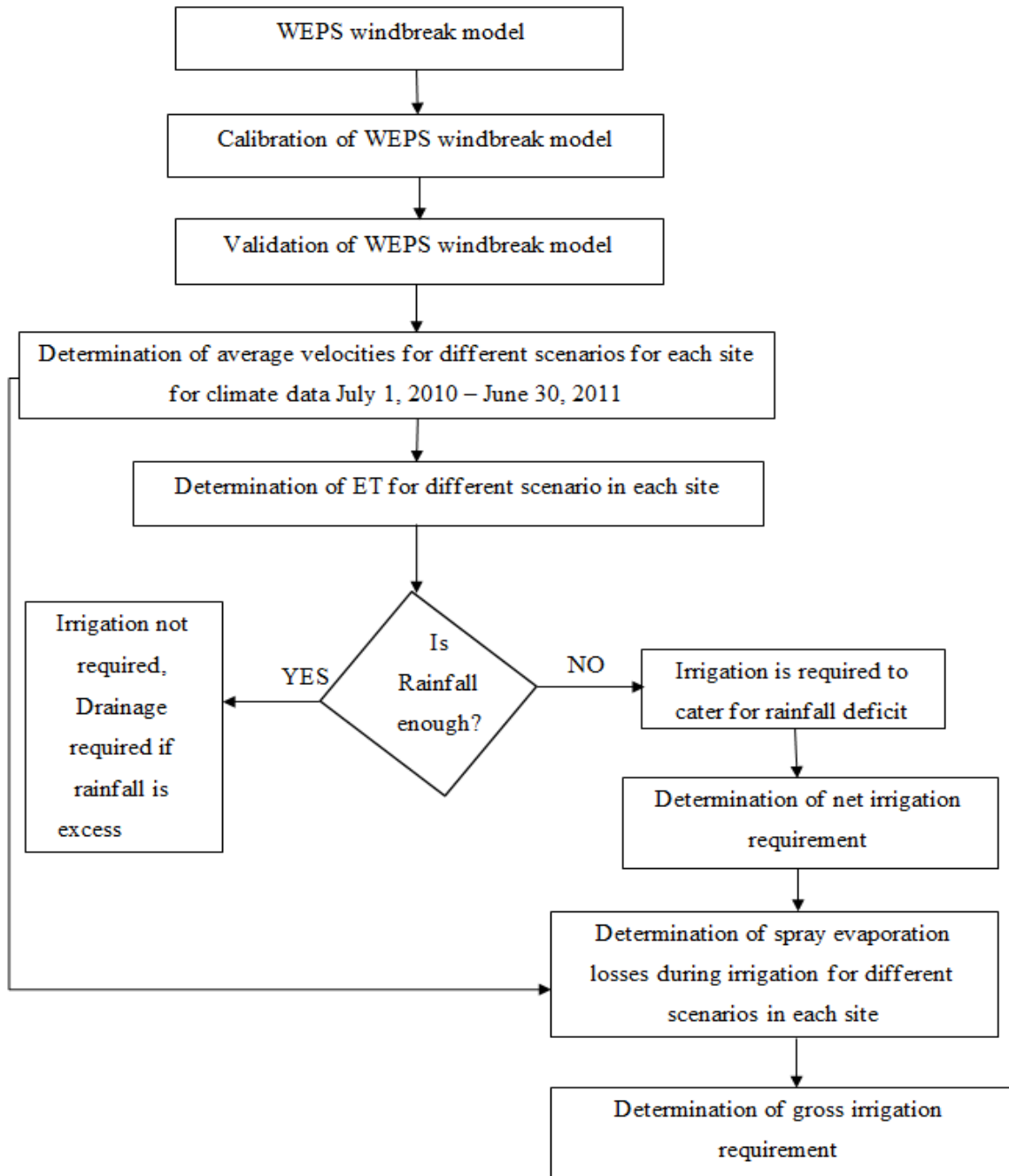
Figure 3-19. Representation of the modelling process of effects of windbreaks on sprinkler irrigation.

3.4.2. Description of the windbreak model

Vigiak et al. (2003) describe in detail the windbreak model as used by the Wind Erosion Prediction System (WEPS), a process-based wind erosion model. The model provides a set of equations which can calculate the reduction in wind velocity behind a single windbreak given a multitude of appropriate parameters. This model was calibrated, validated and used to calculate the reduction in wind speed across the fields.

$$f_{xh}=1-\exp\left[-a\mathrm{xh}^2\right]+b\ \exp\left[-0.003(\mathrm{xh}+c)^d\right] \qquad (3\text{-}10)$$

Where,

- f_{xh} = friction velocity reduction;
- xh = distance from the windbreak in terms of windbreak heights; and
- a, b, c and d are coefficients depending on windbreak porosity θ.

$$a = 0.008 - 0.17\theta + 0.17\theta^{1.05} \qquad (3\text{-}11)$$
$$b = 1.35\ \exp\left(-0.5\theta^{0.2}\right) \qquad (3\text{-}12)$$
$$c = 10(1-0.5\theta) \qquad (3\text{-}13)$$
$$d = 3-\theta \qquad (3\text{-}14)$$

Windbreak porosity is calculated from windbreak optical porosity (op), width (w), with average width measured perpendicular to the main axis of the barrier, and height (h).

$$\theta = \mathrm{op}+0.02\frac{\mathrm{w}}{\mathrm{h}} \qquad (3\text{-}15)$$

The friction velocity is related to the average wind speed through the following

$$u(z) = \frac{u^*}{k}\ln\frac{z}{z_o} \qquad (3\text{-}16)$$

Where,

- $u(z)$ = average wind speed;
- $u*$= wind friction velocity;
- k = von Kármán constant (0.4);
- z = height of instrument; and
- z_o = roughness height.

The friction velocity at a weather station can then be used to calculate the friction velocity on a field.

$$u_*^R = u_*^{WS} \left(\frac{z_o^R}{z_o^{WS}} \right)^{0.067} \tag{3-17}$$

Where,

- u_*^R = friction velocity at the field;
- u_*^{WS} = friction velocity at the weather station;
- z_o^R = roughness height at the field; and
- z_o^{WS} = roughness height at the weather station.

3.4.3. *Calibration and validation of the windbreak model*

Data obtained from the field were used for calibration and validation of the windbreak model in order to ensure that it was fit for the intended use. Measured data obtained from each site were then divided into two: the first half of the measured data were used for calibration while the second were used for validation. Besides calibration and validation, a statistical evaluation of the simulation results was made as described in the next subsections.

a) **Windbreak model calibration**

The windbreak model was calibrated by systematic adjustment of model parameters so that the model outputs accurately reflect the field measured data. Model calibration was performed with the first half of the measured data. This was achieved by adjusting the values of different

windbreak model parameters to bring the model-predicted relative wind speed within the range of the measured mean of the relative wind speed. Adjustment was done by varying the values of optical porosity first, followed by the other parameters; and then a combination of different parameters to obtain a good fit.

b) Windbreak validation

The windbreak model was validated by the calibrated model's prediction with the field measured data, in order to determine whether the model output could be trusted. Once the model was calibrated, it was run with the calibrated parameters, and wind speed reduction factors were predicted for all distances between windbreaks. The predicted values were validated by visual inspection of the graphs that plotted the range of the second half of measured relative wind speed and the predicted relative wind speed for same distances between the windbreaks.

c) Statistical performance evaluation

Statistical validations of the model were also evaluated after validation by visual inspection to identify the accuracy of the model. The first step was to compare the summary of statistics (mean and standard deviation) for observed and predicted data as proposed by Loague & Green (1991). The second statistical validation was done by use of test statistics to compare measured data against simulated results, using the relative root mean square error and model efficiency as proposed by Loague & Green (1991).

i. The Relative mean square error

The Relative Root Mean Square Error (RRMSE) provides a percentage measurement of the difference between the simulated data versus the observed data. The validation is considered to be excellent when the RRMSE is less than 10%, good if the RRMSE is between 10 and 20%, acceptable if the RRMSE is between 20 and 30%, and poor if it is greater than 30% (Jamieson et al., 1991). It was expressed as:

$$\text{RRMSE} = \sqrt{\frac{\sum_{i=1}^{n} (O_i - P_i)^2}{n}} \cdot \frac{100}{\overline{O}} \qquad (3\text{-}18)$$

Where,

- O_i and P_i are the observed and predicted values for the ith pair;
- n is the total number of paired values; and
- $\overline{O}$ is the mean of the observed values.

ii. The modelling efficiency

The modelling efficiency (ME) as defined by Nash & Sutcliffe (1970) was calculated as:

$$\text{ME} = 1 - \frac{\sum_{i=1}^{n}(O_i - P_i)^2}{\sum_{i=1}^{n}(O_i - \overline{O})^2} \qquad (3\text{-}19)$$

In this criterion, ME range from $-\infty$ and 1.0, with a value of 1.0 indicating a perfect model, and a value of zero indicating that the model results are not better than the mean measured value. A value less than zero indicate that the model predictions would be worse than using the mean. In general, model simulations can be judged satisfactory if the ME is greater than 0.50 (Legates & McCabe, 1999).

These two statistical tests (RRMSE and ME) have successfully been used in validation of the WEPS model for prediction of soil loss and PM_{10} (particulates $\leq$10 µm in aerodynamic equivalent diameter) loss from agricultural fields within the Columbia Plateau in the United States (Feng & Sharratt, 2007). After the models were successfully validated, they were used to model the effects of different windbreak characteristics on irrigation management using climate data from National Climate Database of New Zealand (NIWA, 2014).

3.4.4. Climate data

Climate data were obtained from the National Climate Database of New Zealand (NIWA, 2014). Winchmore Research Station was chosen as it is in the mid Canterbury Plains, which made it representative of expected conditions on the farms. Daily climatic measurements of temperature, vapour pressure, wind speed, direct solar radiation, rainfall, and sunshine hours were used for modelling for weather conditions in the period July 1, 2010 to June 30, 2011.

This period was chosen because it had continuous data available for direct use. The other reason for choosing this period was to ensure that the modelling begins during mid-winter in Canterbury which is usually around July, as will be explained in Section 3.4.7. It was assumed that the climatic conditions at both Winchmore Research stations and study sites were similar, and that there was no local variation of the climatic conditions between the two sites and the research station. The daily climatic data obtained were then used for modelling the effects of windbreaks on wind velocity, evapotranspiration, net irrigation requirement, spray evaporation losses and gross irrigation requirement, as explained in the next sections.

3.4.5. *Modelling the effects of windbreaks on wind velocity*

Wind velocity reduction models for each site have already been developed. These models were used to quantify the reduction in wind velocity for the two sites in line with the research objective. Three scenarios were modelled, firstly, leaving the windbreaks as they are and using a centre pivot system. Secondly, reducing the windbreaks height to 2 m to allow for centre pivot irrigation. The third scenario models the complete removal of windbreaks and irrigation with a centre pivot system. The average wind velocity for each scenario at each site was determined using climate data for the period July 1, 2010 to June 30, 2011 for Winchmore, Canterbury. For modelling purposes, it was assumed that each farm is completely bounded by the same windbreaks from all sides, so as to account for the influence of different wind directions on the windbreaks.

3.4.6. *Modelling the effects of windbreaks on evapotranspiration*

Evapotranspiration was calculated in order to estimate crop water requirements for each farm. The reference evapotranspiration (ET_0) was first calculated using the ASCE standardized Reference Evapotranspiration equation (Allen et al., 2005) in Equation (3-20). The actual crop ET was then derived from ET_0 by applying the proper crop and water stress coefficients. This equation is based on the ASCE Penman-Monteith and associated equations. The equation takes into account a variety of factors including parameters affected by windbreaks such as radiation, temperature and wind speed; and is considered to be the most appropriate model to

64

predict ET_0 (Zhang et al., 2010). Daily ET_0 rates were calculated at intervals of 4 m from the windbreak for each scenario and the average obtained for each field.

$$ET_{sz} = \frac{0.408\Delta(R_n - G) + \gamma\frac{C_n}{T + 273}u_2(e_s - e_a)}{\Delta + \gamma(1 + C_d u_2)} \tag{3-20}$$

Where,

- ET_{sz} = standardized reference crop ET (mm d^{-1});
- R_n = calculated net radiation at the crop surface (MJ m^{-2} d^{-1});
- G = soil heat flux density at the soil surface (MJ m^{-2} d^{-1});
- T = mean hourly air temperature at $1.5 - 2.5$ m height ($^{\circ}$C);
- u_2 = mean hourly wind speed at 2 m height (ms^{-1});
- e_s = saturation vapour pressure at 1.5 to 2.5 m height (kPa);
- e_a = mean actual vapour pressure at $1.5 - 2.5$ m (kPa);
- Δ = slope of the saturation vapour pressure-temperature curve (kPa $^{\circ}$C^{-1});
- γ = psychrometric constant (kPa $^{\circ}$C^{-1});
- C_n = numerator constant dependent on reference crop type and calculation time step (K mm s^3 Mg^{-1} d^{-1});
- C_d = denominator constant that changes with reference crop type and calculation time step (sm^{-1}); and
- Units for the 0.408 coefficient are m^2 mm MJ^{-1}.

The Equation (3-20) is valid for both short reference crop evapotranspiration (ET_{os}) and tall reference crop evapotranspiration (ET_{rs}) Values for C_n and C_d are given in Table 3-7. As the modelled crop is pasture (a short reference), ET_{os} was used in the calculations, and wind speed at 2 m height (u_2) was calculated from wind speed at 10 m (u_{10}) from the Equation (3-21), and (3-22) (Allen et al., 2005).

$$u_2 = u_z\frac{4.87}{\ln(67.8z_w - 5.42)} \tag{3-21}$$

Where,

- u_2 = wind speed measured at 2 m above ground surface (m/s);

- u_z = measured wind speed at z_w m above ground surface (m/s); and
- z_w = height of wind measurement above ground surface (m).

Table 3-7: Values for C_n and C_d in ET_{sz} equation

Calculation time step	Short reference, ET_{os}		Tall reference, ET_{rs}		Units for ET_{os}, ET_{rs}	Units for R_n, G
	C_n	C_d	C_n	C_d		
Daily	900	0.34	1600	0.38	mm d^{-1}	MJm^{-2}d^{-1}
Hourly during daytime	37	0.24	66	0.25	mm h^{-1}	MJm^{-2}h^{-1}
Hourly during night time	37	0.96	66	1.7	mm h^{-1}	MJm^{-2}h^{-1}

Source: (Allen et al., 2005).

The computation of all components required for calculating daily ET_0 followed the procedures as set out by Allen et al. (2005). These components, together with ET_0 were calculated in a Microsoft Excel spreadsheet. The accuracy of the spreadsheet was checked by inputting values given, for which the corresponding resultant ET_0 values were also provided. The crop assumed for this study was the permanent grass pasture, which was assumed to have 100% ground cover over the entire growing season. Hence actual ET is equal to ET_0, since the crop factor is equal to one.

3.4.7. *Modelling the effects of windbreaks on irrigation requirements*

Daily soil water balance simulation was done for the entire growing season to determine whether the rainfall was adequate to provide for the crop's ET, and if irrigation was needed. When rainfall was not enough to cater for the crop's ET (such as during summer months), irrigation was scheduled to start when 50% of the total available moisture was depleted so as to return the soil moisture to field capacity. Net irrigation requirement and the spray evaporation losses associated with irrigation for each scenario were determined.

Net irrigation requirement

NIR was determined to estimate the amount of water needed to be supplied through irrigation so as to ensure the crops reached optimal crop yield. The NIR was determined using a

hydrological model by considering the balance between all relevant water fluxes in and out of the cropping system and ignoring the efficiency factors for irrigation systems. In this study, the Water Simulation Model (WaSim) was used to calculate daily irrigation water requirements for different modelling scenarios over the growing season in each site. Many benefits of this model have been cited (Fasinmirin et al., 2008), among which are; (1) ease of operation; (2) minimal data requirements; (3) good visualization of model calculations; and (4) reasonable level of accuracy and flexibility in terms of water management situations that can be simulated.

Description of the WaSim model

HR Wallingford and Cranfield University, UK jointly developed the Water Simulation model, (WaSim) (Hess & Counsell, 2000). WaSim is a one-dimensional, daily, soil water balance model that stimulates the soil water storage and rates of input (infiltration) and output (ET, run-off and drainage) of water in response to weather. Its value in hydrological research has been demonstrated in several applications including estimation of irrigation requirements (Hess, 2010), runoff estimation (Hess, 2010), drainage performance (Hirekhan et al., 2007) and groundwater recharge potential (Holman et al., 2009). It requires daily reference evapotranspiration and rainfall data. Full details of the modelling approach are given in Hess & Counsell (2000).

   a) Model inputs

The model requires specification of inputs of weather data, soil parameters, crop parameter, and model constants, which are described below.

   i.   Climate data

Climate variables used in the calculation of NIR are the average daily reference ET computed using Equation (3-20) and daily rainfall data obtained from the National Climate Database of New Zealand (NIWA) for the period July 1, 2010 to June 30, 2011. Climate data was imported from MS Excel files and screened for missing values. The climate data were then tabulated and saved as a WaSim climate file.

ii. Soil data

In irrigation management, the soil's capacity to store water must be known. Irrigation or rainfall raises the soil's water content to field capacity; water is slowly depleted by evapotranspiration, drainage or deep percolation. Water application in excess of the reservoir capacity is wasted unless it is used for leaching. Irrigation is usually scheduled to prevent the soil water reservoir from becoming so low as to cause plant stress.

The predominant soil type for the two study sites is sandy loam according to New Zealand soil maps and the soil profile is fairly uniform (Landcare Research, 2014).The default soil characteristics for sandy loam in the model where checked against the soil physical properties of normal soils provided by Saxton & Rawls (2006), and adjusted where appropriate. Table 3-8 shows the model input soil data.

Table 3-8. **Soil input data for the two study sites in the Canterbury region.**

Soil data	All sites
Soil type	Sandy loam
Saturation (%)	39%
Field capacity (%)	16%
Permanent wilting point (%)	8.0%
Drainage coefficient (mm/day)	0.37
Hydraulic conductivity (m/day)	1.2
Leaching efficiency (%)	90%
Curve number for run off calculation	61

iii. Drainage data

Free drainage conditions were assumed and the only loss of water from the soil profile is by evapotranspiration. Since there was no ground water pumping, extraction from the ground water was taken as zero.

iv. Crop data

The main purpose of irrigation in the Canterbury region is to irrigate pasture grass for dairy farming. For a permanent grass surface, it was assumed to have 100% ground cover over the entire growing season, so that ET is estimated from:

$$ET_c = K_C ET_{os} \qquad (3\text{-}22)$$

Where,

- K_c = crop factor and
- ET_c = the actual crop evapotranspiration.

Input parameters describing crop data are given in Table 3-9.

Table 3-9. Parameters describing the crop input data for the model.

Crop specifics	Pasture grass
Planting date*	Day 1
Emergence date*	Day 1
20% cover*	Day 1
Full cover*	Day 1
Maturity (days)	365
Harvest (days)	365
Maximum root date*	Day 1
Maximum cover (%)	100%
Planting depth (m)	0.70
Maximum root depth (m)	0.70
Salinity threshold (dS/m)	1.70

*These parameters are set to Day 1 which coincides with the first day of running the model because it is assumed that the pasture crop is already established.

v. *Irrigation data*

Irrigation was scheduled to start when soil moisture was not adequate to cater for crop ET during the dry months of the year and to supplement rainfall during winter. The data related to the volume and time schedule of irrigation is shown in Table 3-10. The start date was selected by design as July 1, 2010 because it is the period of mid-winter when no irrigation is required and the soil can fairly be assumed to be at field capacity at the start of the growing period. Daily average NIR for one growing year was calculated for the period from July 1, 2010 to June 30, 2011.

Table 3-10. **Irrigation data for the two sites.**

General Parameters	Pasture grass
Crop duration	365 days
Water content at start	Field capacity
Timing of irrigation	Irrigate when 50% of total available moisture is depleted
Amount to irrigate	Return irrigation to 0% depletion of total available moisture
Salinity of irrigation water (dS/m)	0.00

The model works by calculating a daily soil water balance and scheduling an irrigation event when pre-defined soil water status criterion is met. As seen from the Table 3-10 above, the criterion chosen for this study is when 50% of the total available water has been depleted. This is the point at which pasture grass starts to suffer water stress (Jensen et al., 1990), and the irrigation amount is set to bring the soil back to field capacity by returning irrigation to 0% depletion of total available water.

b) Model outputs

The model was then run for each scenario for 365 days from July 1, 2010 to June 30, 2011 with the input parameters described above. The model simulations performed soil water balance using a daily time step to give an output including daily values of crop root depth, crop cover, rainfall, runoff, actual ET, net irrigation requirement, irrigation schedules and root zone deficit. The most relevant outputs for this study were the net irrigation requirement and the irrigation schedules, which were used in the calculation of spray evaporation loss and hence the gross irrigation requirement.

3.4.8. Modelling the effects of windbreaks on spray evaporation losses

Knowledge of spray evaporation losses is important because it gives the quantity of the water that is lost due to the atmosphere and hence unavailable for the crop. As a result, the extra water must be pumped from the source to cater for the SEL is known. The net irrigation requirement calculated above was assumed to be supplied using centre pivot machines fitted with Rotator R3000 or Spinner S3000 nozzles as described earlier in this study. For every

irrigation event, SEL was calculated using the developed SEL prediction models based on the prevailing weather condition for that day.

3.4.9. Modelling the effects of windbreaks on gross irrigation requirement

The gross irrigation requirement was calculated for the entire growing season in order to estimate the total amount of water required for the entire growing season. This amount is the summation of the SEL and NIR. It was calculated as:

$$\text{GIR} = \frac{\text{NIR}}{1 - \text{SEL}} \qquad (3\text{-}23)$$

Where,

- GIR = gross irrigation requirement;
- NIR = net irrigation requirement; and
- SEL = spray evaporation (%).

3.4.10. Statistical comparison of scenarios

It was necessary to determine whether there was significant effect on wind velocity, ET, SEL and irrigation requirements when windbreaks are reduced to 2 m or when they are completely removed. Similarly, the effect of different windbreaks on wind velocity, ET, SEL and irrigation requirements were determined. To do this, a paired-samples t-test was conducted to compare if the differences between scenarios was significant at $p = 0.05$.

CHAPTER 4: RESULTS

4.1. Introduction

The results of the research are presented in three major parts, as follows:

1) Analysis of the results from the spray evaporation experiments are presented in Section 4.2. The spray evaporation loss prediction models developed from the spray evaporation loss experiment data are presented. The differences between the models developed in this study and previous models developed using a similar approach are presented. The best fit models in this section are used in Section 4.4 to model the effects of windbreaks on spray evaporation loss;

2) The reduction of wind speed by windbreaks located at the two experimental sites is presented in Section 4.3. Relative wind speed is plotted against horizontal distance to produce a wind reduction profile for each site. The relative wind speed from wind reduction profiles are used to calibrate and validate a windbreak model in Section 4.4;

3) Section 4.4 presents the results of modelling the effects of windbreaks on irrigation efficiency. Windbreak model calibration and validation are presented. Results from the simulation of windbreak scenarios are presented with respect to wind velocity, evapotranspiration, net irrigation requirements, spray evaporation loss and gross irrigation requirement.

Interpretation and discussion of the results detailed in this chapter are presented in Chapter 5, alongside their relevance to sprinkler irrigation practice.

4.2. Spray evaporation loss experiments

A total of 74 spray evaporation loss tests were conducted during the months of February to May and October, 2014, under various climatic conditions and using two different sprinkler nozzle types: Rotator R3000 sprinkler nozzle was used for 40 tests (Experiment A) and the Spinner S3000 sprinkler nozzle was used for 34 tests (Experiment B). Spray evaporation losses were expressed as the ratio of the electrical conductivity values of water in the catch can devices to those in the supply water. It was assumed that all salt remains in the droplets during the evaporation process. SEL values for each experiment were related to the climatic conditions observed during the experiments, and spray evaporation loss prediction models were developed for each experiment. The SEL prediction models developed were then used to model the effect of different windbreak characteristics on spray evaporation losses, and hence to model irrigation requirements.

4.2.1. Average results of spray evaporation losses

Spray evaporation losses varied from one catch can to another within the irrigated area. In compiling the results, the average SEL from individual catch cans within the irrigated area is reported in each test, together with the average climatic conditions during the test. The spray evaporation losses in Experiment A ranged from 1.8% to 32.0% under the climatic conditions shown in Table 4-1, while the spray evaporation losses in Experiment B ranged from 1.7% to 43.1% under the climatic conditions shown in Table 4-3. The average SEL are given in Table 4-2 and Table 4-4 for Experiment A and Experiment B, respectively.

Table 4-1. Ranges of climatic conditions in Experiment A.

	Maximum	Average	Minimum
Air temperature (^{0}C)	27.8	21	11.9
Wind velocity (m/s)	7.6	3.8	0.1
Relative humidity (%)	77	48.7	25
Solar radiation (MJ/m^2)	635	298	46
Vapour pressure deficit (mbar)	28	13.9	3.4

Table 4-2. Summary of all spray evaporation loss tests conducted under various climatic conditions using Rotator R3000 nozzle (Experiment A) operated at a pressure of 1 bar.

Test No.	Mean air Temperature (T_a) (^0C)	Relative humidity (RH) $(\%)$	Vapour pressure deficit $(e_a - e_s)$ $(mbar)$	Solar radiation (I) MJ/m^2	Mean wind velocity (u) (m/s)	Spray evaporation loss (SEL) $(\%)$
1	13.9	70.8	4.6	330	0.6	2.2
2	14.3	66.5	5.5	400	0.1	1.8
3	20.0	45.3	12.8	389	0.7	2.9
4	20.6	58.0	10.2	206	1.5	4.0
5	22.6	35.9	17.6	415	2.6	4.2
6	17.9	52.0	9.8	108	2.7	3.8
7	17.4	55.1	8.9	67	2.3	3.8
8	11.9	69.6	4.2	310	2.4	3.0
9	15.7	61.4	6.9	379	0.4	3.5
10	25.4	45.6	17.7	204	3.2	7.8
11	21.0	33.2	16.6	55	6.7	13.6
12	24.0	48.0	15.5	560	7.6	32.0
13	26.8	32.0	24.0	244	5.3	19.3
14	24.3	44.3	16.9	138	3.0	11.3
15	25.5	42.3	18.8	278	4.8	12.6
16	18.5	29.0	15.1	635	4.5	14.5
17	27.1	33.2	24.0	332	7.2	30.4
18	26.3	30.7	23.7	342	6.5	29.5
19	24.3	35.5	19.6	236	5.8	14.9
20	19.0	55.4	9.8	46	2.1	3.7
21	15.6	48.0	9.2	257	1.1	5.2
22	21.3	44.6	14.1	277	1.3	4.0
23	21.0	45.7	13.5	259	2.2	4.4
24	23.4	44.4	16.0	250	4.0	12.5
25	17.9	58.1	8.6	310	4.3	11.3
26	12.4	63.3	5.3	263	0.2	4.6
27	12.6	75.5	3.6	323	1.4	2.8
28	12.9	77.0	3.4	280	1.3	2.0
29	15.2	66.3	5.8	134	5.3	7.0
30	26.5	34.7	22.6	326	5.3	19.1
31	27.6	43.5	20.9	400	7.2	24.9
32	25.0	43.2	18.0	378	4.2	24.6
33	24.0	64.0	10.7	450	3.2	10.0
34	25.8	56.3	14.5	534	6.1	12.4
35	26.7	45.0	19.3	346	6.4	28.3

Test No.	Mean air Temperature (T_a) (^0C)	Relative humidity (RH) (%)	Vapour pressure deficit (e_a- e_s) (mbar)	Solar radiation (I) MJ/m^2	Mean wind velocity (u) (m/s)	Spray evaporation loss (SEL) (%)
36	27.8	25.0	28.0	227	6.6	31.3
37	19.0	56.3	9.6	235	4.6	12.8
38	22.1	34.7	17.4	351	4.3	13.6
39	21.0	44.4	13.8	332	5.7	10.1
40	23.7	35.0	19.0	343	6.2	13.7

Table 4-3. Ranges of climatic conditions in Experiment B.

	Maximum	Average	Minimum
Air temperature (^0C)	28.1	20.5	13.5
Wind velocity (m/s)	7.8	3.2	0.2
Relative humidity (%)	77.8	49.4	13.3
Solar radiation (MJ/m^2)	655	326	71
Vapour pressure deficit (mbar)	28.3	13.2	4.8

Table 4-4. Summary of all spray evaporation loss tests conducted under various climatic conditions using Spinner S3000 nozzle (Experiment B) operated at a pressure of 1 bar.

Test No	Mean air temperature (T_a) (^0C)	Relative humidity (RH) (%)	Vapour pressure deficit $(e_a - e_s)$ (mbar)	Solar radiation (I) MJ/m^2	Mean wind velocity (u) (m/s)	Spray evaporation loss (SEL) (%)
1	18.9	77.8	4.8	348	1.4	2.9
2	21.6	45.5	14.0	476	0.4	1.7
3	19.1	51.2	10.8	71	0.3	3.5
4	18.1	65.8	7.1	432	1.2	5.9
5	16.3	74.0	4.8	138	0.8	6.3
6	21.8	37.0	16.5	274	2.7	7.5
7	20.6	35.8	15.6	170	1.9	7.2
8	15.0	65.3	5.9	211	0.3	2.3
9	25.1	44.3	17.7	468	5.6	26.6
10	28.1	25.6	28.3	655	4.7	23.4
11	27.0	42.5	20.4	437	4.2	20.8
12	13.9	13.3	13.7	492	3.8	9.5
13	18.8	65.9	7.4	228	3.3	8.4
14	19.2	64.8	7.8	328	4.0	8.8
15	16.1	73.8	4.8	119	3.3	8.3
16	16.5	56.4	8.2	228	2.8	5.9
17	22.9	35.4	18.0	328	4.6	14.9
18	21.9	35.2	17.0	303	3.3	11.6
19	22.5	37.5	17.0	303	6.6	13.6
20	21.5	37.8	15.9	291	6.0	12.8
21	21.9	37.9	16.3	162	5.3	11.4
22	19.3	45.8	12.1	351	0.2	2.8
23	13.8	63.6	5.8	374	1.0	3.4
24	13.5	68.6	4.9	249	0.9	2.8
25	15.2	70.6	5.1	358	1.2	3.5
26	15.4	71.7	5.0	264	0.9	2.5
27	20.5	46.8	12.9	165	1.6	4.0
28	21.3	41.3	14.9	209	2.3	8.1
29	20.9	69.3	7.6	491	1.5	3.9
30	22.2	38.4	16.5	327	7.3	34.7
31	26.0	39.1	20.4	213	7.6	31.4
32	27.4	26.7	26.8	534	7.8	43.1
33	27.2	29.4	25.5	564	5.3	25.7
34	27.3	45.3	19.8	532	3.8	20.6

4.2.2. *The effect of distance from sprinkler on spray evaporation loss*

The effect of distance from the sprinkler nozzle on SEL within the irrigated area was determined. Results showed that SEL in individual catch cans within the irrigated area increased with an increase in distance from the sprinkler. To illustrate the variation of evaporation losses with distance, selected results for different wind conditions are given in Figure 4-1 and Figure 4-2. At very high wind speeds, the results show that SEL increase in the direction of the wind.
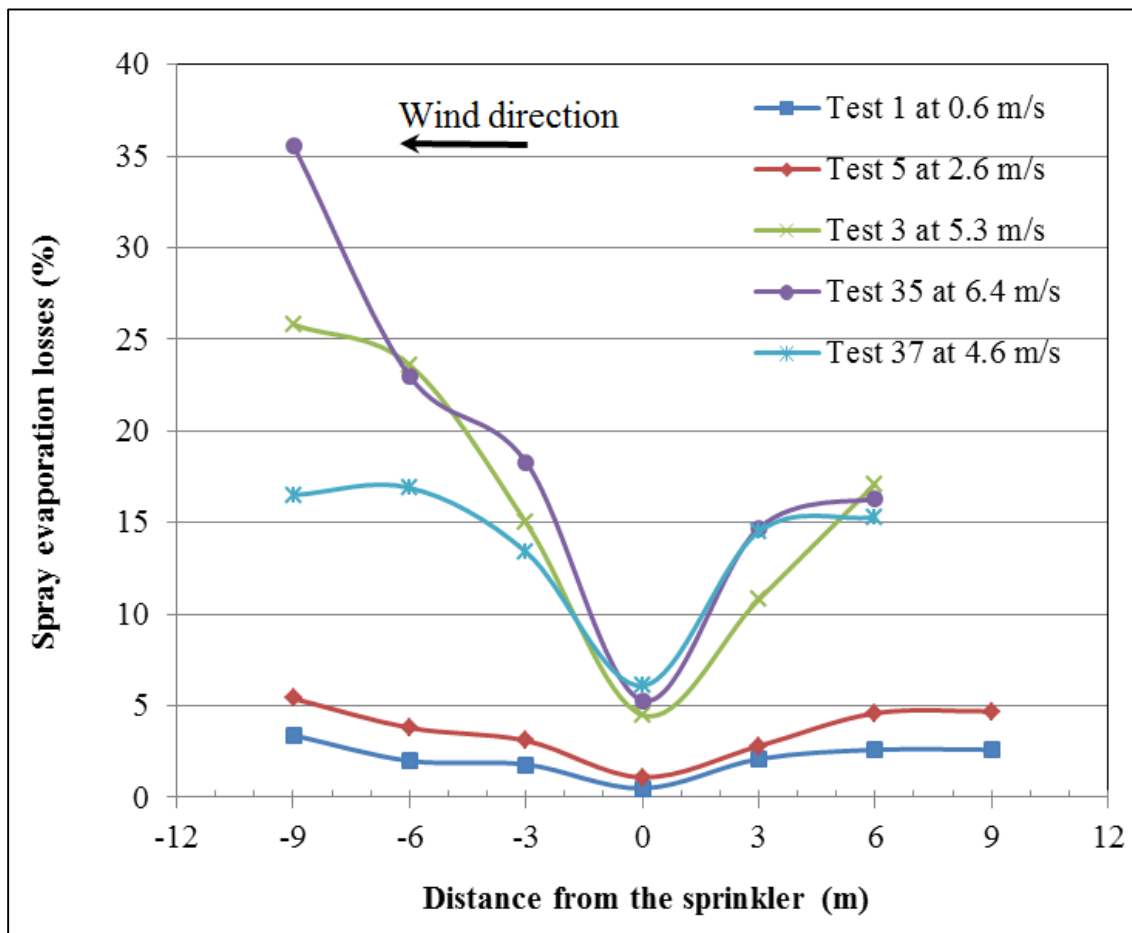
Figure 4-1. Variation of spray evaporation losses in the wind direction with distance under different east – west wind velocities using the Rotator R3000 nozzle.
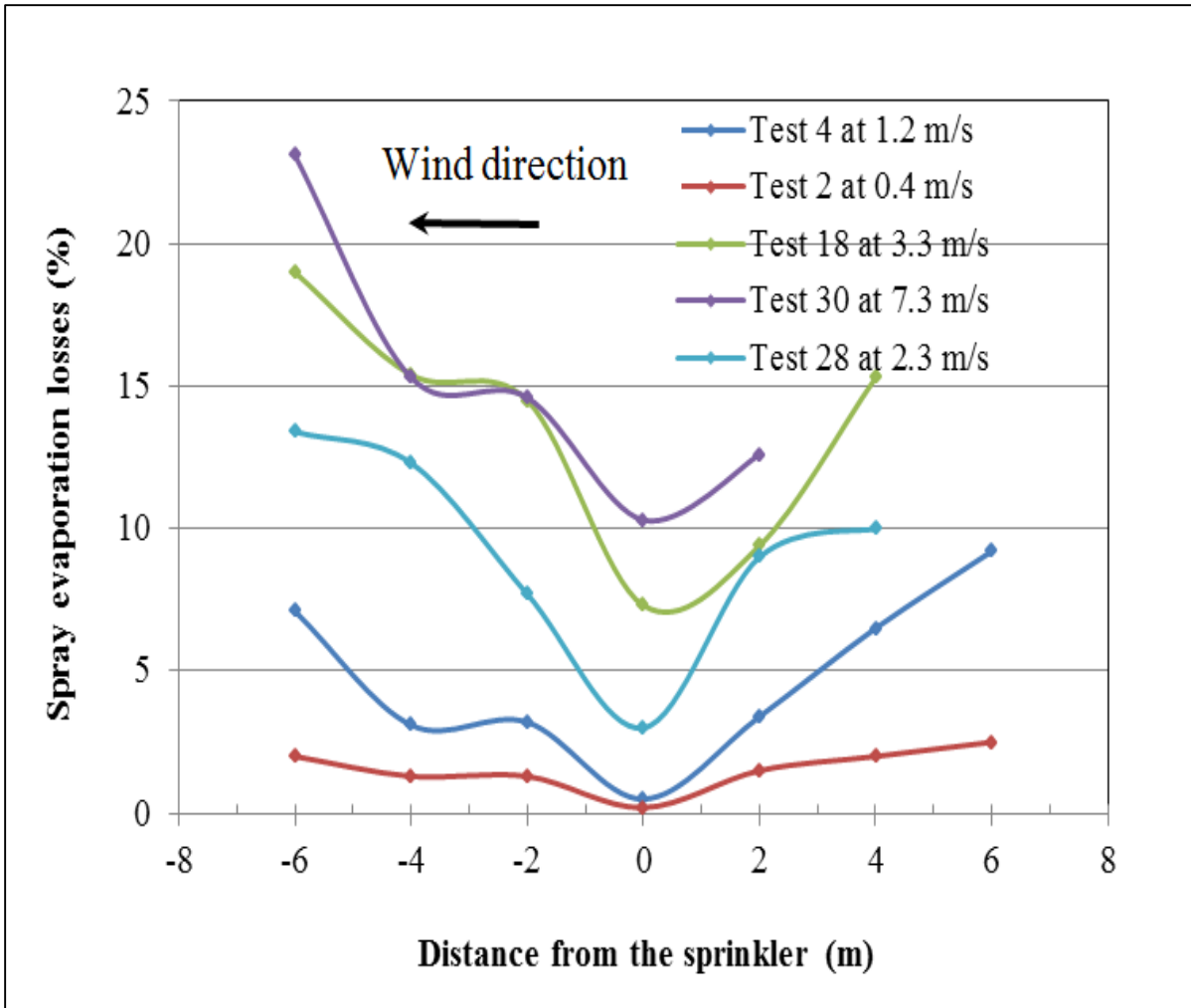
Figure 4-2. Variation of spray evaporation losses in the wind direction with distance under different east – west wind velocities using the Spinner S3000 nozzle.

4.2.3. *Droplet size distribution*

In order to understand the difference between the SEL associated with each sprinkler nozzle, droplet size distribution was quantified. The results of the droplet size distribution tests of irrigation sprays for both sprinkler nozzles, operated at a height of 2 m and a pressure of one bar are shown in Table 4-5. The Rotator R3000 and the Spinner S3000 nozzle atomized water into drops that ranged from 0.4 mm to 6.0 mm and 0.4 mm to 3.5 mm in diameter (Table 4-5), respectively. The larger droplet sizes project the farthest distance, but the Spinner S3000 nozzle is incapable of throwing water past a 6 m radius from the sprinkler. From Table 4-5, it

can be seen that for both the Rotator and the Spinner nozzles, the standard deviation at each point increases with distance from the sprinkler. From Figure 4-3, it can be seen that the mean droplet diameter is higher for the Rotator R3000 than for the Spinner S3000 at corresponding distances from the sprinkler nozzle. It is also apparent that the percent of total drops with small mean droplet sizes is higher under the Spinner S3000 than the Rotator R3000 model.

Table 4-5. The range and mean water droplet sizes (mm) for both sprinkler nozzles operated at a pressure of one bar.

| Distance to sprinkler nozzle (m) | Rotator R3000 nozzle | | | Spinner S3000 nozzle | | |
| | Nozzle diameter = 5.56 mm | | | Nozzle size = 3.57 mm | | |
	Range (mm)	Mean (mm)	σ (mm)	Range (mm)	Mean (mm)	σ (mm)
1	0.4 – 1.1	0.61	0.29	0.4 – 1.1	0.63	0.28
2	0.4 – 2.0	0.79	0.47	0.4 – 1.8	0.85	0.45
3	0.4 – 3.0	1.25	0.79	0.4 – 2.5	1.25	0.66
4	0.4 – 3.0	1.42	0.86	0.4 – 3.0	1.26	0.81
5	0.4 – 4.0	1.83	1.2	0.4 – 4	1.45	1.15
6	0.4 – 6.0	2.27	1.62	0.5 – 3.5	2.1	1.20
7	0.4 – 8.0	2.45	2.03			
8	0.4 – 6.0	3.01	2.4			
9	0.4 – 6.0	3.13	1.63			

σ = standard deviation
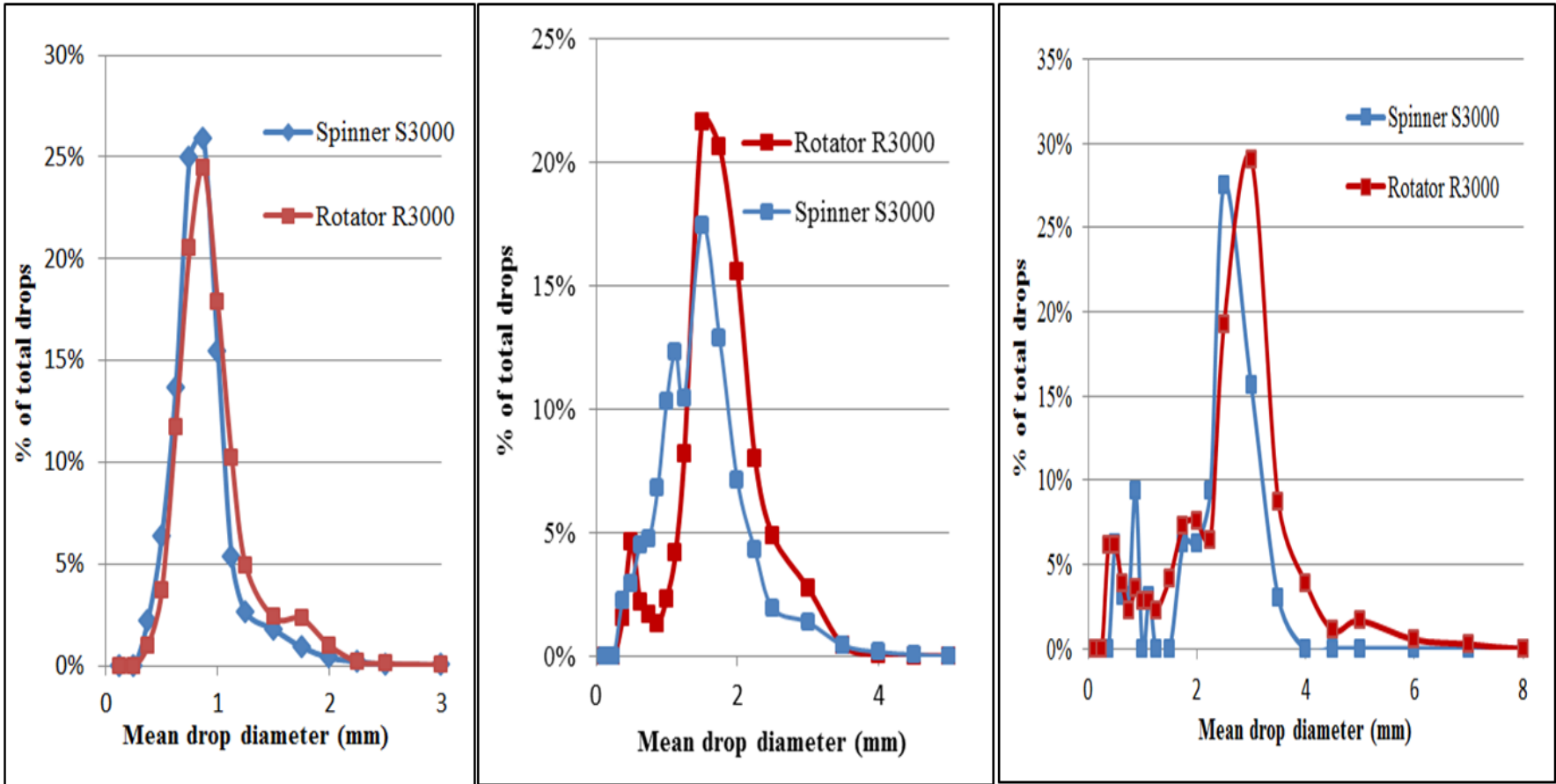
(a) Droplet size distribution at 2m   (b) Droplet size distribution at 4 m   (c) Droplet size distribution at 6 m

Figure 4-3. Comparison of droplet size distributions for the Spinner S3000 and the Rotator R3000 at the same selected distances from the sprinkler nozzle.

4.2.4. *Spray loss evaporation model development*

The results obtained from the tests were used to develop regression models relating evaporation losses as a function of different evaporation controlling variables by multiple regression analysis approach. Two forms of models were developed: in the first form, the evaporation loss was expressed as a function of relative humidity, solar radiation, air temperature and wind speed; in the second form evaporation was expressed as a function of wind speed, solar radiation and vapour pressure deficit. Vapour pressure deficit is derived from air temperature and relative humidity. The two forms of the models were then compared. Operating pressure and rate of water application remained constant throughout the experiment for each test; therefore, they were not included as variables.

a) Model development using air temperature, relative humidity, wind speed and solar radiation

Using air temperature, radiation, wind, and relative humidity, a general linear regression model was first obtained for each sprinkler nozzle as show in Equations (4-1) and (4-2) below.

For the Rotator R3000

$$SEL = 0.701u^{0.418} \ I^{0.262} \ T_a^{0.976} \ RH^{-0.605} \tag{4-1}$$

$$R^2 = 0.766$$

For the Spinner S3000

$$SEL = 0.526u^{0.578} \ I^{-0.088} \ T_a^{1.30} \ RH^{-0.292} \tag{4-2}$$

$$R^2 = 0.837$$

Where,

- u = wind velocity (m/s);
- I = solar radiation (MJ/m^2);
- T_a = Air temperature (^{0}C); and

- RH = relative humidity (%).

Backward elimination of variables was then carried out to test whether the removal of each variable improved the model using the R^2 criterion. The results from elimination of variables showed that the model improved when the radiation variable was omitted. When the radiation factor is omitted, then general prediction equations were obtained as shown in Equations (4-3) and (4-4) below.

For the Rotator R 3000

$$SEL = 1.679u^{0.386}\ T_a^{1.155}\ RH^{-0.584} \qquad (4\text{-}3)$$

$$R^2 = 0.710$$

For the Spinner S3000

$$SEL = 0.334u^{0.574}\ T_a^{1.256}\ RH^{-0.268} \qquad (4\text{-}4)$$

$$R^2 = 0.840$$

A summary of the resulting R^2 values of models when each variable was removed are in Appendix B in Table B-2.

Considering only wind velocity, air temperature and relative humidity in the analysis, the best fit models for both sprinklers were obtained. Wind was expressed in the form e^x while other variables were expressed in the form x^y, where y is an empirical coefficient to be determined. The best fit spray evaporation loss models obtained as a function of wind speed, air temperature and relative humidity are given by Equations (4-5) and (4-6) below.

For the Rotator R3000

$$SEL = 1.027 \exp(0.253\ u)\ T_a^{0.825}\ RH^{-0.345} \qquad (4\text{-}5)$$

$$R^2 = 0.856$$

For the Spinner S3000

$$\text{SEL} = 0.378 \exp(0.286\ u)\ T_a^{0.911}\ \text{RH}^{-0.149} \tag{4-6}$$

$$R^2 = 0.860$$

b) Model development using vapour pressure, solar radiation and wind speed

A general SEL prediction equation for each experiment was obtained using multiple regression analysis and expressed as given in Equations (4-7) and (4-8).

For the Rotator R 3000

$$\text{SEL} = 0.217u^{0.429}\ I^{0.273}\ (e_a - e_s)^{0.683} \tag{4-7}$$

$$R^2 = 0.779$$

For the Spinner S3000

$$\text{SEL} = 1.796u^{0.606}\ I^{-0.051}\ (e_a - e_s)^{0.542} \tag{4-8}$$

$$R^2 = 0.832$$

Then backward elimination of variables was done to check whether the removal of each of the variables improved the model by the R^2 criterion. The results from elimination of variables showed that the model improved when the radiation variable was omitted. When the radiation variable was omitted, the best fit models were those given by Equations (4-9) and (4-10).

For the Rotator R3000

$$\text{SEL} = 0.889u^{0.404}\ (e_a - e_s)^{0.741} \tag{4-9}$$

$$R^2 = 0.751$$

For the Spinner S3000

$$\text{SEL} = 1.390u^{0.603}\ (e_a - e_s)^{0.530} \tag{4-10}$$

$$R^2 = 0.837$$

A summary of the resulting R^2 values of various models when each variable was removed are in Appendix B in Table B-3.

In each of the cases above, each of the independent variables (x) was considered in the following mathematical forms: x, e^x and x^y, where y is an empirical coefficient to be determined (Playán et al., 2005). A non–linear multiple regression analysis was used when wind velocity and vapour pressure deficit were to be included alone in the analysis, due to their narrow range of variables (Bavi et al., 2009; Yazar, 1984). Considering only wind velocity and vapour pressure deficit in the analysis, the best fit SEL models are given by the equations below.

For the Rotator R3000

$$SEL = 0.907 \exp(0.256u)(e_a\text{-}e_s)^{0.508} \tag{4-11}$$
$$R^2 = 0.863$$

For the Spinner S3000

$$SEL = 1.417 \exp(0.299u)(e_a\text{-}e_s)^{0.327} \tag{4-12}$$
$$R^2 = 0.854$$

Where,

$(e_a - e_s)$ = the vapour pressure deficit in mbar.

Examinations of residuals were done to confirm that the residuals were evenly distributed for the best fit models. Other models with different forms of variables which were considered are presented in Appendix B in Table B-3.

In summary, two forms of models for sprinkler nozzles were developed: one form expresses SEL as a function of air temperature, wind velocity and relative humidity; while the second form expresses SEL as function of vapour pressure deficit and wind velocity only. Using air temperature, wind velocity and relative humidity, the best fit models are given by Equation (4-5) and (4-6) for the Rotator R3000 and the Spinner S3000, respectively; while Equations

(4-11) and (4-12) are the best fit models for the Rotator R3000 and the Spinner S3000 respectively; which express SEL as function of vapour pressure deficit and wind velocity. In the next section, the two models are compared in order to select the most appropriate one for each nozzle which can be used to model SEL under given conditions.

4.2.5. *Comparison of different forms of models*

The two forms of best fit models developed for each sprinkler nozzle in Section 4.2.4 were compared to check their accuracy of prediction and the best fit model was selected based on three statistical indices as the criteria: R^2, the Nash &Sutcliffe (1970) modelling efficiency (ME), and relative root mean square error (RRMSE). The results of the statistical indices are shown in Table 4-6.

Table 4-6. Statistical indices R^2, ME and RRMSE used for selection of best model.

Model	Statistic index		
	R^2	ME	RRMSE (%)
Experiment A – the Rotator R3000 models			
Equation (4-5)	0.86	0.83	10.8
Equation (4-11)	0.86	0.83	11.0
Experiment B – the Spinner S3000 models			
Equation (4-6)	0.86	0.87	11.1
Equation (4-12)	0.85	0.84	12.1

Using statistical indices above, the difference between the two forms of the models is very small. Under the R^2 criterion, both forms of the models are nearly the same and give an almost perfect fit. The ME for both forms of the models is above 0.50, indicating that the predictions from both forms of the models are satisfactory (Legates & McCabe, 1999). The RRMSE for both forms of the models range between 10% and 20%, hence both forms of the models can be considered to be good (Jamieson et al., 1991). These results show that predictions using relative humidity, wind velocity and air temperature are nearly the same as predictions using wind velocity and vapour pressure deficit. Different magnitudes of observed SEL from various tests in both experiments were also compared with predictions from the different forms of models developed. The results are shown in Table 4-7 and Table 4-8. In terms of accuracy, there appears to be no preference of one form over the other.

Table 4-7. Comparison of different forms of models in Experiment A.

Test number	Observed SEL (%)	Predicted SEL (%)	
		Equation (4-5)	Equation (4-11)
4	4.0	4.3	4.5
10	7.8	8.9	8.9
12	32.0	25.5	25.4
16	14.5	11.4	11.1
31	24.9	26.8	26.7
35	28.3	21.0	26.7

Table 4-8. Comparison of different forms of models in Experiment B.

Test number	Observed SEL (%)	Predicted SEL (%)	
		Equation (4-6)	Equation (4-12)
4	5.9	3.9	4.0
17	14.9	14.4	14.3
22	13.6	25.7	24.8
32	43.1	42.8	44.0
33	25.7	19.9	19.9

4.2.6. Relationship between spray evaporation losses and climatic variables

The relationship between different climatic variables and SEL was evaluated to determine SEL related to changes in the variables. This information is important because it provides knowledge of the most significant variables if SEL is to be lowered.

Wind velocity

The relationship between spray evaporation losses and wind velocity is shown in Figure 4-4. The analyses of the results of both experiments show a strong exponential relationship between spray evaporation losses and wind velocity.
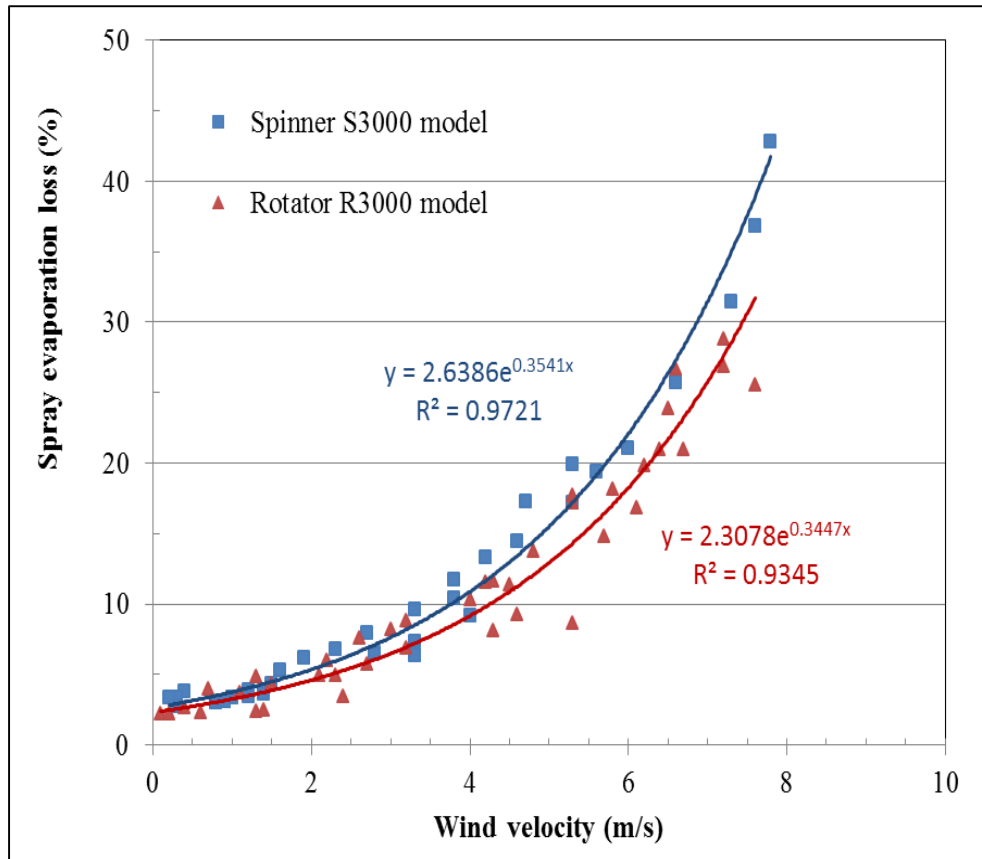
Figure 4-4. The relationship between spray evaporation losses and wind velocity.

Relative humidity

The relationship between spray evaporation losses and relative humidity is shown in Figure 4-5. The relationship between spray evaporation loss and relative humidity shows a poor correlation. However, an increase in relative humidity leads to reduction in spray evaporation loss.
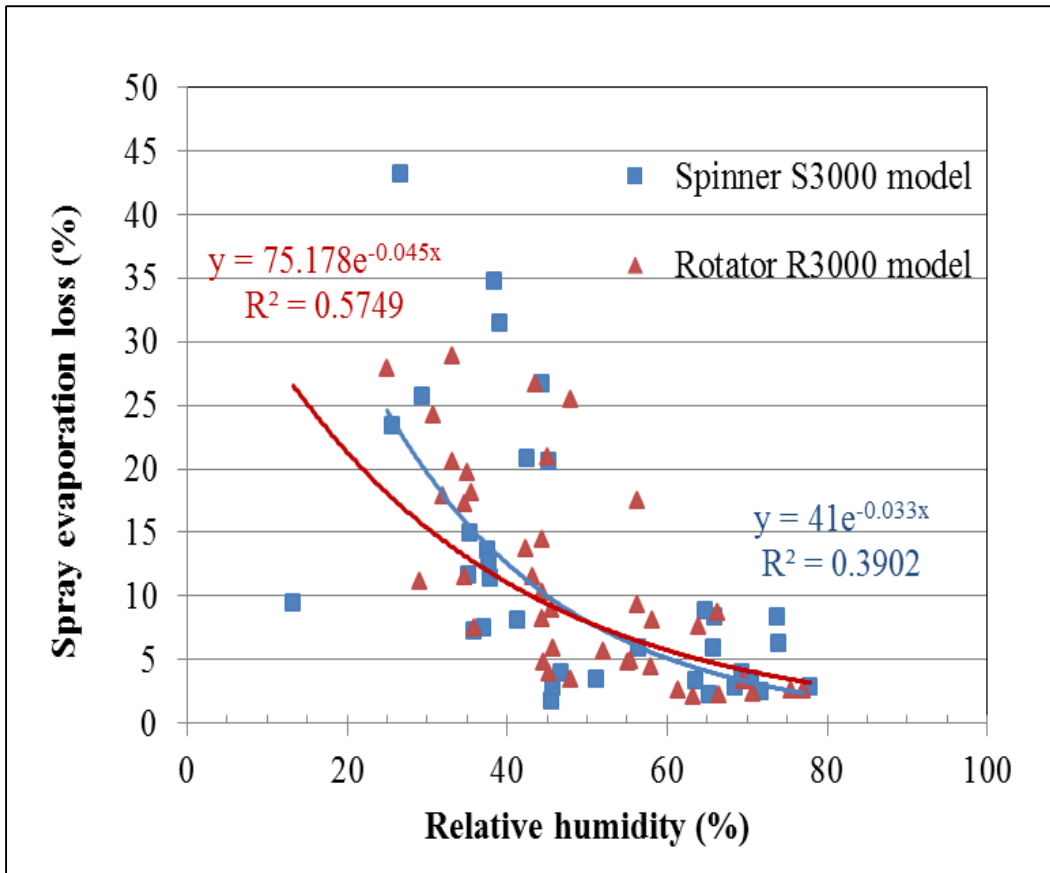
Figure 4-5. The relationship between spray evaporation losses and relative humidity.

Air temperature

The relationship between spray evaporation loss and air temperature is shown in Figure 4-6. Results show that the relationship between air temperature and spray evaporation loss approximates an exponential function.
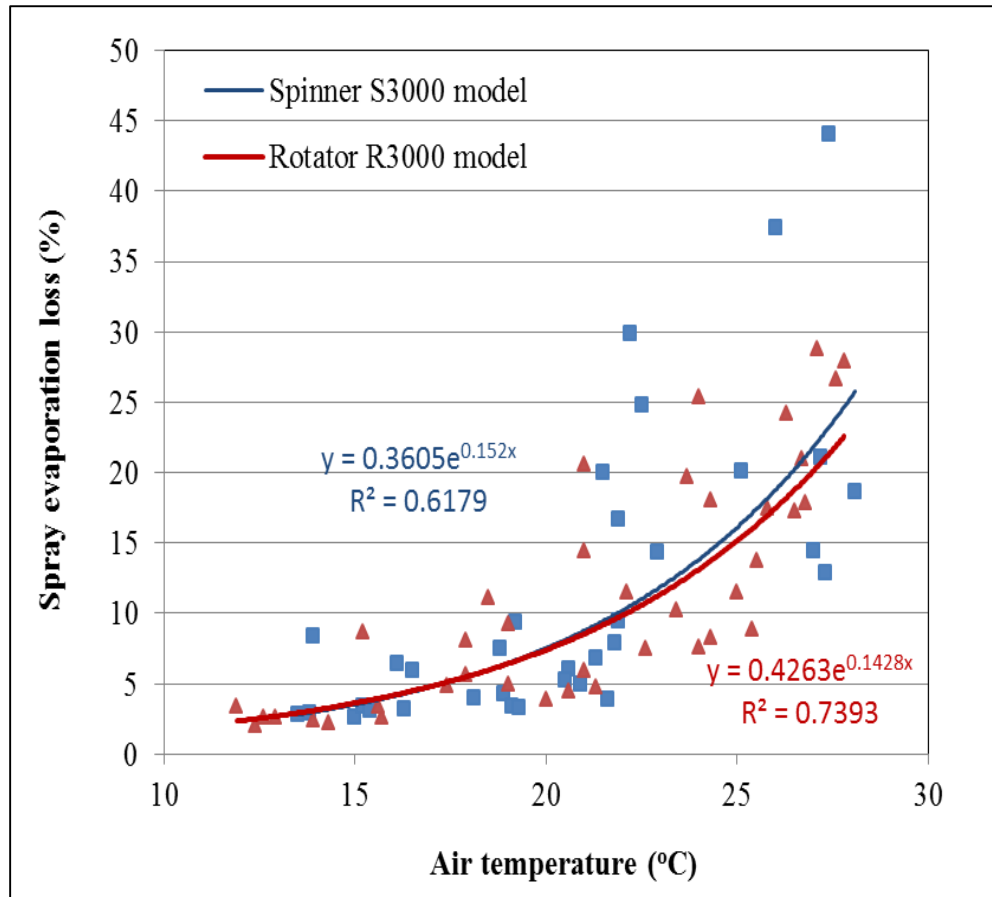
Figure 4-6. The relationship between spray evaporation losses and air temperature.

Vapour pressure deficit

The relationship between spray evaporation loss and vapour pressure deficit is shown in Figure 4-7. The results show that the relationship between spray evaporation loss and vapour pressure deficit is approximately exponential.
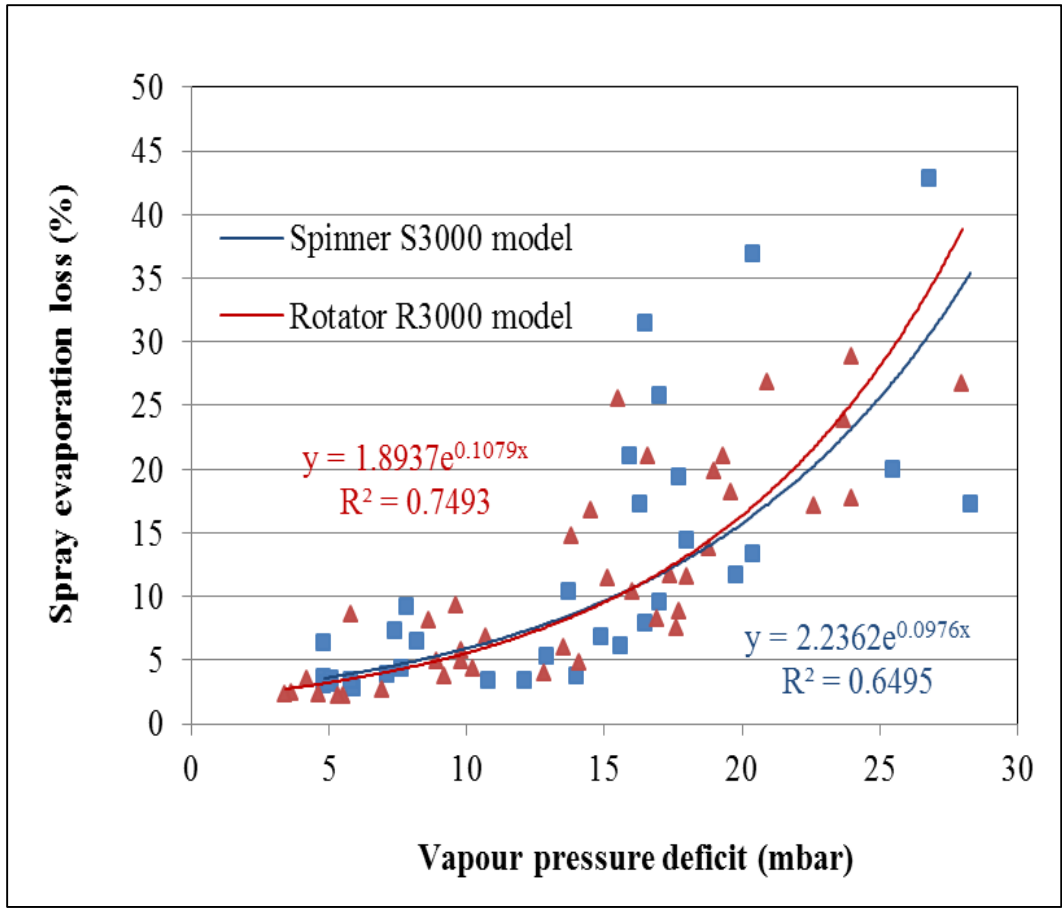
Figure 4-7. The relationship between spray evaporation loss and vapour pressure deficit.

4.2.7. Comparison of the Rotator R3000 model (Equation (4-11)) and the Spinner S3000 model (Equation (4-12))

The best fit models developed in this study were compared in order to identify any difference in the predictions between the two, under the same climatic conditions. The results of comparison between the Spinner S3000 and the Rotator R3000 models to daily spray evaporation losses for Winchmore climate data in the year 2010 - 2011 are shown in Figure 4-8 and Table 4-9. The results show that lower losses are observed during the winter months, while the highest losses are observed during the summer months. A paired samples t- test showed that the mean losses predicted by the Spinner S3000 model were significantly more

(p < 0.05) than those predicted by the Rotator R3000 model under same conditions; with significant peaks in evaporation losses under northwest wind conditions (circled in red).
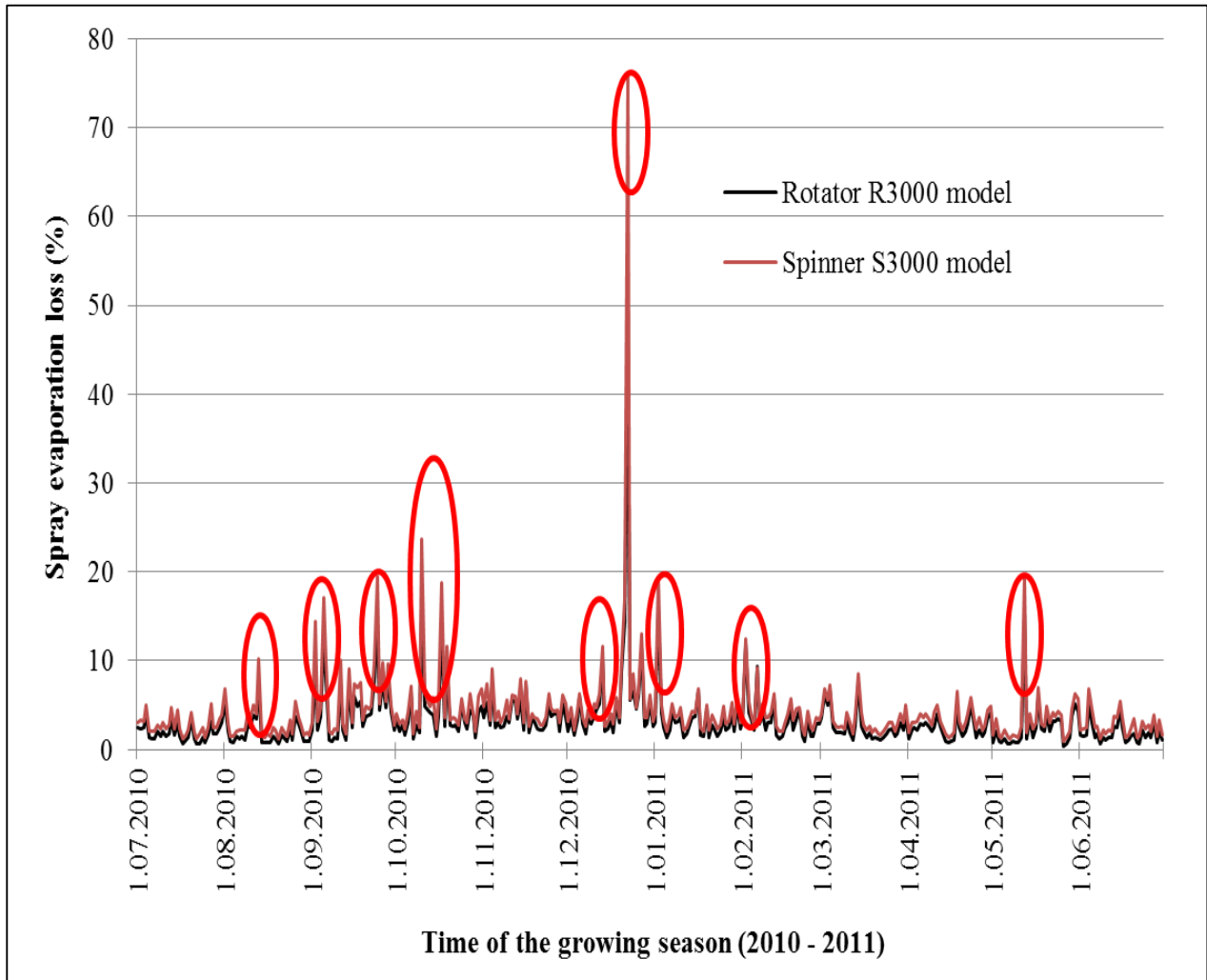
Figure 4-8. Comparison of spray evaporation losses using the best fit Equations (4-11) and (4-12) for the Rotator R30000 and the Spinner R3000 nozzles respectively for continuous data from Winchmore from July 1, 2010 to June 30, 2011.

4.2.8. Comparison of evaporation losses predicted by previous models and models from this study

In order to determine if there was any difference between the SEL predicted by models developed in this study and those developed previously using a similar approach, a comparison was made with the Winchmore climate data for the year 2010 – 2011. These previous models developed using a similar approach are the Yazar's model (Yazar, 1984) and Bavi's model (Bavi et al., 2009). The results of comparison for SEL predicted by the models are presented in Figure 4-9 and Table 4-9. The results show that Bavi's model gives a higher mean SEL than all the other models. However, the Spinner S3000, the Rotator R3000, and the Yazar's model are more affected by northwest wind conditions (circled in red Figure 4-9) than Bavi's model, during the summer months. On the other hand, Bavi's model is minimally affected by northwest wind conditions and the highest SEL is observed in winter months.

Statistical tests were carried out to determine if there were differences between the means of the SEL predicted by the four models. One way ANOVA showed significant differences between SEL predicted by the different models ($p < 0.05$). Pairwise comparison using a simple t-test showed that the means of SEL from different SEL model groups was statistically significantly different. However, SEL predicted by the Spinner S3000 model did not differ significantly ($p < 0.05$) from Bavi's model (as shown in Table 4-10). The means and standard deviations of SEL from the four models are presented in Table 4-9.

Table 4-9. Summary of means and standard deviations for various models.

	Spray evaporation loss (%)			
	Minimum	Maximum	Mean	Standard deviation
Rotator R3000	0.4	48.6	3.2	3.4
Spinner S3000	1.0	75.7	4.3	4.8
Yazar's model	0.1	15.2	1.5	1.4
Bavi's model	3.6	7.6	4.5	0.5

Table 4-10 Summary of *t*- test comparison of means between various SEL models.

Groups compared	p	Remarks
Rotator R3000 vs Spinner S3000	$P < 0.05$	Significant
Rotator R3000 vs Yazar's model	$P < 0.05$	Significant
Rotator R3000 vs Bavi's model	$P < 0.05$	Significant
Spinner S3000 vs Yazar's model	$P < 0.05$	Significant
Spinner S3000 vs Bavi's model	$P > 0.05$	Non-Significant
Yazar's model vs Bavi's model	$P < 0.05$	Significant
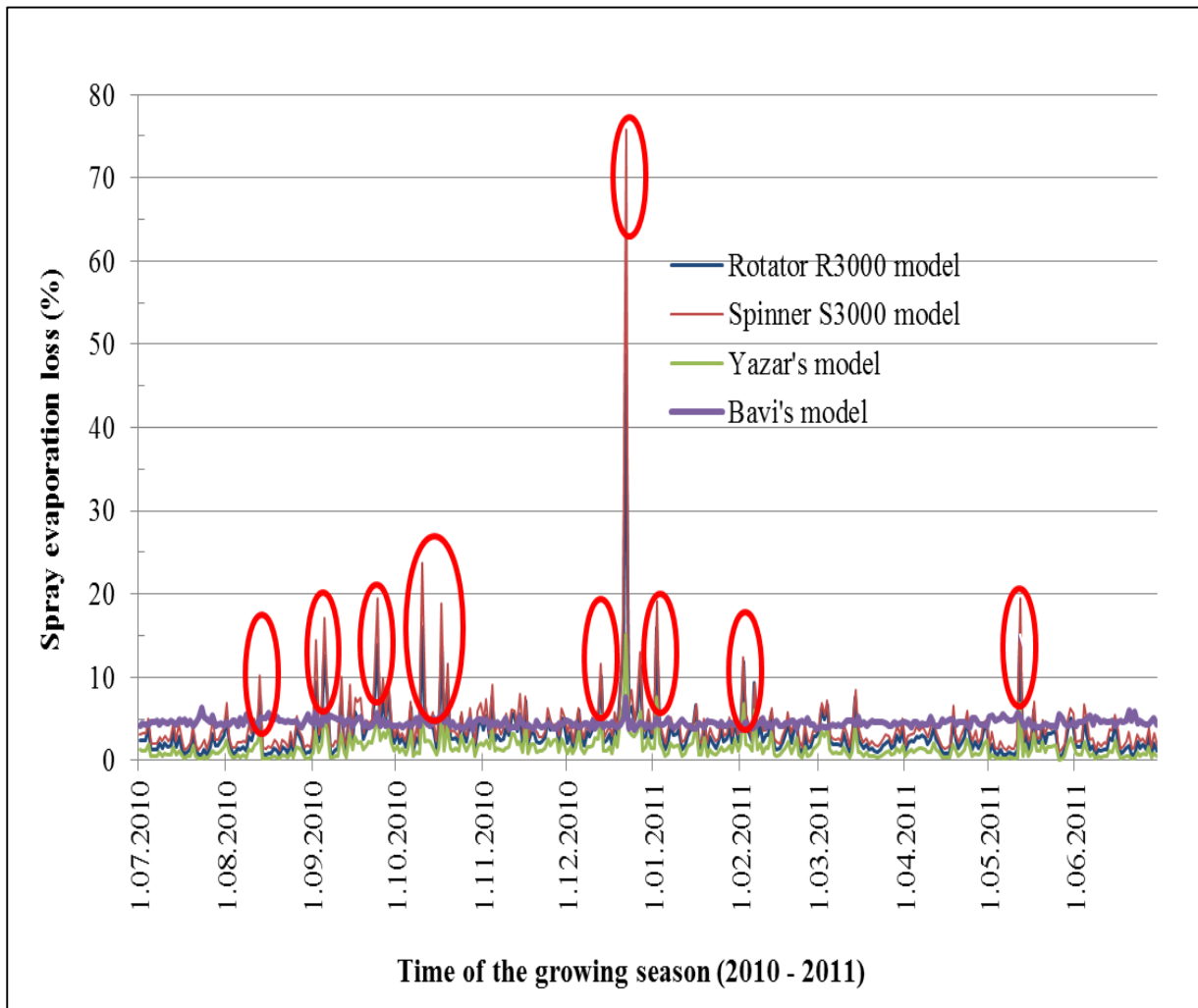
Figure 4-9. Comparison of spray evaporation losses using the best fit Equations (4-11) & (4-12) for the Rotator R30000, the Spinner R3000; Yazar's and Bavi's models for continuous data from Winchmore, July 1, 2010 to June 30, 2011.

4.2.9. Comparative analysis of different models for different climatic variables

A comparative analysis is made by graphical means using a given set of conditions given in Table 4-11 at different wind speeds and different vapour pressure deficits to understand how the different models respond to changes in those variables. This information is important because it provides knowledge indicating which variables are most significant.

Table 4-11. Reference climatic data for comparative analysis.

Date	26 November 2010
Variable	
Maximum temperature ($^\circ$C)	24.5
Minimum temperature ($^\circ$C)	11.6
Mean temperature ($^\circ$C)	18.5
Relative humidity($^\circ$C)	57
Solar radiation (MJ/m^2)	30.18
Vapour pressure deficit (mbar)	10.5

Comparative analysis of wind velocity

A comparison of evaporation losses estimated by different models was made by graphical means using different wind speeds ranging from 0 m/s to 10 m/s for climatic conditions given in Table 4-11.

Figure 4-10 illustrates comparison of the effects of wind velocity from the four models. The results show, in general, that the Spinner S3000 model estimates higher losses at different wind speeds than the other models, followed by the Rotator R3000 model, Yazar's model and Bavi's model, in that order. The relationship between spray evaporation losses and wind velocity is exponential for all models.
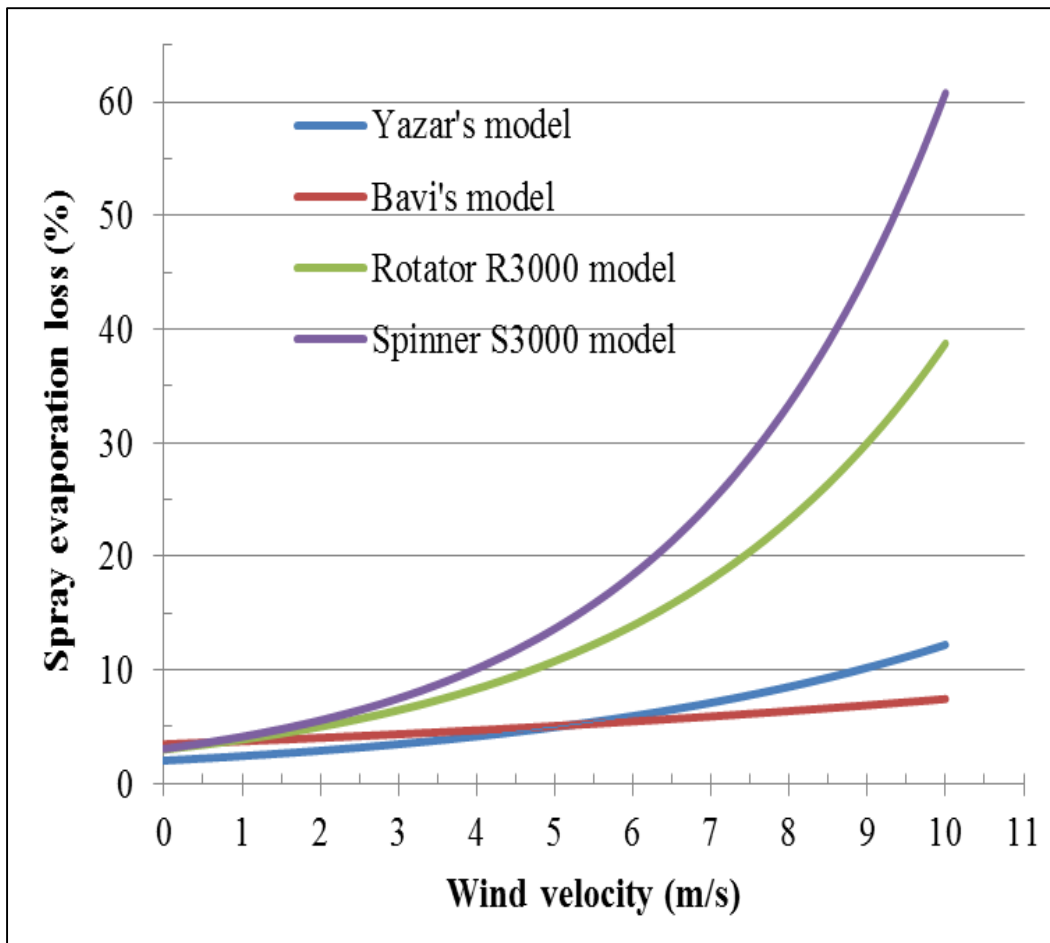
Figure 4-10. Comparison of evaporation losses estimated by various models for a given set of conditions at different wind speeds.

Comparative analysis of vapour pressure deficit

The results of comparison of the effect of SEL on the different models for wind speeds of 3 m/s and vapour pressure deficit range 0 – 20 mbar is shown in Figure 4-11. The results show that evaporation loss increases exponentially with increase in vapour pressure deficit in three models: the Spinner S3000, the Rotator R3000 and Yazar's models. Evaporation losses from the Spinner model are higher than those from both the Rotator R3000 and Yazar's models. However, evaporation losses under Bavi's model decrease exponentially with increase in vapour pressure deficit.
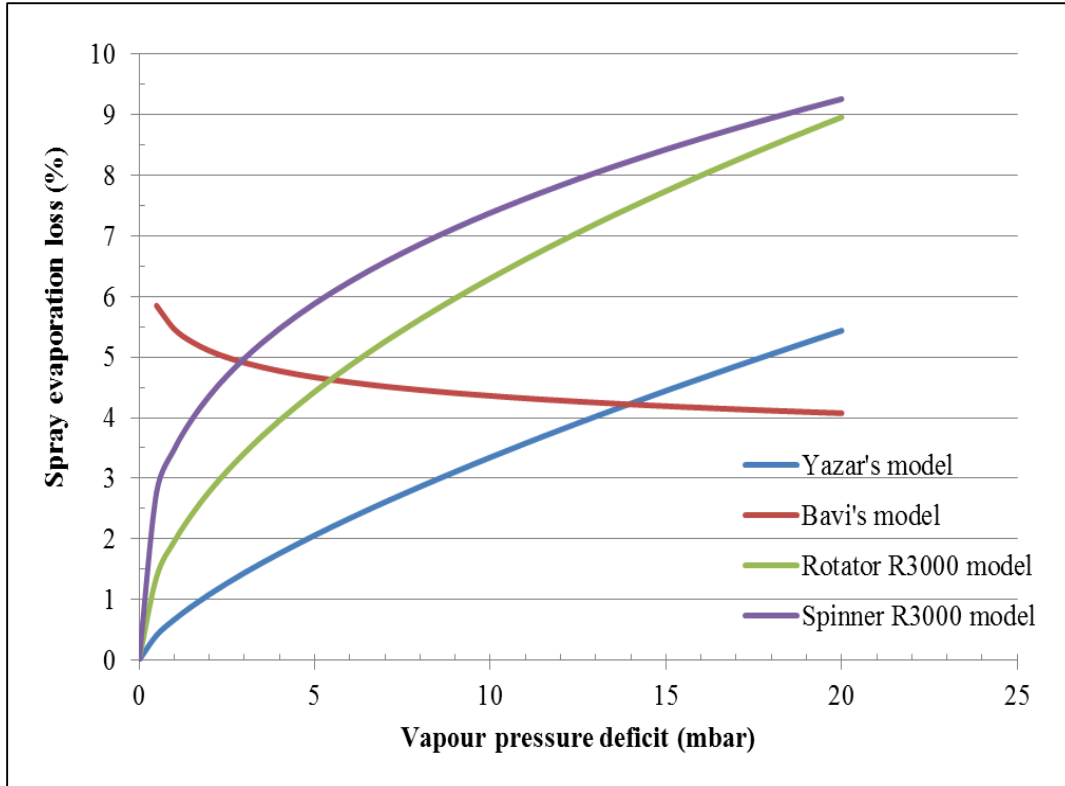
Figure 4-11. Comparison of evaporation losses estimated by various models for a given set of conditions with different vapour pressure deficits.

4.3. Wind speed reduction through windbreaks

Wind data (wind speed and direction) were obtained from Site 1 and 2 for a duration of 81 and 55 days, respectively. Wind loggers recorded average wind direction and speed after every 15 minutes for the entire period. Data from each wind logger were filtered to isolate the events that represented wind speeds that were perpendicular $\pm 22.5°$ to the windbreak in both directions. It was found that 364 and 191 events at Sites 1 and 2 respectively, were perpendicular to the windbreak. The events were then used to calculate relative wind speed and plotted to produce a wind reduction profile curve. The data from the wind reduction profile curve was used in Section 4.4.1 to calibrate and validate a wind speed reduction model.

4.3.1. *Windbreak porosity, height and width estimation*

The photographs taken during the first site visit were analysed for optical porosity by using ArcGIS 10.2 software. Photographs taken from each site were changed into a monochrome figure, as shown in Figure 4-12.
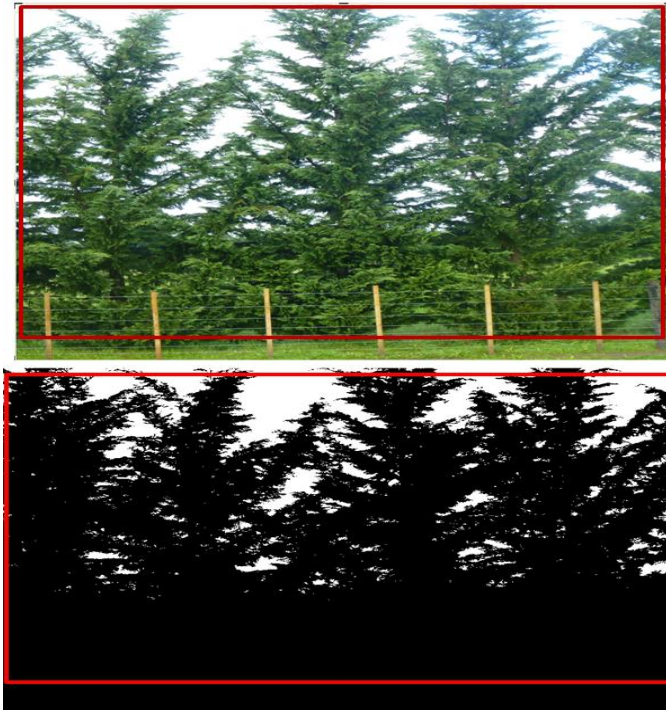
Figure 4-12. The conversion of windbreak photograph to a black and white figure (analysed with ArcGIS 10.1 software).

In this analysis, the optical porosity of the windbreak was estimated as the ratio of white pixels to the total number of both white and black pixels in the area surrounded by the red lines in Figure 4-12. The results of the estimation of average porosity alongside other windbreak characteristics are shown in Table 4-12.

Table 4-12. Estimated porosities of windbreak trees at both Sites 1 and 2.

Site	Windbreak position	Average optical porosity (op) (%)	Barrier porosity (θ) (%)	Average windbreak width (b) (m)	Average windbreak height (h) (m)
1	Northwest	55.4	55.9	1.5	5.5
	Southeast	57.6	58.1	1.5	5.5
2	West	27.9	28.5	2.5	8.0
	East	19.8	20.4	2.5	8.0

The windbreaks at Site 1 can be considered medium porosity windbreaks, while those at Site 2 are low porosity windbreaks. These windbreak parameters were used as input data for calibration and validation of windbreak models as detailed in Section 4.4.1.

4.3.2. *Wind speed and direction distribution at the study site*

The distribution of wind speeds and directions at each study site for each wind logger instrument is shown in the wind rose plots given in Figure 4-13 and Figure 4-14 . From both wind rose plots, it can be seen that the wind at the study sites varies significantly in intensity and direction. It is also apparent that wind speed in the direction of perpendicular to the windbreaks was reduced, compared to wind speeds in the other directions.
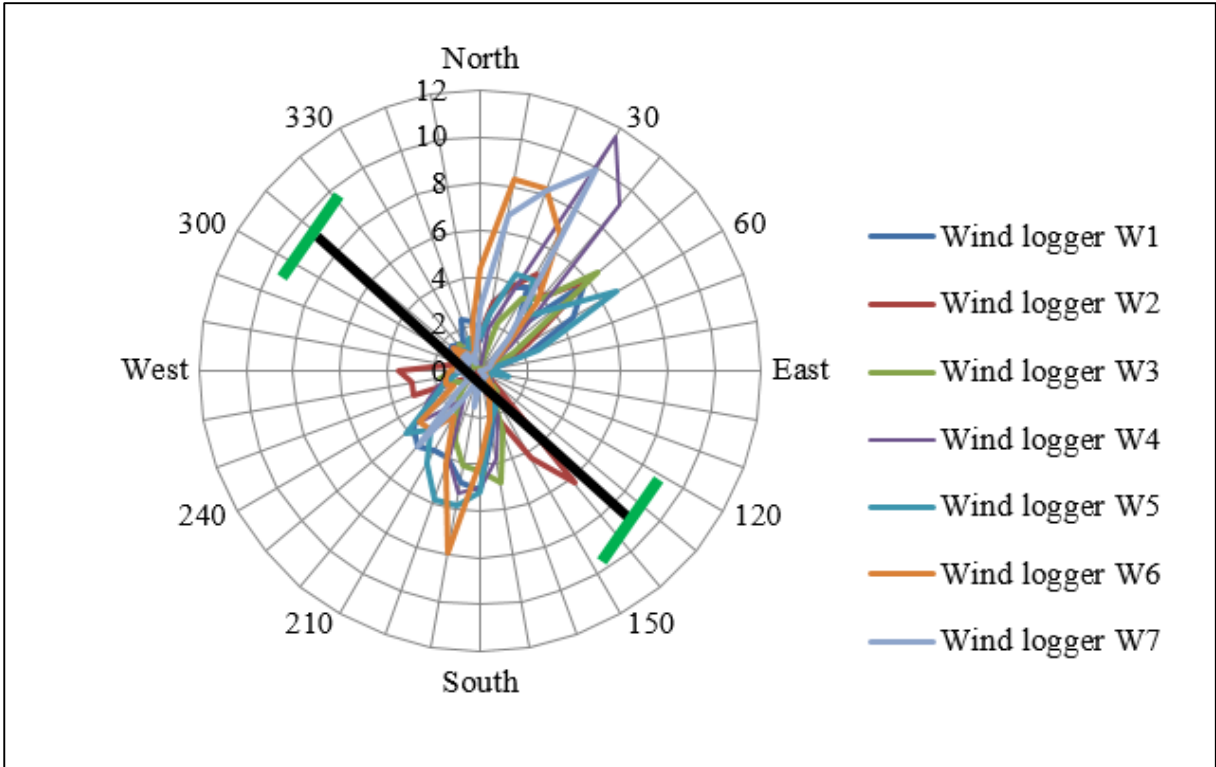
Figure 4-13. Wind rose of each wind logger at Site 1 for the period March 04, 2014 to May 14, 2014. The thick black line shows the direction of the wind logger set-up in the field while the green bars at the end represent the windbreaks (refer to Error! Reference source not found.**Figure 3-14 and Figure 3-15 for the arrangement of wind loggers in the field at Site 1). The y-axis on the scale 0 to 12 represent wind velocity (m/s) from various directions at the site during the study period.**
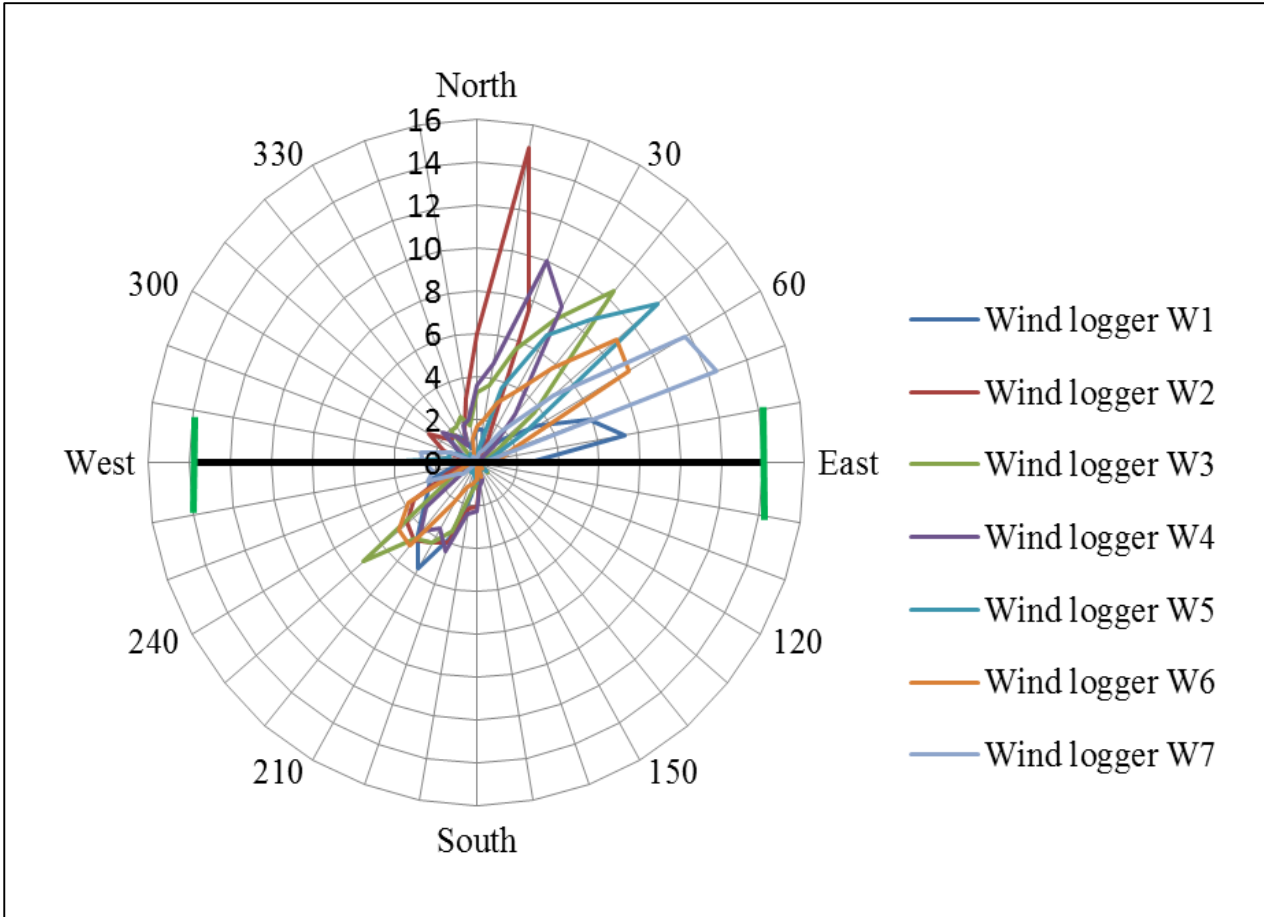
Figure 4-14. Wind rose of each wind logger at Site 2 for the period June 8, 2014 to August 01, 2014. The thick black line shows the direction of the wind logger set-up in the field while the green bars at the end represent the windbreaks (refer to Figure 3-16, Figure 3-17, and Figure 3-18 for the arrangement of wind loggers in the field). The y-axis on the scale 0 to 16 represent wind velocity (m/s) from various directions at the site during the study period.

.

4.3.3. *Wind speed reduction*

Relative wind speed for each observation period in each case was obtained by dividing the wind speed at each wind logger station by the wind speed measurement at the - 5 h windward site. The reduction in wind speed profiles is shown in Figure 4-15 and Figure 4-16 for Site 1 and Figure 4-17 and Figure 4-18 for Site 2. The results show that wind velocity reduced from a distance of -5 h with a reducing distance on the windward side toward the windbreak. In the lee of the windbreaks, wind velocity is reduced with increasing distance from the windbreak, up to a certain distance which is the location of minimum velocity (or maximum velocity reduction). After the point of minimum wind speed, the wind velocity increases gradually up to a maximum at a certain distance where wind speed reduction in the fields is affected by the subsequent windbreak. At the point of maximum wind velocity, the wind velocities do not recover to the open wind velocity and then again start to decrease because the wind speed at this point is affected by the subsequent windbreak.

a) Site 1

The effects of the windbreak on wind speed reduction in the NW - SE and SE - NW direction are shown in Figure 4-15 and Figure 4-16, respectively. The location of the minimum wind speed (at maximum wind speed reduction) is between 1.5 h to 3 h from the windbreak and 1 h to 2 h for NW - SE and SE - NW directions respectively. In both directions the maximum wind reduction is about 70%. The wind speed recovers up to only 55% at 8.5 h and 45% at 8 h for the NW - SW and SW - NW directions, respectively. The vertical bars through the plotted points indicate the standard deviations of the average relative wind speed for a particular wind logger station. As expected, the zone of protection extends from -5 h on the windward side in both directions. The zone of protection covers the entire length of the field between the windbreaks in all wind directions.
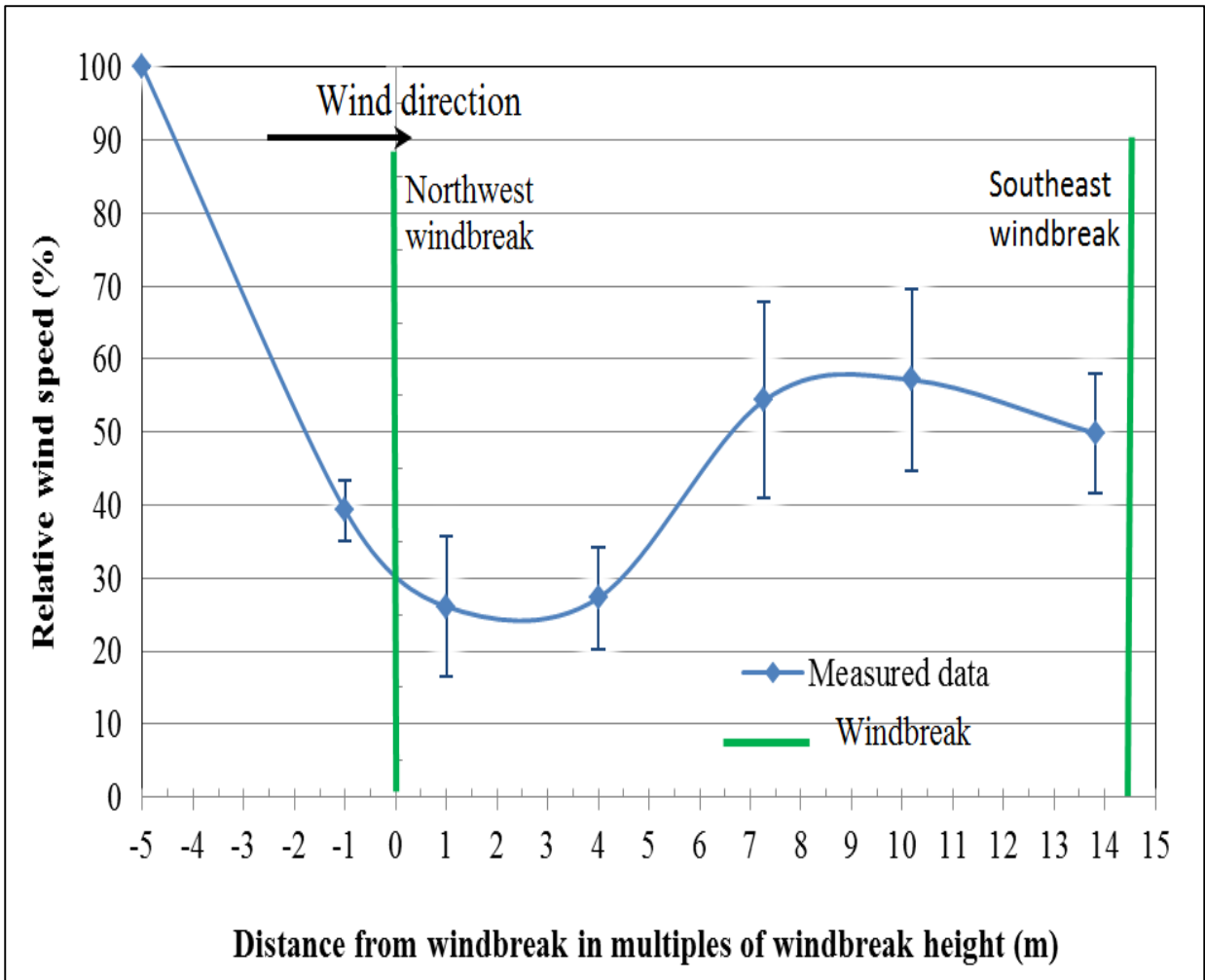
Figure 4-15. Wind speed reduction in the northwest – southeast direction between the two windbreaks at Site 1.
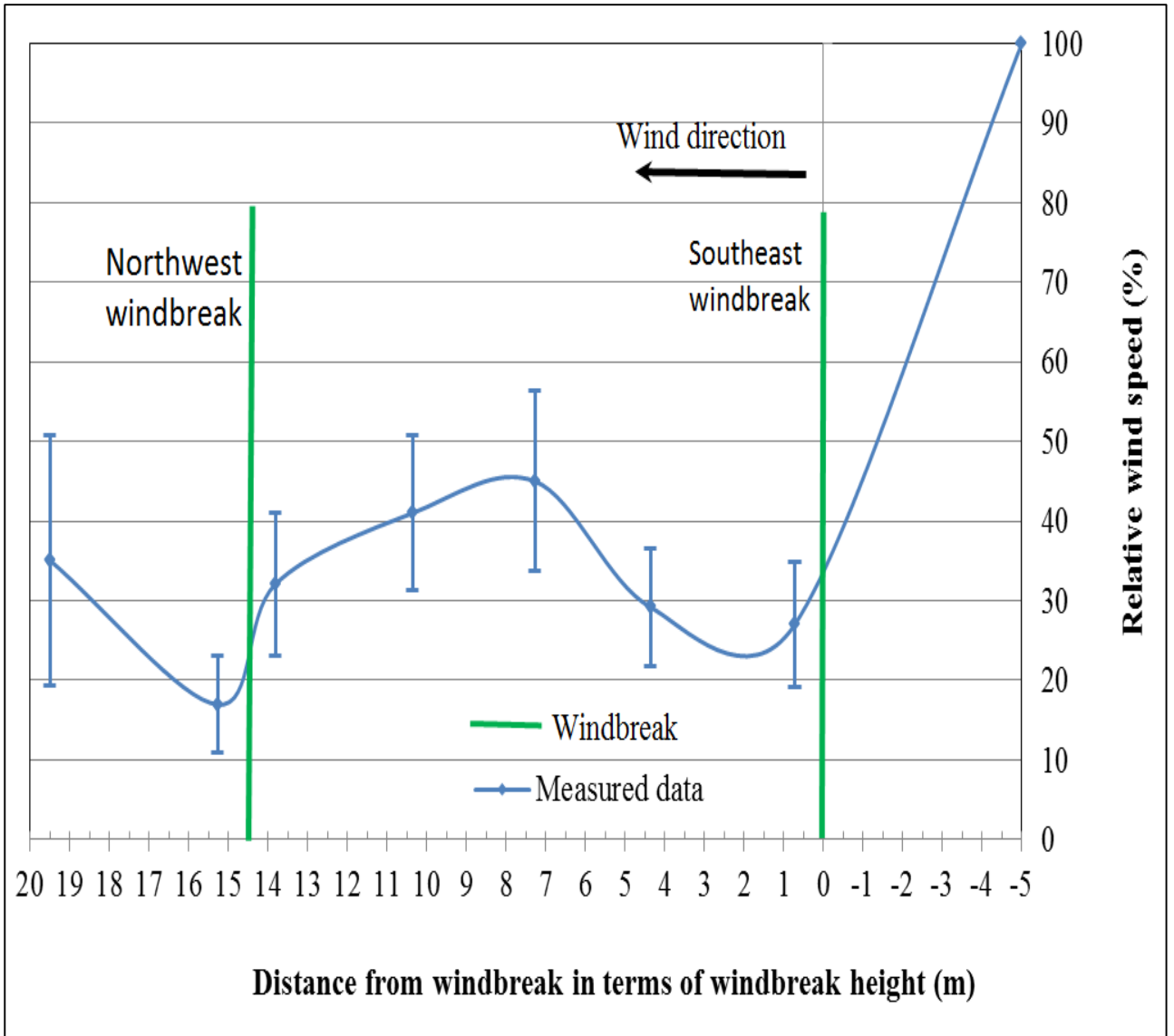
Figure 4-16. Wind speed reduction in the southeast - northwest direction between the two windbreaks at Site 1.

b) Site 2

The effects of the windbreak on wind speed reduction are shown in Figure 4-17 and Figure 4-18. In the west – east direction (Figure 4-17), the location of the minimum wind speed occurs between 1 h to 2 h from the windbreak, with an approximate maximum reduction of 85%; while in the east – west direction (Figure 4-18), the minimum wind speed occurs at 0 h to 1 h, with an approximate maximum reduction of 88%. The vertical bars through the plotted points indicate the standard deviations of the average relative wind speed for a particular wind logger station. The wind speed recovery is up to only 55% of the original wind speed at 10 h and 11.5 h for the west – east and east – west directions, respectively. In both directions, the zone of protection covers the entire field within the windbreaks. As expected, the zone of protection on the windward side in all directions extends up to -5 h.
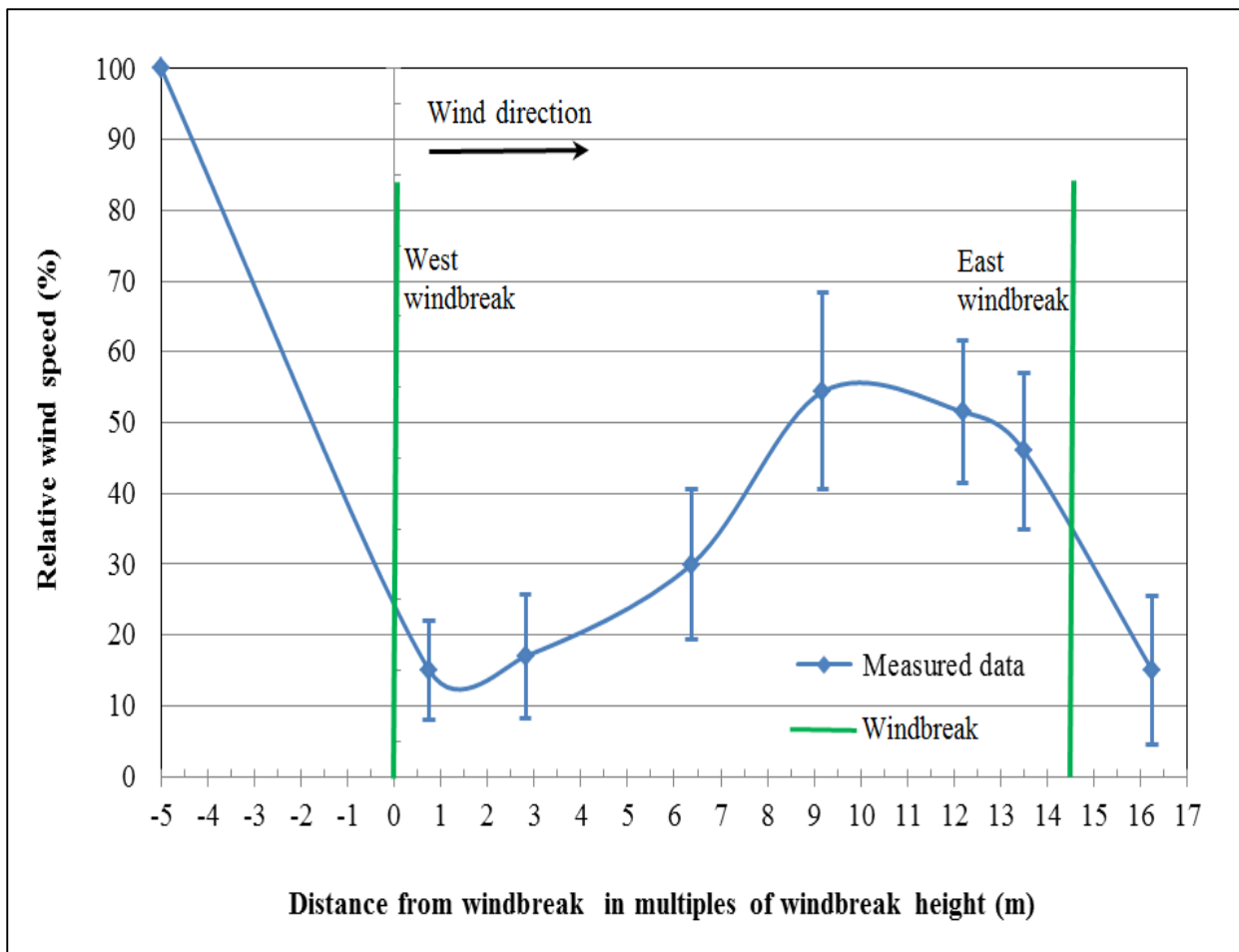
Figure 4-17. Wind speed reduction in the west - east direction between the two windbreaks at Site 2.
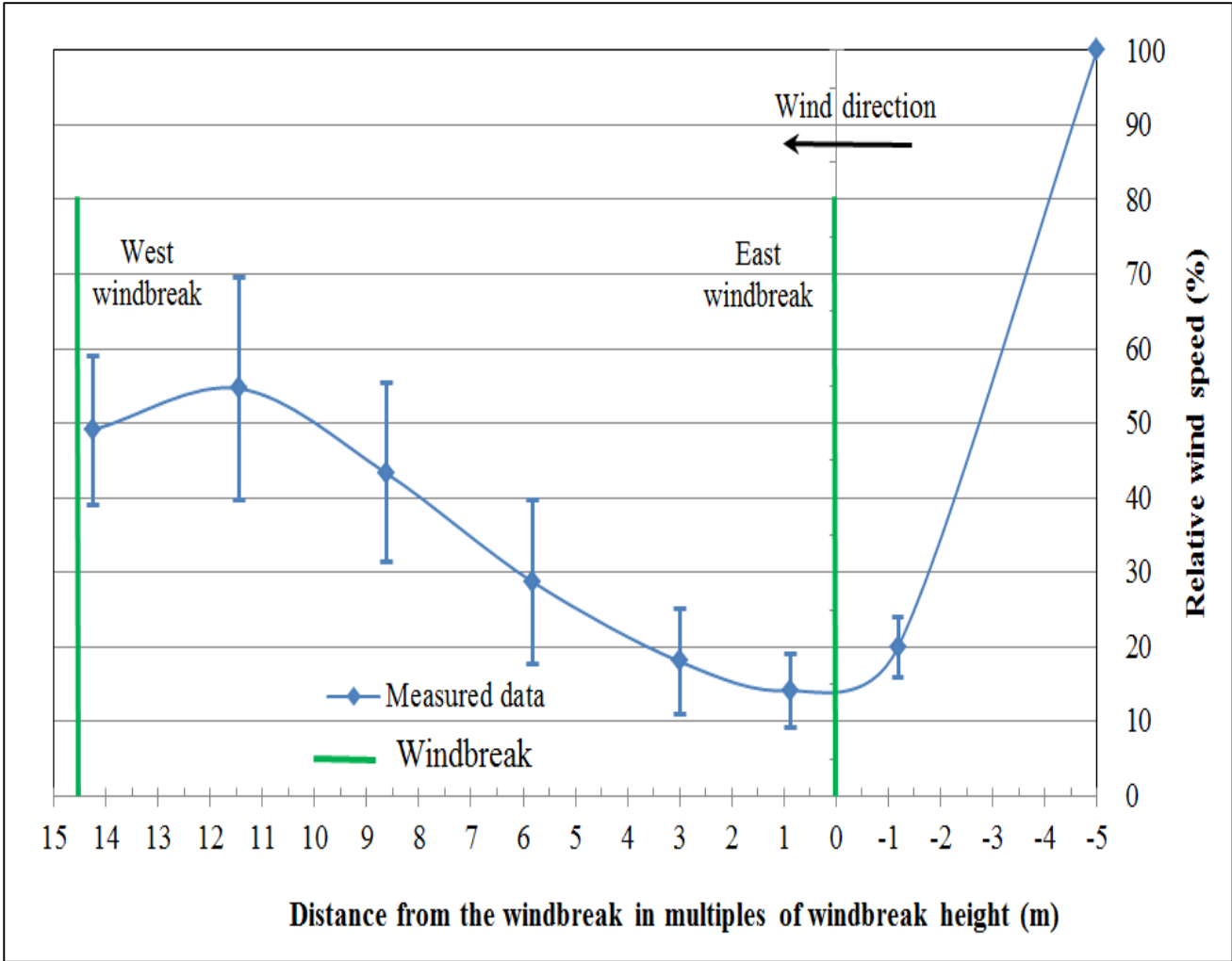
Figure 4-18. Wind speed reduction in the east - west direction between the two windbreaks at Site 2.

4.4. Modelling the effects of windbreaks on irrigation efficiency

Relative wind speed data obtained from field measurements was used to calibrate and validate the WEPS model described in Section 3.4.2 based on windbreak height and porosity. The validated windbreak model was then used to model the effects of wind speed changes for different scenarios: (1) when windbreaks are left as they are in field; (2) when windbreak height is reduced to 2 m; and (3) when wind breaks are completely removed. The reduction in wind speed is then related to evapotranspiration, from which irrigation requirements are calculated.

4.4.1. Calibration and validation of the windbreak model

The set of wind speed measurements were divided into two sets: the first set of the measured data was used for calibration while the second one was used for validation of the windbreak model. The optimum parameters found after calibration are presented in this section. In addition, results from both visual and statistical validation are reported in this section.

a) Calibration

The comparison between the calibrated model and the first set of measured data from the NW – SE direction at Site 1 is shown in Figure 4-19. After calibration, wind equations and parameters that were adjusted in the WEPS model are given in Equations (4-13), (4-14), and (4-15).

$$a = 0.01 \text{ - } 0.17\theta + 0.17\theta^{1.05} \tag{4-13}$$

$$d = 3.01 \text{ - } \theta \tag{4-14}$$

$$b = 1.34 \exp(\text{-}0.5\theta^{0.2}) \tag{4-15}$$

Where,

a, b, c, d are the coefficients described in the original WEPS model described in Section 3.4.2.

The same wind equations and parameters were used to calibrate the WEPS model for the SE – NW wind direction at Site 1 for the same windbreaks. Figure 4-20 shows the comparison between the calibrated model and first set of observed data in the SE – NW direction using

parameters in wind Equations (4-13), (4-14) and (4-15). Similarly, comparison between calibrated models with the first set of the data from Site 2 in the west - east direction is shown in Figure 4-21. The vertical bars through the plotted points indicate the standard deviations of the averaged wind speed reductions for a particular wind logger station. The wind equations and parameters in WEPS models that were adjusted are given in Equations (4-16) and (4-17) below.

$$a=0.01\text{-}0.17\theta+0.17\theta^{1.04} \qquad (4\text{-}16)$$

$$d=2.95\text{-}\theta \qquad (4\text{-}17)$$

The same parameters and wind Equations (4-16) and (4-17) were used to calibrate the windbreak model for wind data in the in the opposite direction (east – west) for the same windbreak. The comparison of the calibrated model in the east – west direction and the first set of the measured data is shown in Figure 4-22. Other wind equations and parameters in the WEPS model remained the same. A summary of optimum parameters and coefficients in WEPS model obtained after calibration for each site is given in Table 4-13.

Table 4-13. Summary of optimum parameters and coefficients obtained after calibration of the WEPS model at both Sites 1 and 2.

Site	Windbreak	Windbreak parameters				coefficients			
		h (m)	w (m)	op	θ (%)	a	b	c	d
1	Northwest	5.5	1.5	45	0.46	0.006	0.87	7.72	2.55
	Southeast	5.5	1.5	47	0.48	0.006	0.87	7.62	2.53
2	West	8.0	2.5	20	0.21	0.007	0.93	8.97	2.74
	East	8.0	2.5	15	0.16	0.007	0.95	9.22	2.79

The results in Table 4-13 show that higher coefficients are obtained for taller windbreaks than for shorter windbreaks. Higher coefficients are also obtained for lower porosity windbreaks at the same height.
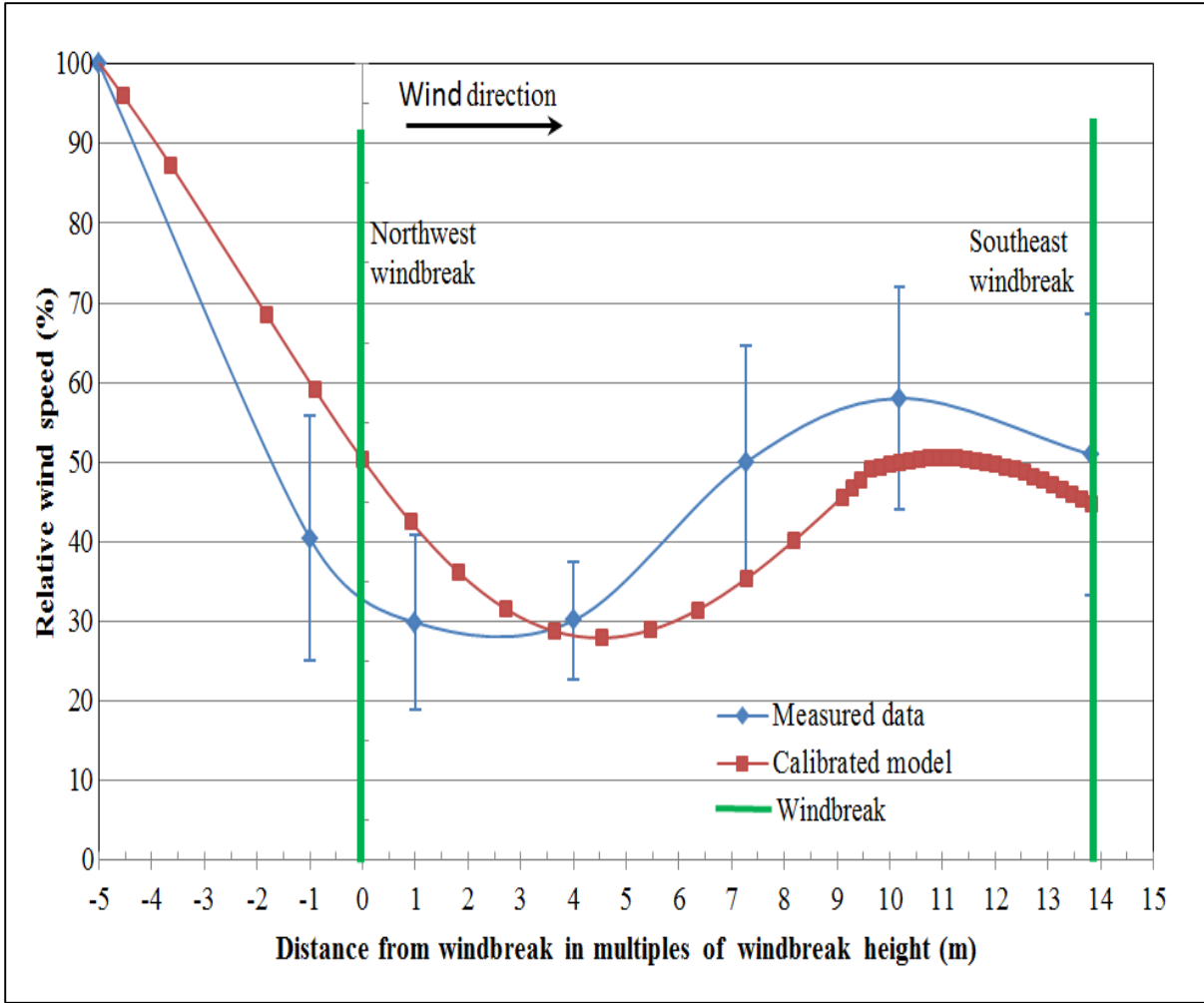
Figure 4-19. Comparison of calibrated model with calibration data in the northwest – southeast direction at Site 1.
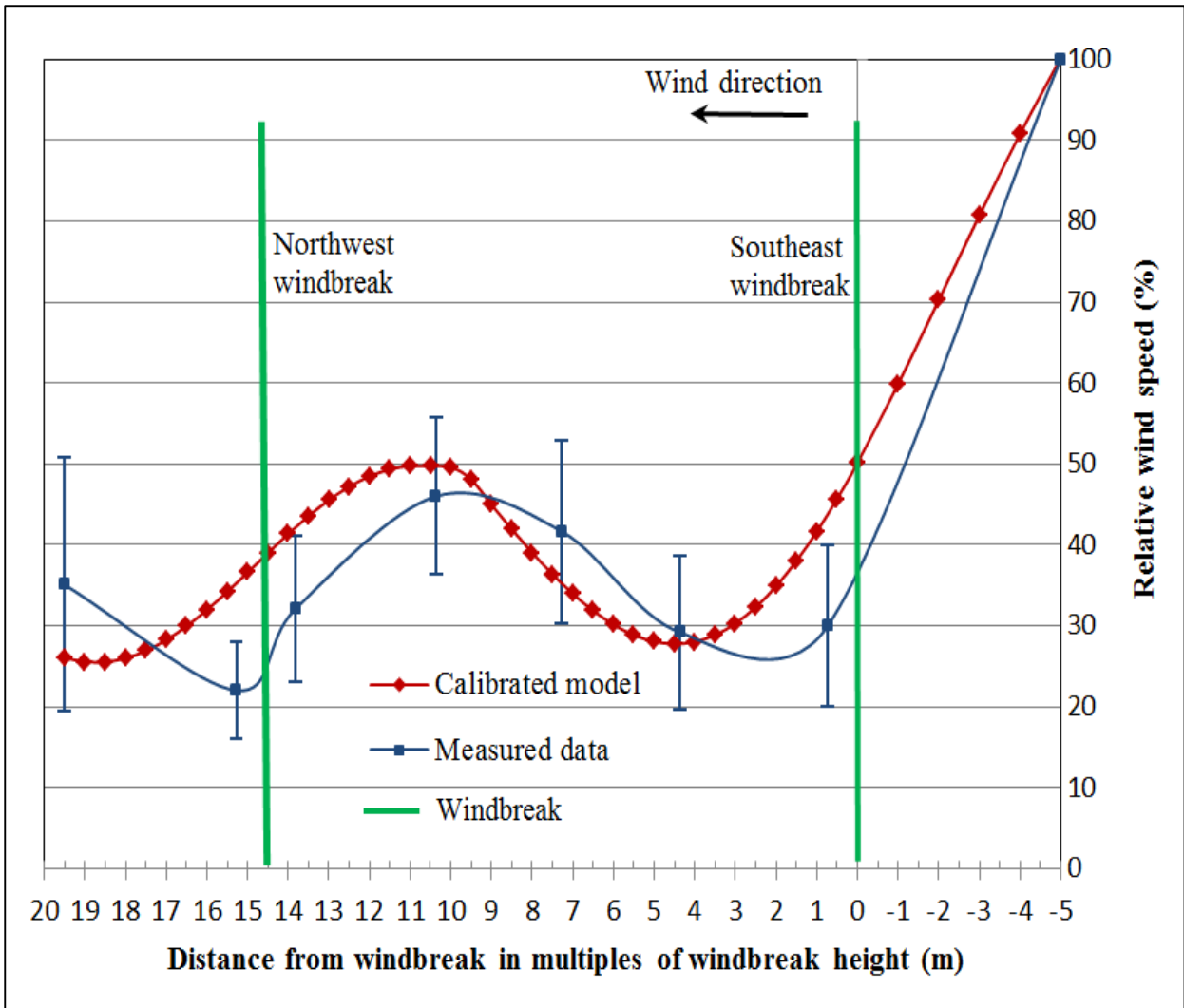
Figure 4-20. Comparison of calibrated model with calibration data in the southeast northwest direction at Site 1.
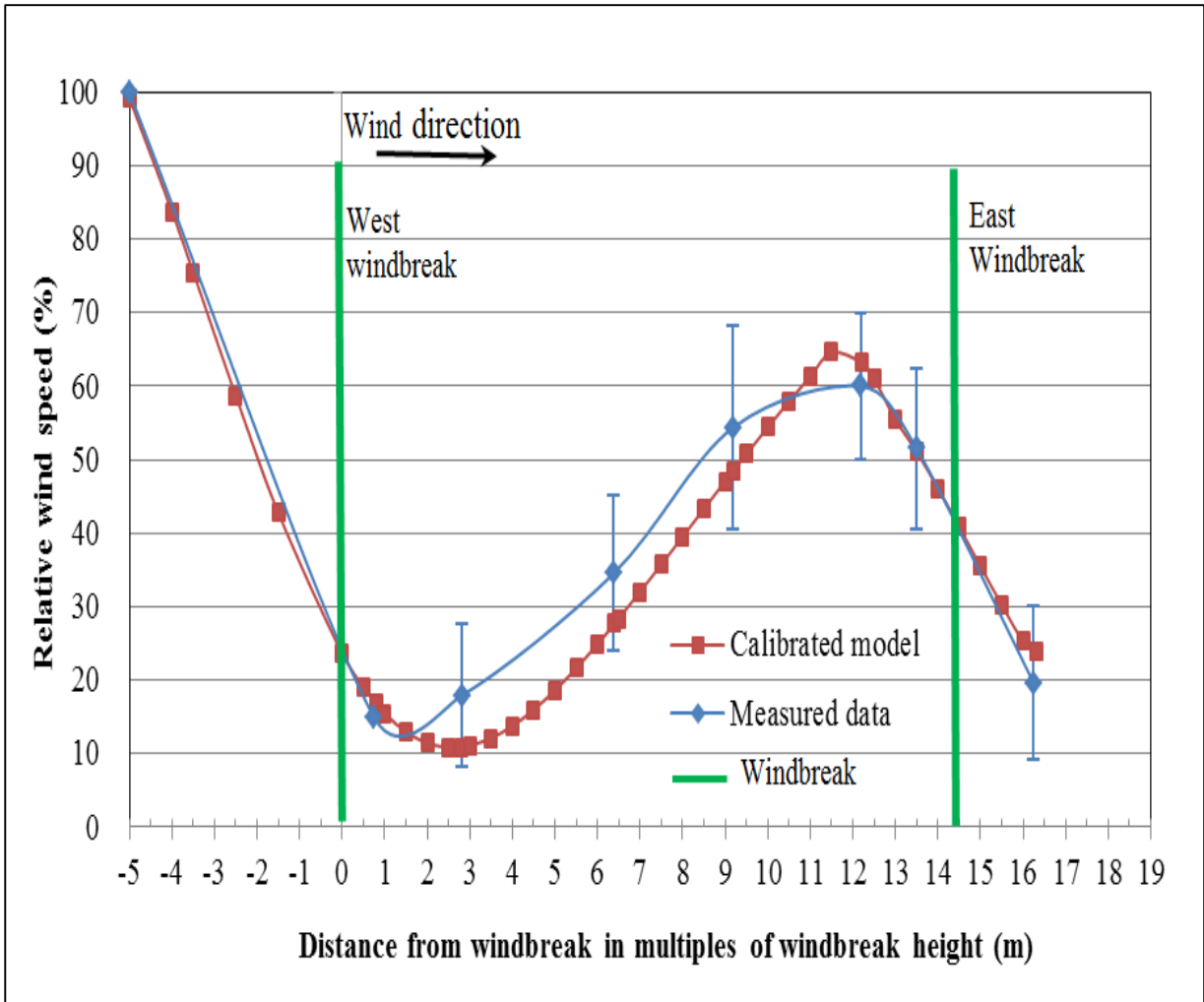
Figure 4-21. Comparison of calibrated model with calibration data in the west - east direction at Site 2.
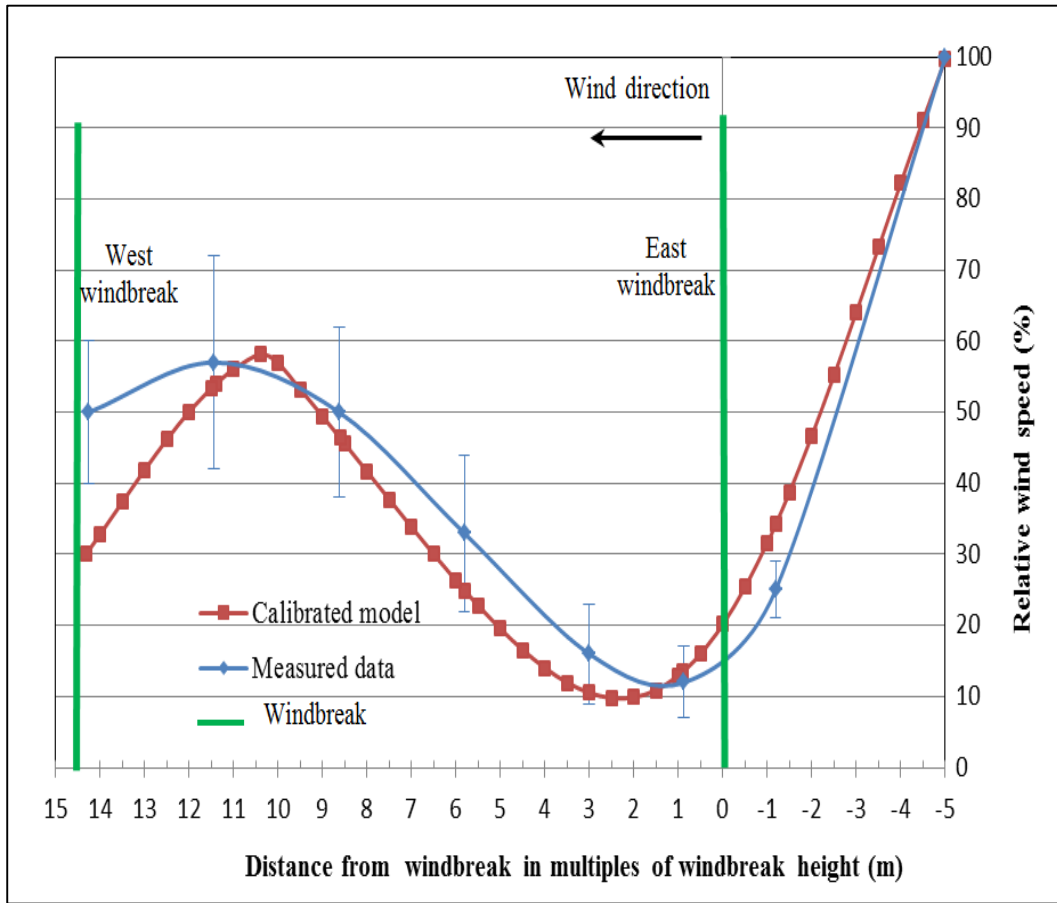
Figure 4-22. Comparison of calibrated model with calibration data for east - west direction at Site 2.

b) Validation

Validation of the calibrated model was done by comparing the calibrated model with the corresponding second data set at each site. Figure 4-23 and Figure 4-24 show the comparison between the calibrated model with the corresponding second half of the validation data at Site 1 for the NW - SE and SE - NW directions, respectively. Similarly, Figure 4-25 and Figure 4-26 show the comparison between the calibrated model with the validation data for the west - east and east - west directions, respectively at Site 2. At both sites, visual comparison shows a good agreement between the measured data and the calibrated model.
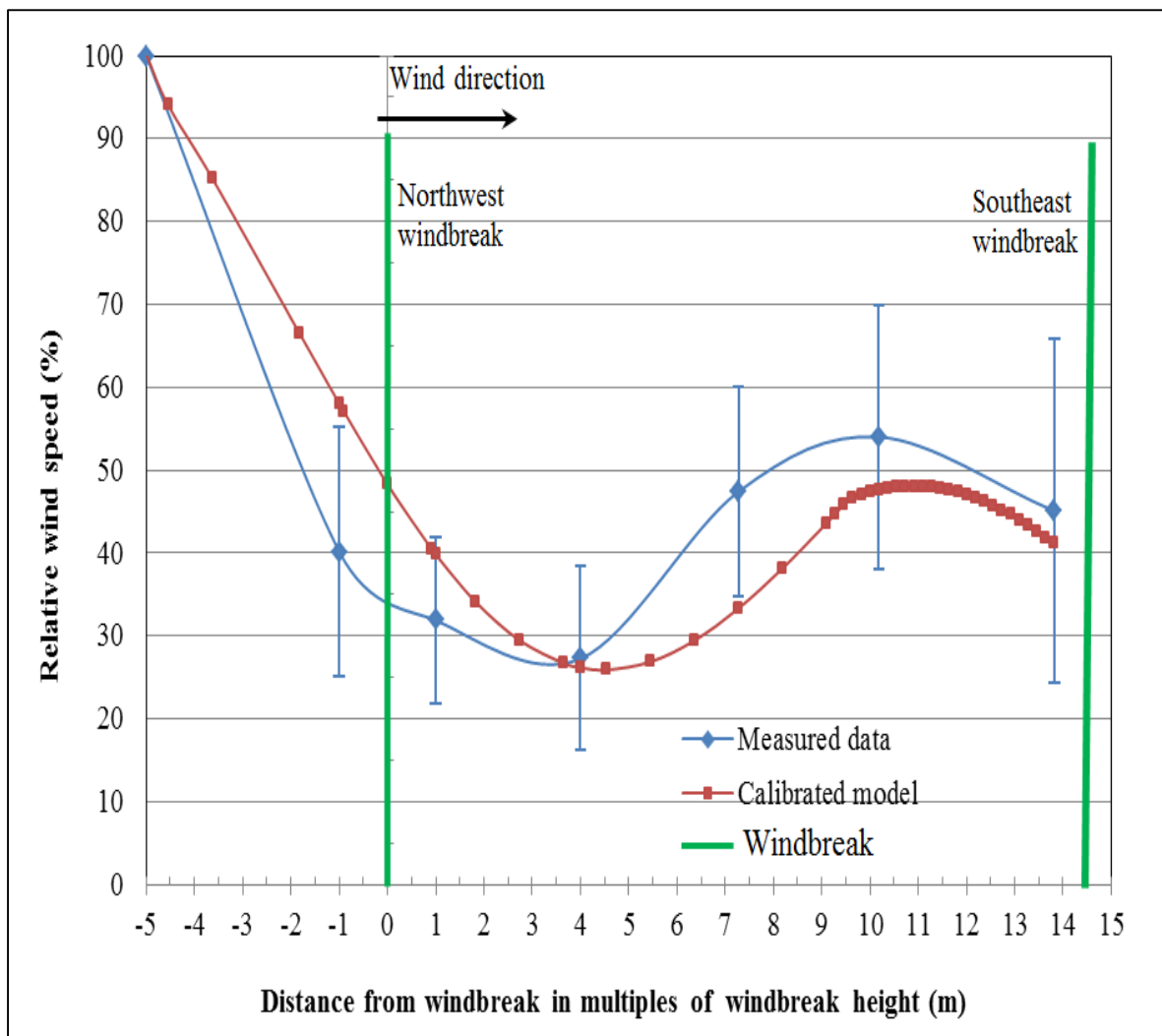
Figure 4-23. Comparison of the calibrated model with validation data for the northwest – southeast direction at Site 1.
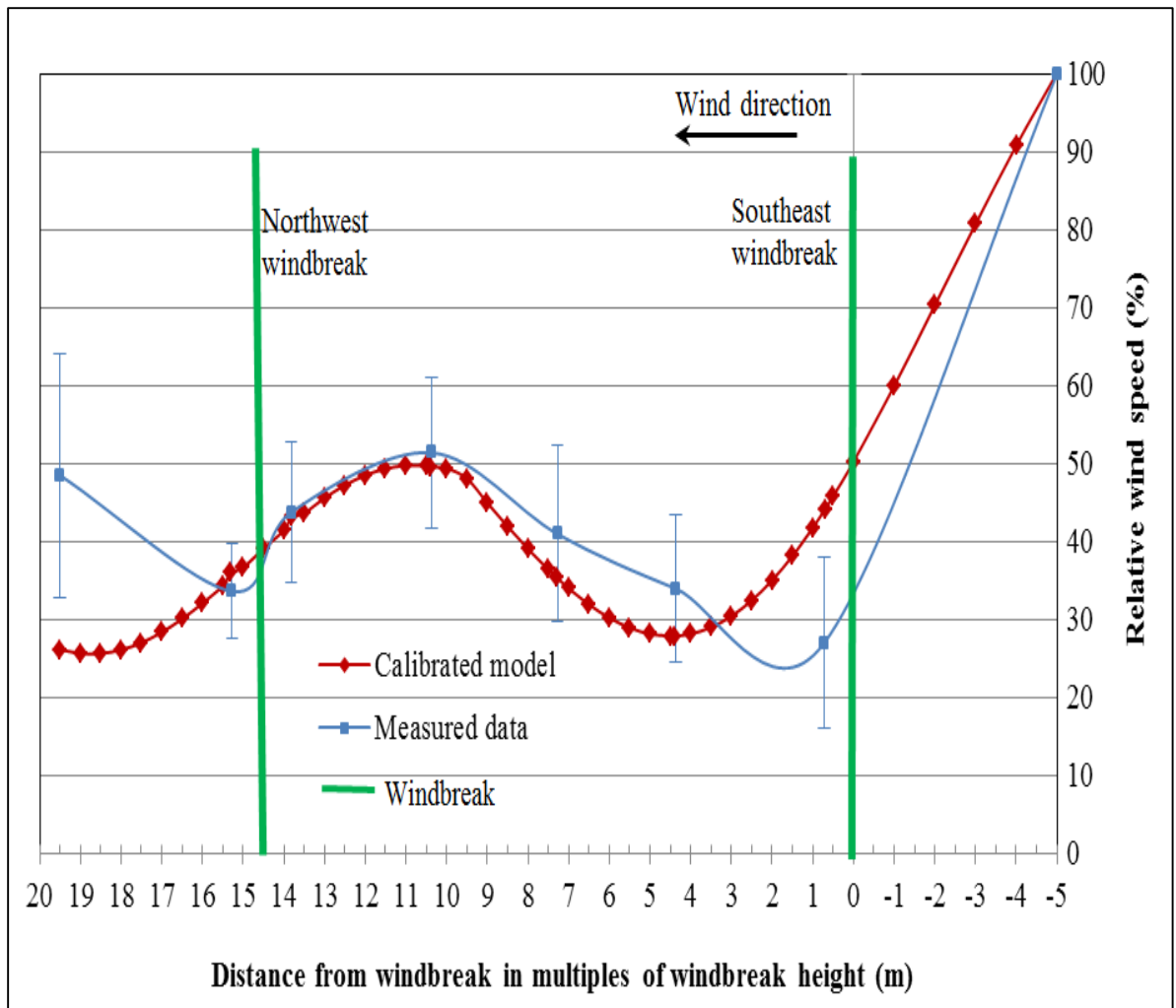
Figure 4-24. Comparison of the calibrated model with validation data for the southeast – northwest direction at Site 1.
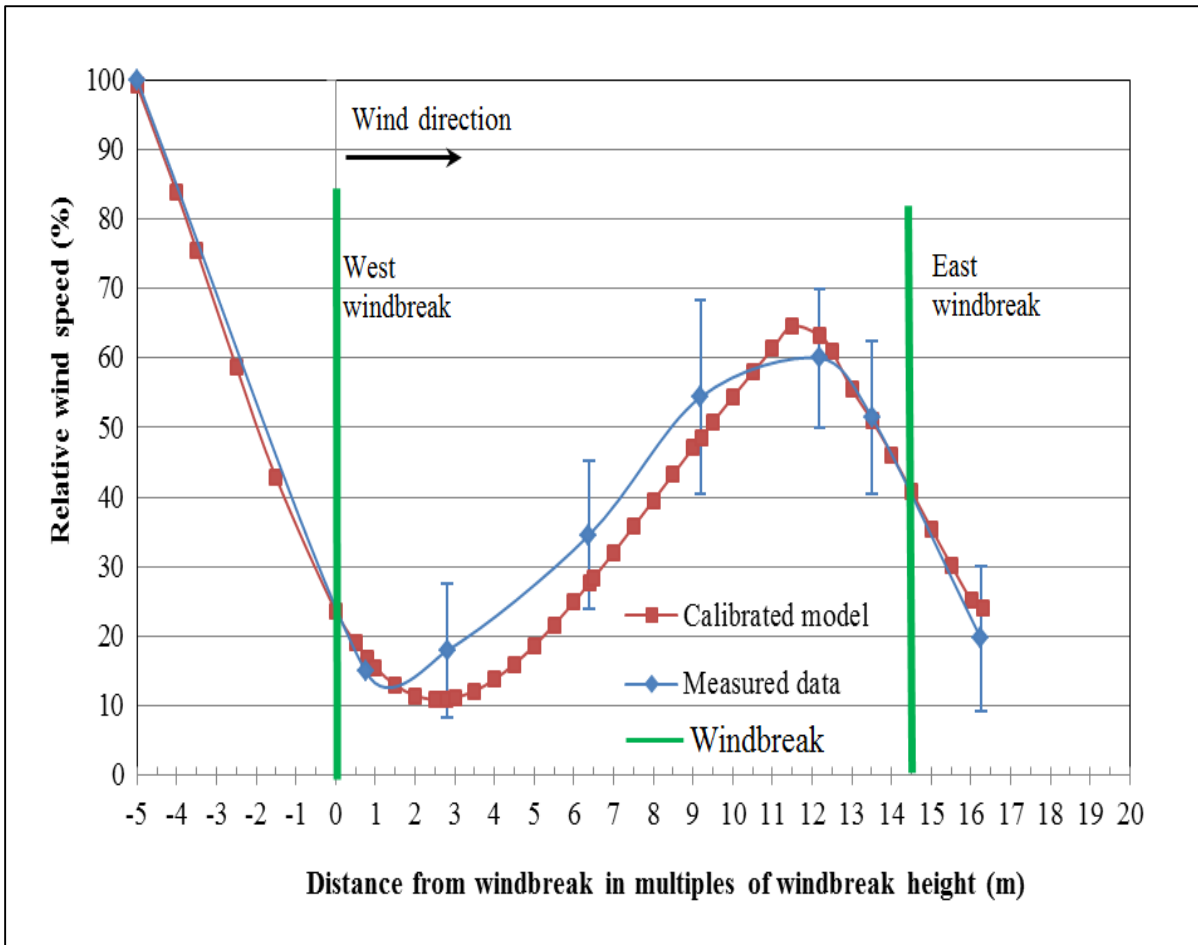
Figure 4-25. Comparison of the calibrated model with validation data for the west – east direction at Site 2.
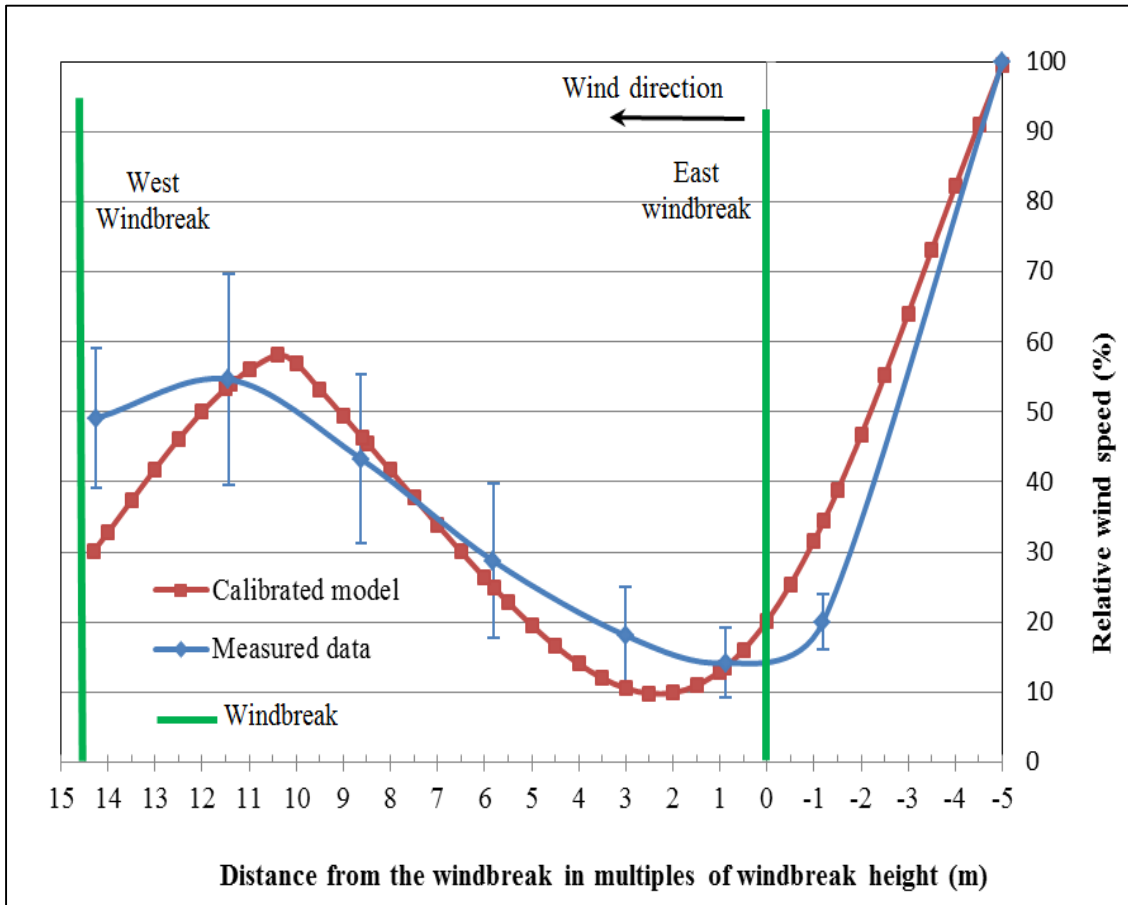
Figure 4-26. Comparison of the calibrated model with validation data for the east - west direction at Site 2.

c) Statistical validation of the windbreak model

After calibration and visual validation, the performance of the models for each site were evaluated, based upon four statistical indices: means of wind reduction; standard deviation of wind reduction; Relative Root Mean Square Error (RRMSE), and the Nash & Sutcliffe (1970) Modelling Efficiency (ME). Values of the four statistical indices for wind speed reduction observed for Sites 1 and 2 in the two directions are given in Table 4-14 and Table 4-15, respectively.

Table 4-14. Results from statistical indices used in evaluating the windbreak model performance in predicting wind velocity reduction at Site 1.

Statistic	Wind direction: Northwest – South East		Wind direction: South East - Northwest	
	Observed	Simulated	Observed	Simulated
Mean reduction in wind velocity (%)	49.41	49.47	48.02	46.22
Standard deviation (%)	22.3	22.7	22.4	23.2
Relative Root Mean Square Error (RRMSE) (%)		13.6		15.2
Modelling Efficiency (ME)		0.82		0.75

Table 4-15. Results from statistical indices used in evaluating the windbreak model performance in predicting wind velocity reduction at Site 2.

Statistic	Wind direction: West – East		Wind direction: East -West	
	Observed	Simulated	Observed	Simulated
Mean reduction in wind velocity (%)	44.1	42.3	41.0	35.85
Standard deviation (%)	28.4	29.5	28.2	29.2
Relative Root Mean Square Error (RRMSE)		9.7		16.2
Modelling efficiency (ME)		0.80		0.75

The results show that the statistical indices obtained from the northwest - southeast direction and the west - east direction are slightly better than those obtained in the corresponding opposite directions: southeast - northwest direction for Site 1 and east - west direction for Site 2.

4.4.2. *Modelling the effect of windbreak on the zone of protection*

The calibrated and validated windbreak models for each site were used for the modelling of different windbreak scenarios as shown in Table 4-16. The results for the effects of windbreaks on wind speed reduction and the zone of protection for various scenarios considered are shown in Figure 4-27 and Figure 4-28. In this subsection, results of modelling the effect of windbreaks on wind speed are presented with respect to the effect of the zone of protection, the minimum wind speed and recovery to maximum wind speed.

Table 4-16. Summary of scenarios modelled.

Site	Area	Scenario (S)	Scenario description
1	80 m by 80 m	S1	When wind breaks are left in situ in field (5.5 m)
		S2	When windbreaks are reduced to 2 m height
		S3	When windbreaks are completely removed
2	120 m by 120 m	S1	When wind breaks are left in situ in field (8 m)
		S2	When windbreaks are reduced to 2 m height
		S3	When windbreaks are completely removed
	Dates modelled: July 1, 2010 to June 30, 2011		

a) Zone of protection

The modelling results show that the zone of protection behind the windbreaks covers the entire area between windbreaks at both sites under Scenario 1. The extent of protection to the windward side at both sites is up to -5 h (- 27.5 m and - 40 m for Sites 1 and 2, respectively). In reducing the windbreak height to 2 m (Scenario 2), the zone of protection both within the windbreaks and to the windward side of the windbreaks reduces. The length of the zone of protection to the windward side reduces from - 27.5 m and - 40 m for Site 1 and Site 2 respectively, to -10 m. The length of the unprotected zone between the windbreaks, which reduces when windbreak height is reduced to 2 m, is 17 m for Site 1 and 52 m for Site 2. The complete removal of windbreaks removes all sheltering effect over the entire fields.

b) Minimum wind speed (at maximum reduction)

Results show that the minimum wind speed occurs at 5 h (27.9 m) and 2 h (16 m) from the windbreaks for Sites 1 and 2, respectively, under Scenario 1. When windbreak height is reduced to 2 m (Scenario 2), the position of minimum wind speed moved closer to the windbreaks for both sites: the position of minimum wind speed occurs at 4 h (8 m) and 2.5 h (5 m) for Sites 1 and 2, respectively. The modelling results show that the maximum wind speed reduction for both Site 1 and 2, are approximately 70% and 88%, respectively. Maximum wind speed remains constant throughout the field under Scenario 3.
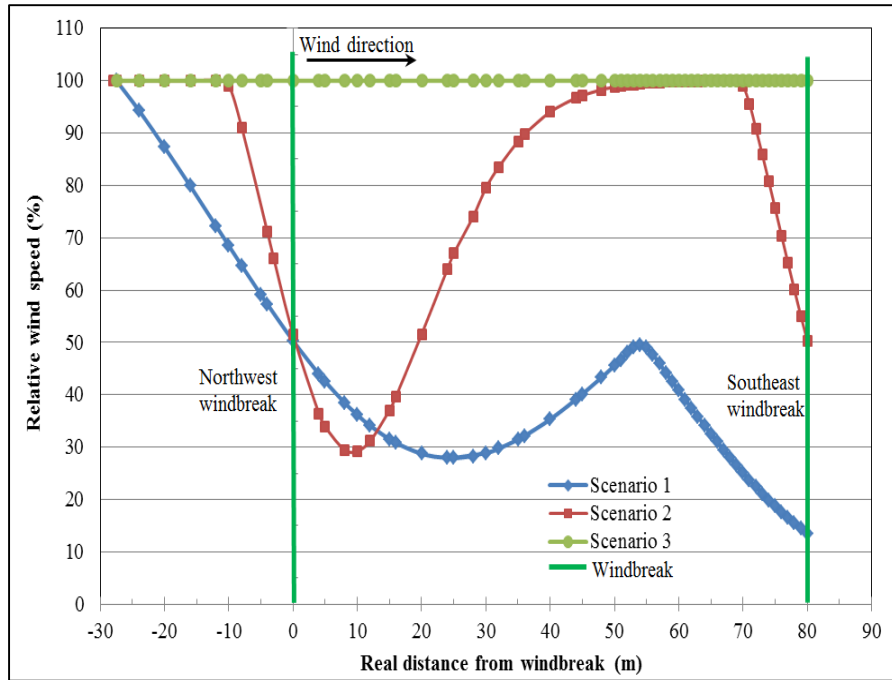
Figure 4-27. Effect of windbreaks on wind speed reduction and zone of protection at Site 1.
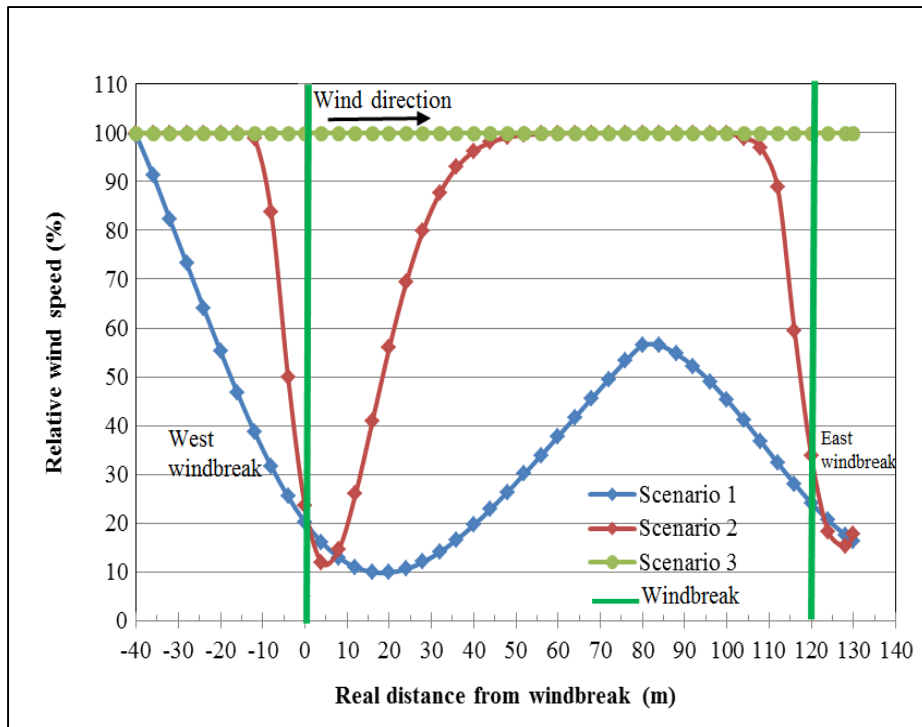
Figure 4-28. Effect of windbreaks on wind speed reduction and zone of protection at Site 2.

c) **Recovery to maximum wind speed**

Wind speed recovers only to 50% and 55% of its original open speed for Sites 1 and 2, respectively, under Scenario 1. Under Scenario 2 (when windbreak height is reduced to 2 m), wind speed fully recovers to open wind speed at 28 h (56 m) and 26 h (52 m) for Sites 1 and 2, respectively. Under Scenario 3, the open wind speed remains throughout the field since no windbreaks are present.

4.4.3. Modelling effects of windbreaks on average wind speed, evapotranspiration and net irrigation requirements

Removal of windbreaks and reduction of windbreak height was expected to cause an increase in the average wind speed across a field. Accordingly, an increase in wind speed was expected to lead to an increase in evapotranspiration. In turn, the net irrigation requirements of a crop are increased. Because these three variables are connected, the modelling results are presented together in Table 4-17 for clear comparison.

Table 4-17. Modelling results on the effect of different scenarios on wind speed, evapotranspiration and net irrigation requirements.

Scenario	Average wind speed (m/s per one year growing season)		Average ET (mm/one year growing season)		Average NIR (mm/one year growing season)	
	Site 1	Site 2	Site 1	Site 2	Site 1	Site 2
S1 (Initial windbreak condition)[1]	0.63	0.58	714.1	707.4	266	262
S 2 (Windbreaks at 2 m)	1.37 (11.7%)[2]	1.49 (156.9%)	782.3 (9.6%)	790.5 (11.7%)	293 (10.1%)	296 (13.0%)
S 3 (No windbreaks)	1.86 (195.2%)[3]	1.86 (220.7%)	823.6 (15.3%)	823.6 (16.4%)	332 (24.8%)	332 (26.7%)

[1] Initial windbreak height: Site 1 was 5.5 m while Site 2 was 8 m.

[2] The bracketed term represent the percentage change when windbreaks height is reduced to 2 m.

[3] The bracketed term represent the percentage change when windbreaks are completely removed.

a) Wind speed

The difference in wind speed as a result of the different windbreak scenarios shows that the average wind speed at Site 1 is significantly different ($p < 0.05$) from the average mean wind speed at Site 2, indicating that windbreak characteristics (porosity and height) affect wind speed in the sites. The changes in wind speed, as a result of changes in windbreak heights, show that wind speed increases in the field when windbreaks are reduced in height or completely removed in both sites. Site 2 experiences higher wind speeds than Site 1 under Scenario 2 (at 2 m windbreak height). However, as expected, both sites experience similar wind speeds under Scenario 3 (when windbreaks are completely removed). Statistical analysis using a paired-sample *t*-test showed that there was a significant increase ($p < 0.05$) in wind speed when windbreak height was reduced from 5.5 m and 8 m to 2 m height, for Sites 1 and 2 respectively. This is also true under Scenario 3; when windbreaks are completely removed for both sites.

b) Evapotranspiration

Evapotranspiration is a function of wind speed, and therefore any change in wind speed is expected to result in a change in ET. The results showed that when wind speeds increase as a result of windbreak reduction or removal, there is a proportional increase in ET. As expected, the ET under Scenario 1 is higher at Site 1 than at Site 2. However, ET is significantly higher ($p < 0.05$) at Site 2 than at Site 1 under Scenario 2. A paired-samples *t*-test showed that there was a significant increase ($p < 0.05$) in ET between the two sites under Scenario 1, indicating that ET is affected by windbreak characteristics. For both sites, a paired-samples *t*-test showed that there was a significant increase ($p < 0.05$) in ET when windbreaks are reduced to a 2 m height and when windbreaks are completely removed, indicating that ET is strongly affected by wind speed.

c) Net irrigation requirements

In the growing season considered, it was found that rainfall was not adequate to cater for ET in some periods of the growing season for all three windbreak height scenarios. As a result, irrigation was scheduled on those days when soil water depletions in the pasture root zone exceeded 50% of the total available soil water. Simulation results show that net irrigation

requirements for both sites increased correspondingly to increases in ET. For both sites, a paired-samples t-test showed that there is a significant increase ($p < 0.05$) in NIR when windbreaks are reduced to a 2 m height and when windbreaks are completely removed, indicating that an increase in wind speed when windbreaks are reduced or removed leads to a significant increase in irrigation requirements.

4.4.4. *Modelling the effects of windbreaks on irrigation frequency*

The number of irrigation events during the entire growing season varied for the different scenarios at both sites. Simulation results for irrigation frequency and net irrigation requirements are shown in Figure 4-29 and Figure 4-30 for sites 1 and 2, respectively. At the start of the simulation (which is winter in Canterbury), the field was assumed to be at field capacity. Consequently, there were no irrigation events until October when the soil water was depleted by increased ET. Results from both sites show that irrigation events started earlier for fields without windbreaks than for fields protected by windbreaks. The number of irrigation events needed to meet the net irrigation requirements increases when windbreaks are reduced in height or completely removed. The effect of reducing windbreak height or removal of windbreaks on the frequency of irrigation events is summarised in Table 4-18.
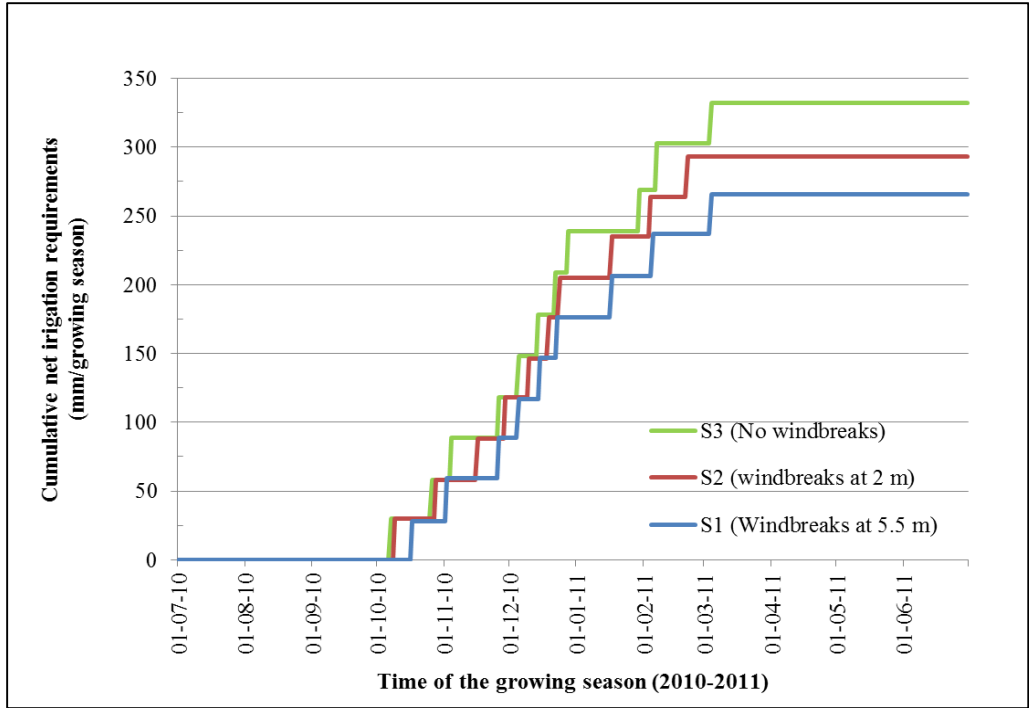
Figure 4-29. Comparison of irrigation frequencies at Site 1 for the different scenarios.
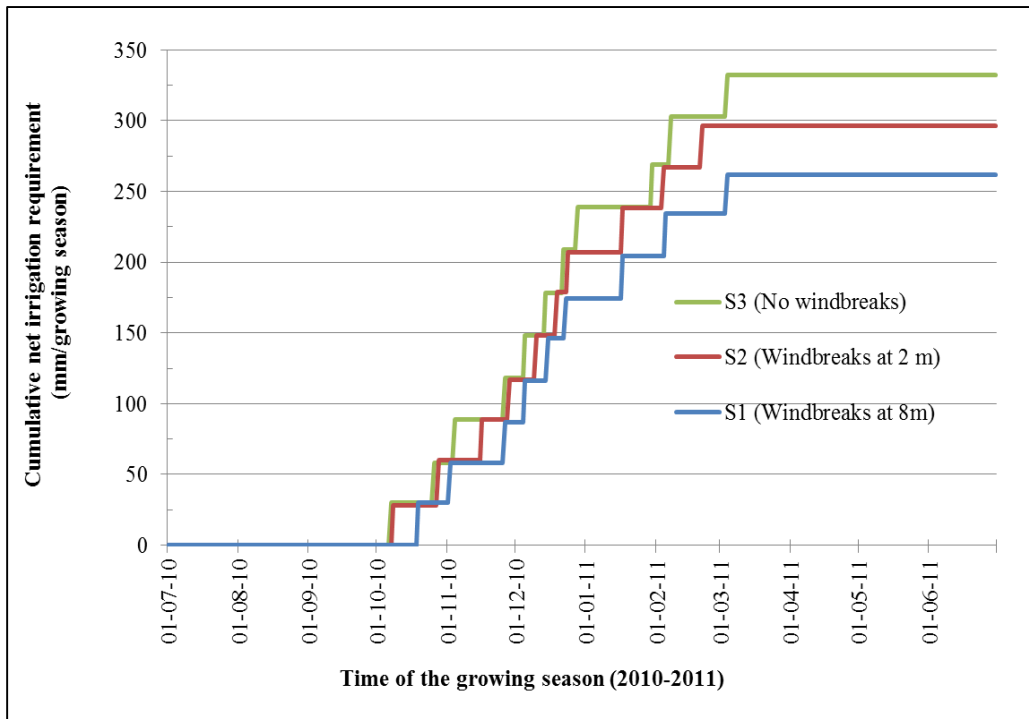
Figure 4-30. Comparison of irrigation frequencies at Site 2 for the different scenarios.

122

Table 4-18. Comparison of irrigation events for different sites under different scenarios.

Scenario	Number of irrigation events per one year growing season	
	Site 1	Site 2
S1	9	9
S2	10	10
S3	11	11

Where S1, S2 and S3 are as earlier defined in Table 4-16.

4.4.5. *Modelling the effects of windbreaks on spray evaporation losses*

In order to supply for NIR, irrigation water is supplied using an irrigation machine fitted with either the Rotator R3000 or the Spinner S3000 sprinkler nozzles, as described in Section 3.2.2. Modelling results show that higher SEL occurred when irrigation was carried out using the Spinner S3000 sprinkler nozzle than when using the Rotator R3000 for all scenarios at both sites. Also, for both sprinkler nozzles, higher SEL occurred when windbreaks were completely removed than when reduced to a 2 m height or when left as they are in fields (Table 4-19).

Table 4-19 Average spray evaporation losses for different scenarios at Sites 1 and 2 over one growing season.

Scenario	Wind speed (m/s)		Spray evaporation loss (mm)			
			When using Rotator R3000		When using Spinner S3000	
	Site 1	Site 2	Site 1	Site 2	Site 1	Site 2
S1 (Initial windbreak condition)[1]	0.63	0.58	8.8 (3.2%)	8.4 (3.1%)	9.7 (3.5%)	9.2 (3.4%)
S 2 (Windbreaks at 2 m)	1.37 (11.7%)[2]	1.49 (156.9%)	10.8 (3.6%)	10.7 (3.5%)	12.7 (4.2%)	12.8 (4.1%)
S 3 (No windbreaks)	1.86 (195.2%)[3]	1.86 (220.7%)	42.1 (11.3%)	42.1 (11.3%)	112 (25.2%)	112 (25.2%)

[1] Initial windbreak height: Site 1 was 5.5 m while Site 2 was 8 m.

[2]The bracketed term represent the SEL in percentage of applied water when windbreaks height is reduced to 2 m.

[3]The bracketed term represent the SEL in percentage of applied water when windbreaks are completely removed.

The results show that when wind speed increases, as a result of wind breaks being reduced to a 2 m height or completely removed, there is a corresponding increase in SEL. This SEL represents the extra water to be pumped from the source. A paired-samples t-test showed that for both sites there was a significant increase ($p < 0.05$) in spray evaporation losses when windbreaks were reduced to a 2 m height and when windbreaks were completely removed.

4.4.6. Modelling the effects of windbreaks on gross irrigation requirements

Gross irrigation requirement (GIR) is the amount of water that must be pumped from the source, which is greater than NIR by a factor that depends on SEL. In this case, GIR does not include extra water needed for special purposes like leaching of salts, or fertilizer application etc. Modelling results show that greater GIR is required when irrigation is done using the Spinner S3000 sprinkler nozzle than when irrigating using the Rotator R3000 sprinkler nozzle, under the same conditions as shown in Table 4-20. The results show a significant increase in GIR when windbreak height is reduced to 2 m or when windbreaks are completely removed. In one growing season, the increase in GIR can be as high 13.8% when windbreak height is reduced to 2m or 63.7% when windbreaks are completely removed, when low porosity windbreaks are considered.

A paired-samples t-test showed that there was a significant increase ($p < 0.05$) in gross irrigation requirement when windbreaks were reduced to a 2 m height or when windbreaks were completely removed for both sites. This indicates that an increase in wind speed leads to a significant increase in spray evaporation losses, which ultimately increases the gross irrigation requirement.

Table 4-20. Average gross irrigation requirements for different scenarios at Sites 1 and 2.

Scenario	Wind speed (m/s per one year growing season)		GIR (mm/growing season)			
			When using Rotator R3000		when using Spinner S3000	
	Site 1	Site 2	Site 1	Site 2	Site 1	Site 2
S1 (Initial windbreak condition)[1]	0.63	0.58	274.8	270.4	275.7	271.2
S 2 (Windbreaks at 2 m)	1.37 (11.7%)[2]	1.49 (156.9%)	303.8 (10.3%)	306.7 (13.4%)	305.7 (10.8%)	308.8 (13.8%)
S 3 (No windbreaks)	1.86 (195.2%)[3]	1.86 (220.7%)	374.1 (36.1%)	374.1 (38.3%)	444.0 (61.0%)	444.0 (63.7%)

[1] Initial windbreak height: Site 1 was 5.5 m while Site 2 was 8 m.

[2]The bracketed term represent the SEL in percentage of applied water when windbreaks height is reduced to 2 m.

[3]The bracketed term represent the SEL in percentage of applied water when windbreaks are completely removed.

CHAPTER 5: DISCUSSION

5.1. Introduction

The results presented in Chapter 4 are discussed and presented in this chapter with respect to the effect of windbreaks on the effectiveness of sprinkler irrigation systems. The chapter is organized into three major sections.

1) Section 5.2 presents a discussion of the results obtained from the spray evaporation experiments. The nature of the spray evaporation patterns during the experimental tests is explained, followed by a discussion of the differences in droplet size distribution from the two sprinkler nozzles used in this research. The differences between the best fit SEL models developed for the Rotator R3000 and the Spinner S3000 sprinkler nozzles is discussed with respect to droplet size distribution. Lastly, the differences between the best fit SEL models developed in this research and those previously developed in other research using a similar approach is discussed.

2) The results of wind speed reduction through the use of windbreaks are discussed in Section 5.3. The difference in wind speed reduction between the two sites studied is discussed with respect to minimum wind speeds, zones of protection and recovery to maximum wind speed.

3) Section 5.4 presents a discussion of modelling results on the effect of windbreaks on irrigation efficiency. The results of simulations of the effects of different windbreak characteristics (based on the scenarios modelled) on ET, SEL, and irrigation requirements are discussed and the effects of windbreak height reduction to 2 m or the complete removal are quantified in terms of water resource use.

5.2. Spray evaporation loss

In this section, the spatial variation of spray evaporation loss in the catch cans within the irrigated area is discussed, followed by an explanation of the differences in the drop size distribution between the Rotator R3000 nozzle and Spinner S3000 nozzle. The differences in droplet size distributions are then used to explain the differences in SEL prediction between the two models and between other models previously developed.

5.2.1.   Spatial patterns of evaporation

Examination of spatial patterns of evaporation within the irrigated area showed that evaporation losses increased with increase in distance from the sprinklers. Thus, the water caught in catch cans on the periphery of the spray pattern exhibited higher rates of evaporation than those nearer the sprinklers. Increase in evaporation with increase in distance from the sprinklers was due to a longer time of travel of the droplets from the sprinkler nozzle to the catch can, which increased the time available for evaporation to occur. Similar results were reported by Hermsmier (1973) and Yazar (1984); however, they differed from the results of George (1957) who observed greater evaporation losses near the sprinklers and at the periphery of the application pattern.

SEL in the individual catch cans was found to increase in the direction of the wind direction at high wind speeds. This was due to the smaller water droplets being carried by the wind further distance, which increased their flight path and hence increased the time available for evaporation to occur. When a stream of water is emitted by a sprinkler nozzle, it will reach further from the nozzle if its trajectory is with the wind and nearer the nozzle if the trajectory is against the direction of the wind. As a result, droplets from the sprays whose trajectory is with the wind direction travel further and have more time available for evaporation to occur than those droplets whose trajectory is against the wind direction.

127

5.2.2. *Droplet size distribution*

Droplet size distribution from the nozzles was related to nozzle size. The results showed that, under same operating pressure, the Rotator R3000 nozzle produced larger water droplets when compared to the Spinner S3000 nozzle. The Rotator R3000 and the Spinner S3000 nozzles atomized water into droplets that ranged from 0.4 mm to 6.0 mm and 0.4 mm to 3.5 mm in diameter, respectively. The difference in droplet size can be attributed to the difference in nozzle diameter and spray plate geometry. The Rotator R3000 has a 5.56 mm nozzle diameter while the Spinner S3000 has a 3.55 mm nozzle diameter. Previous studies have found that the droplet sizes produced in sprinkler irrigation are directly proportional to the nozzle diameter of the sprinkler (Dadiao & Wallender, 1985; Solomon et al., 1985). Larger nozzle diameters produce larger droplets, while smaller nozzle diameters tend to break up water jets from sprinkler nozzles into finer droplets. With regard to spray plate geometry, both nozzles used a 8-channel spray plate; however, the spray plates differed in the shapes of the channels and the velocity of rotation of the spray plate. Generally, the spray plates in spinner nozzles rotate faster than in rotator nozzles. Consequently, spinner sprinklers generally tend to produce smaller water droplets than rotator sprinklers (DeBoer, 2002). As a result, the Spinner S3000 nozzle had a greater proportion of smaller droplets than Rotator R3000 nozzle. This suggests that, at a specified operating pressure and height, droplet size is a function of the sprinkler type.

It was also observed that larger droplets project the farthest distance, with the Spinner S3000 nozzle being incapable of throwing water past a 6 m radius from the sprinkler. As noted, the Rotator R3000 nozzle has a bigger nozzle diameter which makes it generate bigger water droplets, and those droplets are thus blown further distance due to their mass and velocity as they leave the nozzle when compared to the Spinner S3000 nozzle. The smaller water droplets from the Spinner S3000 nozzle do not have enough momentum to reach great distances from the sprinkler. From both tests, the standard deviation of droplet sizes at each point increased with the distance from the sprinkler nozzle. This suggests that the range of water droplet sizes furthest from the sprinkler is wider than those nearer the sprinkler. This could be due to the smaller droplets being drifted by wind to the further distance and also as a result of the larger

droplets being projected farther due to their mass and velocity (the principle of momentum) as they leave the nozzle. Since the two nozzle sizes were operated at same pressure level, no conclusion can be drawn with respect to any effects of operating pressure.

5.2.3. *Statistical spray evaporation prediction models*

Results from the multiple regression analysis enabled the selection of the simplest model that best estimated SEL for sprinkler nozzles. In developing the models, SEL was expressed in two forms: in the first, as a function of air temperature, wind velocity, solar radiation and relative humidity; and, in the second form, as function of wind velocity, vapour pressure deficit and solar radiation. The R^2 criterion was used to check the significance of inclusion or exclusion of each variable in the models. The R^2 in all models changed very little or was nearly the same as when all variables were included in the model analysis. This suggests that radiation has very little effect on SEL from irrigation sprays during sprinkler irrigation. The most likely reason for this is because radiation indirectly influences air temperature and relative humidity or heat exchange by radiation alone is so small, due to the short flight time, that it can be neglected (Hardy, 1947). Thus, it was found that SEL can accurately be determined using a model in two forms: with air temperature, wind velocity and relative humidity only or wind velocity and the vapour pressure deficit (VPD) as the only variables. The VPD can be calculated using different empirical expressions depending on the availability of data.

Statistical comparison using R^2, ME and RRMSE indices between the different forms of models for each experiment showed that the models using air temperature, relative humidity and wind velocity - i.e. Equations (4-5) and (4-6) - have slightly better prediction than models using VPD and wind velocity - Equations (4-11) and (4-12). This was expected because Equations (4-5) and (4-6) use directly observed data, while in Equations (4-11) and (4-12), the VPD term was computed using empirical equations. Empirical equations are only approximations of the actual value and are usually subject to errors (Allen et al., 2005). However, when different magnitudes of observed SEL from various tests in both experiments were compared with predictions from the different forms of models, the predictions were

found to be nearly the same, and no trend was observed for the differences in the predictions. Hence, there appears to be no preference of one form of the model over the other. Air temperature and relative humidity can be represented by VPD, which is calculated using various empirical equations (Allen et al., 2005) depending on data availability. Models which only use VPD and wind velocity are preferable because of the flexibility of obtaining VPD in regard to data availability. VPD is also a realistic way of representing the evaporative potential of air. As noted by Yazar (1980), relative humidity is not a direct measure of the evaporative potential of air. The factor driving the actual evaporation process is the VPD: combining it with wind velocity gives a simple, yet flexible model. Thus, the two models selected for this study express SEL as a function of VPD and wind velocity. These results are in agreement with Seginer et al. (1991) who reported that average SEL determination using a single-sprinkler pressure combination can be formulated as function of the vapour pressure deficit of the air, and wind velocity. Similar results were also reported by Bavi et al. (2009) and Yazar (1984). Throughout this thesis, all calculations of SEL are based on wind velocity and VPD as the climatic variable.

5.2.4. *The relationship between spray evaporation losses and climatic variables*

The response of SEL to an increase in climatic variables measured in the experiments was analysed. The results from the two experiments suggest that the relationship between SEL and wind velocity is exponential. These results are in agreement with the results of Bavi et al. (2009) and Yazar (1984). However, the results differ from those of Christiansen (1942), George (1957) and Kraus (1966) who found no clear relationship between evaporation loss and wind velocity, but they observed that high wind velocities had the effect of increasing spray losses. The results in this study also differ from those reported by Frost & Schwalen (1955), who observed an approximately linear relationship between SEL and wind velocity.

The relationship between VPD and SEL was found to be exponential, corresponding to the findings of Bavi et al. (2009) and Yazar (1984) who used similar approach to determine SEL. There is an indirect relationship between spray evaporation loss and relative humidity:

increases in relative humidity lead to decreases in SEL. These findings are similar to results reported by Christiansen (1942) and Frost & Schwalen (1955), which also show that an increase in air temperature leads to an increase in SEL. These results differ from those reported by Abo-Ghobar (1992), Hermsmier (1973) and Lorenzini (2002); in that, in this study, the relationship between SEL and air temperature was approximately exponential.

5.2.5. *Comparison of the Spinner S3000 and the Rotator R3000 models*

The Spinner S3000 model predicts higher evaporation losses than the Rotator R3000 model. One possible reason could be the droplet size distribution produced by each nozzle, which is influenced by the nozzle geometry with regard to nozzle diameter and spray plate shape, as described in Section 5.2.2. The Rotator R3000 nozzle produced larger droplets than Spinner S3000 nozzle. Larger droplets are more resistant to drift and present less surface area to volume ratio for evaporation to occur (Kohl et al., 1987). Smaller droplets are more sensitive high wind velocity, which increases the flight time and hence the more time available for evaporation to occur. Greater evaporation losses are also associated with smaller droplets because they present a large surface area to volume ratio for evaporation to take place (Kohl et al., 1987); temperature and humidity also have great influence on them (Molle et al., 2012).

A comparison of SEL estimated by Yazar's model (Yazar, 1984) and Bavi's model (Bavi et al., 2009), developed using a similar approach showed that SEL varied between models for the same climatic conditions. Models developed in this study predicted higher estimates of SEL than previous models. A possible reason for the difference is due to droplet size distribution, which is influenced by the types of sprinklers used. Both Yazar's and Bavi's models used single-nozzle impact sprinklers while rotating spray plate sprinkler nozzles were used in this study. Rotating spray plate sprinklers (RSPS), which include the Rotator R3000 and the Spinner S3000 used in this study, produce droplets of smaller diameters with higher proportions of very small drops than impact sprinklers (DeBoer, 2002). Smaller droplets are more sensitive to evaporation than larger diameter droplets because they present a larger surface area to volume ratio for evaporation to take place, hence there are greater evaporation

losses (Molle et al., 2012). In that case, slightly more evaporation could be taking place in using RSPS than in using the impact sprinklers.

Another reason for the variation could be the conditions for which each model was derived. The Canterbury region is often characterised by high wind speeds, with very high short gusts (Salinger, 1979). Such conditions during experiments could have led to high SEL. According to Ortíz et al. (2009), wind gusts in short periods of time can lead to evaporation and drift loss values which are not explained by the mean wind speed. Again, in the previous models, the estimation of SEL for the Canterbury conditions required significant extrapolation for the climatic conditions in the Canterbury region. Table 5-1 shows the temperature, wind speed and VPD ranges for the Winchmore 2010 climate data used in the study, as well as the climatic conditions under which the statistical models were determined. It can be seen that in the cases of both Yazar's and Bavi's model, calculating the evaporation losses required extrapolation for the climatic data used. Values obtained by predictions outside the range for which a model was developed are subject to a level of uncertainty.

Table 5-1. Air temperature, wind speed and vapour pressure ranges used to develop different models.

Location	Temperature range ($^\circ$C)	Wind velocity range (m/s)	Vapour pressure deficit (mbar)
Winchmore, Canterbury , NZ	1.3 - 29.4	1.9 - 10.5	0.2 - 24.7
Mead, NE (Yazar's model)	18.9 - 36.7	0.9 - 6.7	4.2 - 33.1
SE Khuzestan province, Iran (Bavi's model)	19.8 - 45.4	3.0 - 9.5	0.70 - 8.9
Canterbury, New Zealand (Spinner S3000 model)	13.5 - 28.1	0.2 - 7.8	4.8 - 28.3
Canterbury , New Zealand (Rotator R3000 model)	11.9 - 27.8	0.1 - 7.6	3.4 - 28.0

Both the Spinner S3000 and the Rotator R3000 models showed a higher standard deviation of predicted SEL than other models under Canterbury conditions. Similarly, the two models predicted a significantly higher maximum and average SEL than the other models. These maximum SEL correspond to the SEL predicted during northwest wind conditions. Therefore, it can be concluded that these two models are more susceptible to northwest wind conditions,

because of the smaller droplets produced from the irrigation sprays. The other possible reason for this difference is that, during these northwest wind conditions, the prediction of SEL is by extrapolation rather than by interpolation. As shown in Table 5-1, the calculation of SEL from both the Rotator R3000 and the Spinner S3000 for the period considered required extrapolation because of the limited data range that was used to develop the models. This is very significant with wind velocity, hence there can some level of uncertainty in the predicted SEL at higher wind speeds.

Comparison of the actual SEL for the climatic data in the period considered shows that evaporation rates varied between models; with the Spinner S3000 model showing more susceptibility to northwest wind conditions. It can also be seen that the maximum SEL is significantly higher for both the Spinner S3000 and the Rotator R3000 models than for the other models (Table 5-2). This maximum SEL corresponds to northwest wind conditions for which the model predictions were outside the range for which the models were developed.

Table 5-2. Summary of seasonal spray evaporation losses during July 1, 2010 to June 30, 2011 for Winchmore climate data.

Model	Spray evaporation loss (%)		
	Minimum	Average	Maximum
Spinner S3000	1.0	4.3	75
Rotator R3000	0.4	3.2	48
Yazar	0.1	1.5	15.2
Bavi	3.6	4.5	7.6

For the majority of the growing year, Bavi's model predicts fairly constant values of spray evaporation losses, with the highest evaporation losses observed during the Canterbury winter months. The reason for this is unclear; however, it suggests that SEL under this model are more dependent on wind speed, which is unaffected by solar radiation during winter. On the other hand, both models developed from this study and Yazar's model predict high evaporation losses during the summer months with peak SEL occurring during northwest storms when temperatures (over 30^0C) and wind speeds (over 10 m/s) are high. This suggests that these models are very sensitive to climatic data in different ways, as described in the next section.

5.2.6. Comparative analysis under different climatic variables

Wind velocity

Results from comparison of responses to wind velocity show that the Spinner S3000 model is more sensitive to wind velocity, followed by the Rotator R3000 model and then Yazar's model, with Bavi's model being less sensitive to wind speeds under the same climatic conditions. The difference is due to the differences in droplet size distribution from the sprinkler nozzles, which are dependent on the nozzle geometry. Larger nozzle diameters produce larger droplet diameters which are more resistant to drift, hence only a short time frame is available for evaporation to occur. Larger droplets also present less surface area per unit mass for evaporation to occur hence less evaporation occurs. On the other hand, smaller nozzle diameters tend to produce the finer droplets, which have a large surface per unit mass ratio hence leading to greater evaporation losses.

Vapour pressure deficit

Evaporation losses were found to increase exponentially with increase in vapour pressure deficit in three models: the Spinner S3000, the Rotator R3000 and Yazar's model. Evaporation losses from the Spinner S3000 model are higher because the sprinkler produces smaller droplets compared to those from either the Rotator R3000 or Yazar's model. Smaller droplets are the most sensitive to temperature and wind, and present a larger surface area per unit mass for evaporation to take place, hence greater evaporation losses occur (Molle et al., 2012). However, SEL under Bavi's model was found to decrease with an increase in vapour pressure deficit. The reason for this trend is unclear because it is normally expected that any increase in vapour pressure deficit should result in an increase in evaporation; however, it may suggest that losses under this model are only affected by wind speed.

5.2.7. Conclusions

In summary, the results from the spray evaporation tests have demonstrated that three major variables affect SEL from agricultural sprays: the vapour pressure deficit of air; wind

velocity; and droplet size distribution, which is a function of nozzle size. Two statistical models have been developed for each sprinkler nozzle considered, which can be used to predict spray evaporation losses under the Canterbury conditions. Among the two climatic variables, it is more practical to pay attention to wind velocity than to vapour pressure deficit if SEL is to be minimized in the case of water scarcity. This is because wind velocity in a farm can effectively be controlled by windbreaks. Droplet size distribution from irrigation sprays determines SEL. Droplet diameters produced by larger diameter nozzle are higher than those produced by smaller nozzle diameters. Thus, more SEL is expected in irrigation spray from smaller nozzle diameters than from larger nozzle diameter under the same climatic conditions. For this reason, it is reasonable to use nozzles with larger diameters because they produce larger droplets which present less surface area to volume ratio for evaporation to occur.

It has also been demonstrated it is difficult to get reliable results of SEL in Canterbury by using either Yazar's or Bavi's models because they were derived from conditions completely different to those found in the Canterbury region. Furthermore, both Yazar's and Bavi's models were developed using impact sprinklers, whose droplet sizes are larger than those from RSPS (i.e. the Spinner S3000 and the Rotator R3000). Impact sprinklers are currently not in use in the Canterbury region and therefore neither Yazar's nor Bavi's model can be applied to predict SEL from RSPS in the Canterbury situation. If both the Spinner S3000 and the Rotator R3000 models are correct, however, they can be used to estimate evaporation losses under Canterbury conditions.

5.3. Wind speed reduction through windbreaks

The wind speed reduction by the windbreaks in this study was similar to that reported in other studies in some aspects when a single windbreak was considered. On the windward side of the windbreaks, wind velocity reduced with a reducing distance to the windbreak from a distance of -5 h. The reduction of wind velocity as the wind approaches the windbreak is caused by air pressure on the ground building up on the windward side (the side toward the wind), and

135

larger quantities of air moving up and over the top of the windbreak. The air pressure increases as the wind approaches the windbreak and reaches a maximum at the windward edge (-5 h) of the barrier. After this point, pressure drops as the wind passes through the barrier. Then wind velocity starts decreasing as it passes through the windbreak.

In the lee of windbreaks, wind velocity reduced with an increasing distance from the windbreak, up to a certain distance: between 1h -3h and 0h – 1h for Site 1 and 2, respectively, which is the location of minimum velocity (or maximum velocity reduction). This is because, as the wind passes through the windbreak, air pressure continues to drop until it reaches a minimum value, where minimum wind velocity occurs. In this case, the wind that passes through the windbreak is filtered. The position of the minimum wind velocity at both sites is in agreement with those reported by other authors (Heisler & Dewalle, 1988; McNaughton, 1988; Vigiak et al., 2003). The difference in the specific location of minimum velocity between the two sites is due to differences in windbreak porosity. A low porosity windbreak (Site 2) will obstruct and deflect air flow, creating a small but very still sheltered zone close to the windbreak before turbulent wind eddies contact the ground. In contrast, a medium porosity windbreak (Site 1) will filter or diffuse the air flowing through it, creating a sheltered zone over a longer distance before turbulent flow contacts the ground.

After the point of minimum wind velocity, the wind velocity gradually increases up to a maximum value at a certain distance. At this point, the wind velocity still does not reach its original open air speed because it is affected by the subsequent windbreak at this point. However, the location of this maximum velocity is nearer to the windbreak in Site 1 than it is Site 2: wind velocity increases to a maximum at about 8h and 10h for sites 1 and 2, respectively. The difference in the location of the maximum wind velocity in the field between the windbreaks is due to the differences in porosity, height and spacing of the two windbreaks in each site. The windbreak porosity influences the rate of recovery of wind speed and hence the positions of maximum wind speed. For windbreaks spaced more closely (in Site 1 at 80 m), the wind velocity reaches a maximum earlier than in Site 2 where spacing between windbreaks is wider (at 120 m). Other factors that influence the recovery to maximum wind velocity are: the slope of the terrain, surface roughness, and the angle of incidence of the wind

(Cleugh, 1998; Kenney, 1987; McNaughton, 1988; Vigiak et al., 2003; Wang et al., 2001). These factors were not considered in the analysis and thus are not discussed further.

At the point of maximum wind velocity, the wind velocity does not recover to the open wind velocity, but starts to decrease as a result of the influence of the subsequent windbreak. Thus, in the entire field, wind velocity reduction is not only affected by a single windbreak but by subsequent windbreak as well. Observed wind reductions from both sites are in agreement with the simulated wind velocity reductions. Statistical comparison of the observed and simulated wind reductions is discussed in the next section.

5.4. Modelling the effects of windbreaks on irrigation

Previous sections have shown that wind speeds in a field can be significantly reduced by windbreaks. It has also been shown that, in the fields selected for this research, wind velocity reductions are influenced by the combined effect of having two windbreaks in the fields. In addition, a wind velocity reduction model for each site has been calibrated and validated. Since both ET and SEL are influenced by wind velocity, a change in wind velocity should lead to a corresponding change in both ET and SEL, and hence a change in irrigation water requirements. In this section, modelling results for simulations of the effects of windbreaks on wind velocity are discussed. The effects of wind speed changes are further discussed in terms of water resource use with regard to ET, SEL and irrigation requirement.

5.4.1.   Calibration and validation of windbreak models

In all cases both measured data and simulated data showed good agreement by visual inspection. Exceptions occurred with the measured data where there was a point of inflection, i.e. at minimum and maximum wind velocity. At these points, it was not possible to establish the exact value due to limited measured data. However, these points seemed to fall within the standard deviations of the measured values.

There was a very slight difference (less than 1%) between the means and the standard deviations of the simulated and observed relative wind speeds, which indicates a good agreement between observed and simulated values. The relative root mean squared error (RRMSE) was 13.6% and 15.2% in the NW - SE and SE - NW directions, respectively for Site 1; and 9.7% and 16.2% in the W - E and E - W directions respectively, for Site 2. The modelling efficiency (ME) at Site 1 was 0.82 and 0.75 for NW - SE and SE - NW, respectively; while the ME for Site 2 was 0.80 and 0.75 for W - E and E - W directions for Site 2, respectively. It can be seen that the ME and RRMSE for wind direction NW - SE (Site 1) and a wind direction of W - E (Site 2) are better than those of the SE - NW and E - W wind directions for the corresponding sites. This difference is because calibration parameters developed using the wind data for the NW - SE and W - E were used for calibration in the SE - NW and E - W directions for Sites 1 and 2, respectively. These statistical indices indicate a good agreement between observed and simulated relative wind speeds. In general, it is desirable to have values of ME close to 1 and RRMSE less than 10% (Loague & Green, 1991). The validation of the models is thus considered good based on the RRMSE (Jamieson et al., 1991); while the simulations from the models are considered satisfactorily based on ME. Legates & McCabe, (1999) showed that that a value of ME greater than 0.5 represents a satisfactory model performance. Therefore the statistical indices indicate that the models have good precision, and are thus thought to be acceptable for purposes of this research.

5.4.2. Effects of windbreaks on the length of the zone of protection

The horizontal length of the zone of protection was found to be dependent on the height of the windbreak for the both two sites. Comparison of the zone of protection afforded by windbreaks on the windward side showed that windbreaks at Site 2 gave more length of protection than the windbreaks at Site 1: i.e., 27.5 m and 40 m for Site 1 and Site 2, respectively under Scenario 1. This is due to the fact that the windbreak height at Site 2 (8 m) is higher than at Site 1 (5.5 m). Under Scenario 2, the zone of protection on the windward side of the northwest windbreak at Site 1 was reduced from 27.5 m to 10 m, which represents a

63.6% reduction in the zone of protection; in Site 2, the zone of protection on the windward side of the west windbreak reduced from 40 m to 12 m, which represents a 70% reduction in the zone of protection. Since the simulated zone of protection at both sites is nearly the same under Scenario 2, the main controlling factor is the wind break height. This is in agreement to Heisler & Dewalle (1988) and Vigiak et al. (2003) who reported that the distance sheltered by a windbreak is increased proportionately by increasing the windbreak height, while windbreak porosity only affects the maximum reduction.

On the leeward side of the windbreaks, the zone of protection covers the entire field between the windbreaks before the windbreaks are reduced to 2 m or completely removed. However, when the windbreaks are reduced to 2 m, there is a reduction in the length of the zone of protection at both sites. At Site 1, there is a section of unprotected zone of 22 m between windbreaks, which represents 27.5% of the total length of the field. At Site 2, the unprotected area is 56 m, midway between the two windbreaks, which represents 46% of the total length of the field. The difference between the lengths of the protected zones is due to the differences in windbreak height and the spacing between the two windbreaks. These results suggest that the length of the protected zone is dictated by windbreak height. With a close spacing (such as Site 1), the subsequent windbreak falls within the zone of protection of the upstream windbreak, suggesting that the zone of protection is influenced by the two windbreaks. Thus, a greater zone of protection is achieved when windbreaks are closely spaced.

5.4.3.   Effects of windbreaks on wind velocity

Minimum wind speed

The position of the minimum wind velocity (or maximum wind velocity reduction) is nearer the windbreak for a low porosity windbreak (Site 2) than for a medium porosity windbreak (Site 1) for the same windbreak height. When all windbreak heights were reduced to 2 m, the position of the minimum wind speed (maximum wind speed reduction) in the protected fields moved closer to the windbreaks for both sites. Minimum wind speed with 45% and 48%

porous windbreaks occurred at about 8 m (4 h); whereas, with 19% and 28% porous windbreaks, it occurred at about 5 m (2.5 h). This suggests that windbreak porosity is the factor which influences the position of the minimum wind velocity. Hence, the position of minimum wind velocity moves closer to the windbreak with decreasing porosity.

Windbreak tree species may also be the reason why the location of the minimum wind velocity is different for the two sites. According to Loeffler et al. (1992) windbreak tree species can influence minimum wind velocity reduction in that they affect the rigidity of different tree leaves for different wind speeds, and therefore the leaves open or move differently at given wind speeds. The degree of branch movement at high wind speeds also affects the drag force of the windbreak on the wind, and therefore impacts on the leeward shelter effects. Nevertheless, the effect of different windbreak species and different wind speeds is beyond the scope of this study.

Average wind velocity

Average wind velocity between the two sites under Scenario 1 was found to be significantly different ($p < 0.05$). This difference is attributed to windbreak height and porosity. The windbreaks at Site 1 have medium porosity while the windbreaks at Site 2 have low porosity. Higher porosity at Site 1 means that large openings (gaps) exist in the windbreak structure, which channels wind through the openings, increasing wind speed, as opposed to the low porosity windbreaks at Site 2 which are more efficient in reducing wind velocity. Higher windbreak height at Site 2 than at Site 1 means that a larger zone is protected at Site 2 than at Site 1. The combined effect of both the windbreaks at Site 2 is more effective than at Site 1 because they are taller and denser.

A reduction of windbreak height to 2 m caused the average wind velocity in both fields to increase significantly, irrespective of the windbreak porosity. The wind speed significantly increased from 0.63 m/s to 1.37 m/s and from 0.58 m/s to 1.47 m/s for Site 1 and Site 2, respectively. These wind speed increments represent 117.5% and 156.9% at Site 1 and Site 2, respectively. The increase in wind velocity at both sites is due to a reduction in the length of protection, as a result of a decrease in the windbreak height. Reduction in the length of the

zone of protection leads to larger zones of the fields being unprotected by any windbreaks (where wind speeds are equal to the open field wind velocity) than when they were under the initial conditions (Scenario 1). As a result, the average wind velocity across the whole field increases.

The rate of wind velocity recovery is faster in the near lee of the windbreak (between 0 h and 10 h), and slower afterwards for both Scenarios 1 and 2 at both sites. However, the rate of recovery to open wind velocity is faster in the lower porosity windbreaks (Site 2) than it is in the medium porosity windbreaks (Site 1) for the same windbreak height (at 2 m). At a 2 m windbreak height, the average wind velocity recovered to open wind speed at 28 h and 26 h at Site 1 and 2, respectively. Therefore, a larger section of unprotected field, exposed to open wind speed occurred at Site 2 than at Site 1 under Scenario 2, hence the reason for a higher average wind velocity at Site 2 than at Site 1 under Scenario 2. The other possible reason why Site 2 had a higher average wind velocity than Site 1 was due to a difference in windbreak spacing. The windbreaks are spaced more widely at Site 2 than at Site: 120 m for Site 1 and 80 m for Site 1. Therefore, at the same windbreak height, a larger section of the field at Site 2 is unprotected than at Site 1.

When the windbreaks are completely removed, the average wind speed in the fields is the open field wind speed. The average wind speed increases by 195.2% and 220.7% at Sites 1 and 2, respectively. This means that windbreaks significantly reduce wind speeds across a field, with taller windbreaks with low porosity affording the greatest protection. The effects of this increased wind speed as a result of windbreak removal or reduction is quantified next in terms of water use by crops.

5.4.4.   *Effects of windbreaks on evapotranspiration*

Evapotranspiration is a function of wind speed, and any change of weed speed is expected to result in a change in ET. The results of this study showed that when wind speeds increased as a result of windbreak reduction or removal, ET increased proportionately as well.

Comparison between the two sites of Scenario 1 and 2 shows that there is a significant difference between average seasonal ET between the sites. However, Scenario 3 indicates that the average seasonal ET is affected by wind speed. This difference in ET for different sites under different scenarios is attributed to the difference in wind speed when windbreaks were either completely removed or reduced to a 2 m height at both sites, ET increased proportionately to increase in wind speed. The increase in ET due to an increase in wind speed is because increasing wind speed lowers the aerodynamic resistance to the transfer of water vapour, and crops transpiration is increased (Nuberg, 1998). The process of evapotranspiration moves water vapour (humid air) from the ground and crop surfaces to an adjacent shallow layer that is only a few centimetres thick. When an increase in wind velocity removes this layer, replacing it with drier air, the crop will increase its rate of transpiration while evaporation from the ground increases. The increase in ET with an increase in wind speed, when windbreak height is reduced or when windbreaks are removed, suggests that crops grown in fields protected by windbreaks require less water due to a lower rate of ET when compared with crops grown in unprotected fields. The results also show that reducing windbreak height leads to an increase in ET, hence higher crop water use.

ET is a combination of soil evaporation and plant transpiration, which represent evaporative processes: the difference between the two rests in the path by which water moves from the soil to the atmosphere. Water lost by transpiration must enter the plant via the roots, and then pass to the foliage, from where it is vaporized and lost to the atmosphere through tiny pores in the leaves known as stomata. In contrast, water lost through soil evaporation passes directly from the soil to the atmosphere. In this research, the pasture grass crop was considered to fully cover the ground surface; hence, only contribution to ET was through transpiration of the grass. At the times of the various seasons when rainfall is inadequate to supply for ET, irrigation is necessary to supplement the deficit. Irrigation requirements for different scenarios will be discussed in the next section in order to understand the effect of windbreaks on irrigation requirements, given the climatic conditions in the Canterbury region.

5.4.5. *Effects of windbreaks on irrigation*

The ET calculated for different scenarios in the previous section provides average estimates of seasonal water use by crops and thus can assist in making all the important decisions about when to apply water and how much water to apply through irrigation. In the growing season considered here, natural rainfall was not adequate to cater for the crop's ET; hence irrigation was necessary to replenish soil moisture to meet the amount of ET that was consumed by plants during the growing season. Irrigation requirements will be discussed below with respect to net irrigation requirements and irrigation frequency.

a) Net irrigation requirements

The net irrigation requirements are a direct function of ET under the same rainfall conditions in all scenarios. For the same rainfall conditions, crops grown in sheltered fields require less net irrigation than crops grown in unsheltered fields. Reducing windbreak height reduces the protected zone and thereby increases wind velocity, which in turn increases ET. Higher ET means more water is needed by the crop and, in the absence of adequate rainfall, the deficit must be supplied through irrigation. As a result of increased ET, crops protected by short windbreaks require more irrigation water than crops protected by tall windbreaks.

Reducing windbreak height to 2 m increases the net irrigation water requirements by 10.2% and 13.0% for fields protected by medium porosity and low porosity windbreaks, respectively. Complete removal of windbreaks would require an extra 24.8% and 26.7% of the net irrigation water requirements for medium porosity and low porosity windbreaks, respectively. Therefore, removing windbreaks or reducing their height to 2 m in a farm leads to an increase in net irrigation required by crops.

b) Irrigation frequency

Simulation results for the number of irrigation events show that no irrigation is required from the start of the growing season (which is winter in the Canterbury region) until mid-October. This was expected, because both fields were assumed to be at field capacity at the start of the simulation and rainfall was enough to cater for ET. When the dry season in the Canterbury

143

region starts (around October), high temperature, low humidity, and high solar radiation increase ET, and the crops transpire more. As a result, soil water is depleted through increased ET and irrigation is necessary, due to inadequate rainfall to maintain soil water potential at a higher level so that the soil can supply water fast enough to meet the crops' demand without placing the plants under water stress.

The results from both sites further show that irrigation events are required to start earlier in a field without windbreaks than in a field protected by windbreaks. This is because crop ET in a field unprotected by windbreaks is high, which is a consequence of high evaporative demand, due to an increase in wind speed upon windbreak removal or reduction in height to 2 m. As a result, in fields with shorter windbreaks or without windbreaks, soil moisture is depleted faster due to increased transpiration because of increased wind speed.

It can also be seen that the number of irrigation events needed to meet net irrigation requirements increase when windbreaks are reduced in height or removed all together. The reason for the increase is because in fields unprotected by windbreaks, irrigation events need to start earlier because of increased ET due to higher wind speeds so as to cater for crops' water requirements. Increase in the frequency of irrigation events has an implication for labour costs associated with moving irrigators, in case of sprinkler irrigation, and pumping costs are higher due to the increased energy required to pump extra water from the source.

5.4.6. Spray evaporation losses

Spray evaporation losses are losses which need to be catered for while applying water to the crop and these losses affect sprinkler irrigation efficiency during water application. For this research, the net irrigation requirements were to be supplied by sprinkler irrigation using a sprinkler system fitted with either the Rotator R3000 or the Spinner S3000 nozzle. Spray evaporation losses from both nozzles increased significantly (at $p < 0.05$) when windbreak height were reduced to 2 m or completely removed. This increase was due to a corresponding increase in wind speed when windbreaks are reduced in height or completely removed. The difference in spray evaporation losses for both sites when windbreaks were reduced to 2 m

was very small (i.e. approximately 0.4%), suggesting that sprinkler irrigation systems could still be operated within windbreaks at a height of 2 m with minimal spray evaporation loss. However, when windbreaks were completely removed, the spray evaporation losses significantly ($p < 0.05$) increase by 8.1% and 21.8% when irrigating using the Rotator R3000 nozzle and the Spinner S3000 nozzle, respectively.

Results from both sites and all scenarios show that spray evaporation losses are higher when irrigating using the Spinner S3000 nozzle than when using the Rotator R3000 nozzle. The explanation for this difference is due to the droplet size of the irrigation sprays, which are a function of sprinkler nozzle geometry with regard to nozzle diameter. A larger nozzle diameter in the Rotator R3000 nozzle produces larger diameter droplets, while smaller nozzle diameter Spinner S3000 breaks irrigation sprays into finer droplets. The large droplets produced by a larger nozzle diameter are more resistant to drift and present less surface area per unit mass for evaporation to occur than smaller droplets (Kohl et al., 1987). This means that irrigation water can be saved if a proper choice of sprinkler nozzles is made with regard to the droplet size distributions produced by the sprinklers.

5.4.7. *Gross irrigation requirements*

ET is the principal factor in determining irrigation water requirements, but losses in storage, conveyance and applying water, and the need for soil leaching are additional factors (Jensen, 1981). The gross irrigation water requirements (GIR) are the depth of water needed to meet the water losses and crop ET in a field. For this research, losses are assumed to occur during water application (spray evaporation loss) only. Thus, the GIR calculated are a combination of spray evaporation losses and net irrigation water requirements, which represent the total quantity of water to be pumped from the source. In general, GIR increase significantly in direct proportion to the increase in spray evaporation losses and the net irrigation requirement, when wind velocity increases due to windbreak height reduction or complete removal. GIR are highest when windbreaks are completely removed and lowest when the fields are protected with windbreaks. High irrigation requirements in areas not protected by windbreaks are attributed to high wind speeds, which increase the total irrigation requirements due to

145

spray evaporation loss. For the size of the fields considered, which are 80 m by 80 m (Site 1) and 120 m by 120 m (Site 2), significant extra irrigation water of up to 14% is needed when windbreaks are reduced to 2 m. Further, if windbreaks are completely removed from the fields, extra irrigation water of up to 39% and 64% is needed when irrigating using the Rotator R3000 nozzle and the Spinner S3000 nozzle, respectively. Therefore, the removal of windbreaks in a field lead to significant increases in water resource use in irrigated agriculture.

5.4.8.   Conclusions

A wind speed reduction model was calibrated and validated, and then used for modelling the effects of windbreak heights on wind velocity. Changes in wind velocity were directly related to ET and irrigation requirements. The results showed that greater reduction in wind speed is achieved with low porosity windbreaks than medium porosity windbreaks. Crop ET is thus lower for fields protected by low porosity windbreaks than those protected by medium porosity windbreaks.

The results further showed that a reduction in windbreak height or complete removal of windbreaks results in an increase in wind velocity across a field, which in turn increases the crop ET. The increase in ET further leads to an increase in net irrigation requirements. In addition, SEL is also increased with an increase in wind velocity which further increases the gross irrigation requirements when windbreaks are reduced to a 2 m height or completely removed. Thus, more irrigation water is needed for crops that are not protected by windbreaks than those protected. It was also shown that unprotected fields require more irrigation events than protected fields. Increases in the frequency of irrigation lead to additional labour and pumping costs. Lastly, it was demonstrated that for the same fields, SEL are higher when irrigating with a Spinner R3000 nozzle than when using Rotator R3000 nozzle. Therefore, water can be saved if the proper choice of nozzle is made.

CHAPTER 6: SUMMARY, CONCLUSIONS AND RECOMMENDATIONS

6.1. Summary

In the recent and on-going expansion of irrigation systems in the Canterbury region, modern sprinkler irrigation methods, namely centre pivot and lateral spray irrigation technology, have replaced the old border-dyke systems. This has been due to the need to increase irrigation flexibility and efficiency to guarantee pasture growth for dairy production in dry periods. This conversion has required windbreaks to be reduced to a 2 m height or sometimes to be removed completely so as to accommodate centre pivots or linear move irrigation systems. However, the removal of windbreaks can potentially increase ET and SEL on the irrigated farms. Hence, this research study was done to quantify the effects of windbreak removal on water resource use in the Canterbury region.

Field experimental work was conducted to quantify the effects of windbreaks on reduction in wind speeds. A windbreak model to estimate wind speed reduction was developed and validated to quantify the effects of windbreaks on ET, irrigation requirements and spray evaporation losses. Spray evaporation loss during irrigation was determined for two sprinkler nozzles under different climatic conditions. The data obtained from the experiments were used to develop regression models for the two nozzles to predict SEL that may occur in the Canterbury region. The reduction of wind speed by different windbreak characteristics was then modelled with respect to evapotranspiration, spray evaporation loss, and irrigation requirements.

6.2. Conclusions

The following conclusions can be drawn from the spray evaporation loss studies:
- For sprinkler nozzles operating at a fixed height and at a given pressure, the main factors that affect SEL are wind velocity, air temperature, relative humidity, and droplet size. Solar radiation was found to have little or no effect on SEL for the ranges

of climate data measured. As a result, SEL can be determined from both wind velocity and vapour pressure deficit since air temperature and relative humidity can be represented by the former.

- Reduction in water resource use can be achieved in sprinkler irrigation by proper selection of irrigation nozzles because SEL is dependent on droplet size which in turn is influenced by nozzle geometry with regard to nozzle diameter and spray plate configuration. Results from this study have shown that significant reduction in water resource, as high as 11%, can be achieved in one year growing season by changing sprinkler irrigation nozzles from the Spinner S3000 to the Rotator R3000. Therefore, in addition to selecting sprinkler nozzles based on agronomic needs, it is important to take into account the expected SEL associated with the nozzle type.

Results from the windbreak studies showed that wind speed reduction is affected by both the height and porosity of windbreaks. By simulating the effects of windbreak characteristics on wind velocity, the following conclusions were reached:

- The porosity of windbreaks was found to determine the rate of wind velocity recovery, and the position of minimum wind speed. At the same windbreak height, wind velocity recovery was found to be faster for a low porosity windbreak than for a medium porosity windbreak.
- For the two windbreaks studied, the location of minimum wind speed was found to occur nearer the lee of a low porosity windbreak than a medium porosity windbreak. At the same windbreak height, wind velocity recovery was found to be faster for a low porosity windbreak than for a medium porosity windbreak.
- The degree of wind speed reduction was found to depend on windbreak porosity; with maximum wind speed reduction reported for low porosity windbreak (at 88%), while medium porosity windbreaks gave a maximum wind speed reduction of 70%.
- The length of the zone of protection was found to be dependent on the windbreak height, with taller windbreak trees protecting a greater zone. Thus, taller windbreaks are more efficient in protecting agricultural fields. In order to improve the efficiency of windbreaks, windbreak height should not be reduced.

The benefits of windbreaks in reducing wind speed were related to ET and SEL. By simulating the effects of windbreaks on water resource use in irrigated fields in Canterbury, the following conclusions were reached:

- Windbreaks can significantly reduce ET of crops in windbreak protected fields. Hence, crops protected by windbreaks require less water for growth than crops growing in unprotected zones. The degree to which ET is reduced by windbreaks is dependent on windbreak height and porosity. Results from this study have shown that for a field of 120 m by 120 m protected by 8 m high low porosity windbreaks, reduction in windbreak height from 8 m to 2 m can lead to an 12% increase in ET in one year's growing season. The increase in ET can reach 16% in one year's growing season if the same windbreaks are completely removed. Thus, in order to reduce crop water use, windbreaks must be maintained.

- The net irrigation requirements (NIR) in a field protected by windbreaks are also reduced under irrigated systems as a function of ET being reduced by windbreaks. Less irrigation water is required for crops grown in a field protected by windbreaks. The modelling results of this study have shown that NIR can increase by 13% when low porosity windbreaks are reduced in height from 8 m to 2 m, and by 27% when the same windbreaks are completely removed.

- Windbreaks can reduce the frequency of irrigation events, because less irrigation water is required for a field protected by windbreaks than for a field not protected by windbreaks. In order to reduce the frequency of irrigation and associated labour and pumping costs, windbreaks must be maintained within the existing irrigated system. The results of this study have shown that both reduction of windbreak height and complete removal of windbreaks lead to an increase in irrigation events in one growing season.

- Windbreaks significantly reduce SEL, and therefore irrigation water is saved, which in turn increases irrigation efficiency. Modelling results showed that SEL increase with reduction of windbreak height or when windbreaks are completely removed.

- Reduction in water resource use can be achieved in irrigated agriculture if sprinkler irrigation systems can be designed to operate under existing windbreaks. The potential reduction in the amount of irrigation water required is significant and can be as high as 39% in one year's growing season for a field of 120 by 120 m which is protected by low porosity windbreaks when considering savings in water losses related to combined ET and SEL.

- With climate projections showing that the Canterbury region will become hotter, windier and drier, the losses associated with sprinkler irrigation may increase. Therefore, windbreaks can be used to help to mitigate water losses expected under the future climatic conditions of higher wind speeds, higher temperatures and lower relative humidity. In turn, this can lower the projected water demand.

- The benefits of windbreaks quantified in this study can be used to convince farmers to conserve already established windbreaks and instead adapt irrigation systems to operate under existing windbreaks. Also, the reported results can inform designers of irrigation systems to improve centre pivot irrigation technology.

- The SEL prediction models developed in this study on basis of experimental data, can be used to aid irrigators to predict SEL which may occur in other locations, not solely the Canterbury region but also in the rest of New Zealand using local climate data, provided irrigation is carried out using nozzles similar to those discussed in this research. Such results can provide important information to farmers regarding the additional amount of water required to meet the evaporation losses.

- The results from this study can also be applied to other areas of the world with similar climatic conditions (i.e. with high temperatures, high wind velocity and low relative humidity), where water is scarce. In applying these results to other areas, some variables must be taken into account: the type of sprinkler nozzles used for sprinkler irrigation, the type of windbreaks and the size of the fields, and wind speed reduction by windbreaks must be measured for the size of the field. Considering these variables, the effectiveness of windbreaks can be estimated in the same manner, using local meteorological data, of the total amount of water required from the source.

6.3. Recommendations for future research

This research work was conducted on a small scale, using a stationary irrigation experimental set up fitted with single sprinkler nozzle at a fixed height. It is hoped that this research can be continued.

- Further spray evaporation tests should be conducted for northwest wind conditions under high temperature (above 28°C), low relative humidity, and wind speeds above 8 m/s. The results could then be used to improve the already developed SEL predictive models so as to avoid the problems of extrapolation when predicting SEL under northwester conditions.

- An experimental set-up fitted with multiple sprinklers should be used to account for nozzle overlap, because the total number of operating sprinklers and their combination influence the rate of spray evaporation by reducing air evaporative demand.

- Research on spray evaporation losses for a wider range of sprinkler nozzles, with different diameters and spray plate configurations, is needed. The results from different tests using various nozzles can be combined and a single SEL model developed that accounts for nozzle diameter and spray plate configuration.

The results from experimental studies on windbreaks were obtained from fields which are smaller in size than typical fields under in which centre pivots operate. Furthermore, only fields affected by two windbreaks were considered. Due to time limitations, it was not possible to extend the research to other larger fields (e.g. 200, 300 and 600 m). It should be noted that specific results and conclusions could be expected to be impacted by the size of the field (windbreak spacing). However, it is hoped that this research can be continued in this field along the lines of the following recommendations:

- Experiments should be conducted to quantify the effects of multiple windbreaks on wind reduction. A GIS model should be developed that accounts for differences in wind direction and wind speed.

- The research can be extended to find the optimum windbreak characteristics, in terms of porosity and height, which can provide the best protection and hence minimize both SEL and ET.

- Research could also be extended to determine the best windbreak spacing, which can offer the best protection to fields from the effects of SEL and ET.

- Wind speed reduction should be quantified as affected by different windbreak tree species in the Canterbury region. The manner in which aerodynamic porosity changes with wind speed depends on tree species; for example, cedar leaves are less rigid than pine leaves, and therefore move differently at given wind speeds. Furthermore, the degree of tree branch movement at high wind speeds also affects leeward shelter.

- The literature also shows that windbreaks create shadow close to the barrier, which reduce radiation received by crops and thus can reduce ET. Hence, this research work could be extended to account for the reduction of ET and SEL due to shadow created by windbreaks, in addition to the reduction of wind velocity.

REFERENCES

Abo-Ghobar, H. M. (1992). Losses from low-pressure center-pivot irrigation systems in a desert climate as affected by nozzle height. *Agricultural Water Management, 21*(1), 23-32. doi: 10.1016/0378-3774(92)90079-C

Allen, R. G., Walter, I. A., Elliot, R. L., Howell, T. A., Itenfisu, D., & Jensen, M. E. (2005). *The ASCE standardized reference evapotranspiration equation.* . Prepared by the Task Committee on Standardization of Reference Evapotranspiration of the Environmental and Water Resources Institute of the American Society of Civil Engineers. Reston, VA: American Society of Civil Engineers/ The Irrigation Association.

Bavi, A., Kashkuli, H. A., Boroomand, S., Naseri, A., & Albaji, M. (2009). Evaporation losses from sprinkler irrigation systems under various operating conditions. *Journal of Applied Sciences, 9*(3), 597-600. doi: 10.3923/jas.2009.597.600

Bird, P. R. (1998). Tree windbreaks and shelter benefits to pasture in temperate grazing systems. *Agroforestry Systems, 41*(1), 35-54. doi: 10.1023/A:1006092104201

Blaney, H. F., & Criddle. (1952). Determining water requirements in irrigated areas from climatological and irrigation data. *In: Technical paper 96. USDA Soil of Conservation service*.

Brandle, J. R., Hodges, L., & Zhou, X. H. (2004). Windbreaks in North American agricultural systems. *Agroforestry Systems, 61*(1), 65-78. doi: 10.1023/B:AGFO.0000028990.31801.62

Brown, K. W. (1974). Calculations of evapotranspiration from crop surface temperature. *Agricultural Meteorology, 14*(1), 199-209. doi: 10.1016/0002-1571(74)90019-3

Caborn, J. M. (1957). Shelterbelts and microclimate *Forestry Commission Bulletin No 29*. Edinburgh H.M. Stationery Office.

Caborn, J. M. (1965). *Shelterbelts and windbreaks*. London: Faber & Faber.

Chawla, J. K., & Singh, S. R. (1975). Sprinkler irrigation losses as affected by climatic and operating conditions. *Journal of Agricultural Engineering, India, 14*(n1), 20-27 (E).

Christiansen, J. E. (1942). Irrigation by sprinkling. *California Agricultural Experimental Station Bulletin 670*(Book, Whole).

Clark, R. N., & Finley, W. W. (1975). Sprinkler evaporation losses in the sourthen plains. *American Society of Agricultural Engineers, Paper No. 75-2573*.

Cleugh, H. A. (1998). Effects of windbreaks on airflow, microclimates and crop yields. *Agroforestry Systems, 41*(1), 55-84. doi: 10.1023/A:1006019805109

Crawley, M. J. (2013). *The R book*. Chicester, United Kingdom: John Wiley & Sons.

Dadiao, C., & Wallender, W. W. (1985). Droplet size distribution and water application with low-pressure sprinklers. *Transactions of the American Society of Agricultural & Biological Engineers 28*(2), 511 - 516.

de Vries, T. T., Cochrane, T. A., & Galtier, A. (2010). *Saving irrigation water by accounting for windbreaks.* Paper presented at the Sustainable Irrigation Conference, Bucharest, Romania.

De Wrachien, D., & Lorenzini, G. (2006). Modelling jet flow and losses in sprinkler irrigation: Overview and perspective of a new approach. *Biosystems Engineering, 94*(2), 297-309. doi: 10.1016/j.biosystemseng.2006.02.019

DeBoer, D. W. (2002). Drop and energy characteristics of a rotating spray-plate sprinkler. *Journal of Irrigation and Drainage Engineering 128*(3), 137-146. doi: 10.1061/(ASCE)0733-9437

Dickey, G. L. (1988). Crop water use and water conservation benefits from windbreaks. *Agriculture, Ecosystems and Environment, 22*(23), 381-392. doi: 10.1016/0167-8809(88)90033-3

Edling, R. J. (1985). Kinetic energy, evaporation and wind drift of droplets from low pressure irrigation nozzles. *Transactions of the American Society of Agricultural & Biological Engineers, 28*(5), 1543-1550.

Edmondson, L. (2012). Irrigation efficiency under under northwester storm conditions . Waterways Centre for Freshwater Management Report 2012-002. Christchurch: University of Canterbury & Lincoln University.

Estévez, J., Gavilán, P., & Berengena, J. (2009). Sensitivity analysis of a Penman-Monteith type equation to estimate reference evapotranspiration in southern Spain. *Hydrological Processes, 23*(23), 3342-3353. doi: 10.1002/hyp.7439

Fasinmirin, J., Olufayo, A., & Oguntunde, P. (2008). Calibration and validation of a soil water simulation model (WaSim) for field grown Amaranthus cruentus. *International Journal of Plant Production, 2*(3), 269-278.

Feng, G., & Sharratt, B. (2007). Validation of WEPS for soil and PM10 loss from agricultural fields within the Columbia Plateau of the United States. *Earth Surface Processes and Landforms, 32*(5), 743-753. doi: 10.1002/esp.1434

Frost, K. R., & Schwalen, H. C. (1955). Sprinkler evaporation losses. *Agricultural Engineering, 36*, 526 - 528.

George, T., J. (1957). *Evaporation from irrigation sprays as determined by an electrical conductivity method.* Unpublished M.S Thesis. University of California. Berkeley.

Goulter, C. (2010). Dairy shelter on Canterbury Plains *SFF Project L09/023 Report. Lincoln: AgResearch Ltd.*

Guan, D., Zhang, Y., & Zhu, T. (2003). A wind-tunnel study of windbreak drag. *Agricultural and Forest Meteorology, 118*(1), 75-84. doi: 10.1016/S0168-1923(03)00069-8

Hardy, J. K. (1947). Evaporation of drops of liquid *Aeronautical Research Council, Reports and Memoranda, No. 2805, March 1947*. London: H.M. Stationery Office.

Hargreaves, G. H., & Samani, Z. A. (1985). Reference crop evapotranspiration from ambient air temperature. *American Society of Agricultural Engineers (Microfiche collection)(USA). no. fiche no. 85-2517.*

Heisler, G. M., & Dewalle, D. R. (1988). Effects of windbreak structure on wind flow. *Agriculture, Ecosystems and Environment, 22*(23), 41-69. doi: 10.1016/0167-8809(88)90007-2

Hermsmier, L. F. (1973). Evaporation during sprinkler application in a desert climate. *Americal Society of Agricultural Engineers*, Paper No. 73-216.

Hess, T. M. (2010). Estimating green water footprints in a temperate environment. *Water, 2*(3), 351-362.

Hess, T. M., & Counsell, C. (2000). A water balance simulation model for teaching and learning-WaSim. *Paper presented at the ICID British Section Irrigation and drainage research day, 29 March 2000. http://dspace.lib.cranfield.ac.uk/handle/1826/2455*

Hirekhan, M., Gupta, S., & Mishra, K. (2007). Application of WaSiM to assess performance of a subsurface drainage system under semi-arid monsoon climate. *Agricultural water management, 88*(1-3), 224-234.

Holman, I., Tascone, D., & Hess, T. (2009). A comparison of stochastic and deterministic downscaling methods for modelling potential groundwater recharge under climate change in East Anglia, UK: Implications for groundwater resource management. *Hydrogeology Journal, 17*(7), 1629-1641.

Irmak, S., Payero, J. O., Martin, D. L., Irmak, A., & Howell, T. A. (2006). Sensitivity analyses and sensitivity coefficients of standardized daily ASCE-Penman-Monteith equation. *Journal of Irrigation and Drainage Engineering, 132*(6), 564-578. doi: 10.1061/(ASCE)0733-9437(2006)132:6(564)

Jamieson, P. D., Porter, J. R., & Wilson, D. R. (1991). A test of the computer simulation model arcwheat1 on wheat crops grown in New Zealand. *Field Crops Research, 27*(4), 337-350. doi: 10.1016/0378-4290(91)90040-3

Jensen, M. E., Burman, R. D., & Allen, R. G. E. (1990). *Evapotranspiration and irrigation water requirements: A manual (ASCE manuals and reports on engineering practice*

No. 70) (Vol. no. 70). New York, N.Y: American Society of Civil Engineers. Committee on Irrigation Water.

Kenney, W. A. (1987). A method for estimating windbreak porosity using digitized photographic silhouettes. *Agricultural and Forest Meteorology, 39*(2), 91-94. doi: 10.1016/0168-1923(87)90028-1

Kincaid, D. C., & Longley, T., S. (1989). A water droplet evaporation and temperature model. *Transactions of the American Society of Agricultural & Biological Engineers, 32*(2), 457- 463.

Kohl, K. D., Kohl, R. A., & DeBoer, D. W. (1987). Measurement of low pressure sprinkler evaporation loss. *Transactions of the American Society of Agricultural & Biological Engineers, 30*(4), 1071 - 1074.

Kraus, J. H. (1966). Application efficiency of sprinkler irrigation and its effects on microclimate. *Transactions of the American Society of Agricultural & Biological Engineers, 9*(5), 642 - 645.

Landcare Research. (2014). New Zealand Soils. Retrieved 15 October 2014, from https://soils.landcareresearch.co.nz/contents/index.aspx

Legates, D. R., & McCabe Jr, G. J. (1999). Evaluating the use of 'goodness-of-fit' measures in hydrologic and hydroclimatic model validation. *Water Resources Research, 35*(1), 233-241. doi: 10.1029/1998WR900018

Loague, K., & Green, R. E. (1991). Statistical and graphical methods for evaluating solute transport models: Overview and application. *Journal of contaminant hydrology, 7*(1), 51-73. doi: 10.1016/0169-7722(91)90038-3

Loeffler, A., Gordon, A., & Gillespie, T. (1992). Optical porosity and windspeed reduction by coniferous windbreaks in Southern Ontario. *Agroforestry Systems, 17*(2), 119-133.

Lorenzini, G. (2002). Air temperature effect on spray evaporation in sprinkler irrigation. *Irrigation and Drainage, 51*(4), 301-309. doi: 10.1002/ird.68

Lorenzini, G. (2004). Simplified modelling of sprinkler droplet dynamics. *Biosystems Engineering, 87*(1), 1-11. doi: 10.1016/j.biosystemseng.2003.08.015

McLean, R. K., Ranjan, R., & Klassen, G. (2000). Spray evaporation losses from sprinkler irrigation systems. *Canadian Agricultural Engineering 42*(1), 1-8.

McNaughton, K. G. (1988). Effects of windbreaks on turbulent transport and microclimate. *Agriculture, Ecosystems and Environment, 22*(C), 17-39. doi: 10.1016/0167-8809(88)90006-0

Molle, B., Tomas, S., Hendawi, M., & Granier, J. (2012). Evaporation and wind drift losses during sprinkler irrigation influenced by droplet size distribution. *Irrigation and Drainage, 61*(2), 240-250. doi: 10.1002/ird.648

Nash, J. E., & Sutcliffe, J. V. (1970). River flow forecasting through conceptual models Part I — a discussion of principles. *Journal of Hydrology, 10*(3), 282-290. doi: 10.1016/0022-1694(70)90255-6

NIWA. (2014). CliFlo (the National Climate Database). Retrieved 15 October 2014, from http://cliflo.niwa.co.nz/

Nuberg, I. K. (1998). Effect of shelter on temperate crops: A review to define research for Australian conditions. *Agroforestry Systems, 41*(1), 3-34. doi: 10.1023/A:1006071821948

O'Donnell, L. (2007). Climate change: An analysis of the policy considerations for climate change for the review of the canterbury regional policy statement. Christchurch, New Zealand: Environment Canterbury.

Ortíz, J. N., Tarjuelo, J. M., & de Juan, J. A. (2009). Characterisation of evaporation and drift losses with centre pivots. *Agricultural Water Management, 96*(11), 1541-1546. doi: 10.1016/j.agwat.2009.06.015

Penman, H. L. (1948). *Natural evaporation from open water, bare soil and grass.* Paper presented at the Proceedings of the Royal Society of London A: Mathematical, Physical and Engineering Sciences.

Playán, E., Salvador, R., Faci, J. M., Zapata, N., Martínez-Cob, A., & Sánchez, I. (2005). Day and night wind drift and evaporation losses in sprinkler solid-sets and moving laterals. *Agricultural Water Management, 76*(3), 139-159. doi: 10.1016/j.agwat.2005.01.015

Price, L. W. (1993). Hedges and shelterbelts on the canterbury plains, new zealand: Transformation of an antipodean landscape. *Annals of the Association of American Geographers, 83*(1), 119-140. doi: 10.1111/j.1467-8306.1993.tb01925.x

Ranz, W. E., & Marshall, W. R. (1952). Evaporation from drops: Part 1. *Chemical Engineering Progress, 48*(3), 141-146.

Salinger, M. J. (1979). New Zealand climate: The temperature record, historical data and some agricultural implications. *Climatic Change, 2*(2), 109-126. doi: 10.1007/BF00133218

Saxton, K., & Rawls, W. (2006). Soil water characteristic estimates by texture and organic matter for hydrologic solutions. *Soil Science Society of America Journal, 70*(5), 1569-1578.

Seginer, I., Kantz, D., & Nir, D. (1991). The distortion by wind of the distribution patterns of single sprinklers. *Agricultural Water Management, 19*(4), 341-359. doi: 10.1016/0378-3774(91)90026-F

Smajstrla, A. G., & Zazueta, F. S. (2003). Evaporation loss during sprinkler irrigation. In I. o. F. a. A. S. Agricultural and Biological Engineering Department, University of Florida, USA. (Ed.).

Solomon, K. H., Dennis, C. K., & James, C. B. (1985). Drop size distributions for irrigation spray nozzles. *Transactions of the American Society of Agricultural & Biological Engineers, 28*(6), 1966-1974. doi: 10.13031/2013.32550

Steiner, J. L., Kanemasu, E. T., & Clark, R. N. (1983). Spray losses and partitioning of water under a center pivot sprinkler system. *Transactions of the American Society of Agricultural Engineers, 26*(4), 1128-1134.

Sturrock, J. W. (1988). Shelter: Its management and promotion. *Agriculture, Ecosystems and Environment, 22*(C), 1-13. doi: 10.1016/0167-8809(88)90004-7

Tapper, N., & Sturman, A. (2006). *The weather and climate of Australia and New Zealand.* South Melbourne; Oxford: Oxford University Press.

Tarjuelo, J. M., Ortega, J. F., Montero, J., & de Juan, J. A. (2000). Modelling evaporation and drift losses in irrigation with medium size impact sprinklers under semi-arid conditions. *Agricultural Water Management, 43*(3), 263-284. doi: 10.1016/S0378-3774(99)00066-9

Thompson, A. L. (1986). *Sprinkler water droplet evaporation simulated above a plant canopy.* Doctoral Thesis, University of Nebraska, Lincoln.

Thorrold, B. S., Clark, D. A., Caradus, J. R., Monaghan, R. M., & Sharp, P. (2007). Issues and options for future dairy farming in New Zealand. *New Zealand Journal of Agricultural Research, 50*(2), 203-221. doi: 10.1080/00288230709510291

Ucar, T., & Hall, F. R. (2001). Windbreaks as a pesticide drift mitigation strategy: A review. *Pest Management Science, 57*(8), 663-675. doi: 10.1002/ps.341

Uddin, J., Smith, R., Nigel, H., & Foley, J. (2010). *Droplet evaporation losses during sprinkler irrigation: An overview.* Paper presented at the One Water Many Future, Australian Irrigation Conference and Exhibition,, Sydney, 8-10 June 2010.

Vigiak, O., Sterk, G., Warren, A., & Hagen, L. J. (2003). Spatial modeling of wind speed around windbreaks. *Catena, 52*(3–4), 273-288. doi: 10.1016/S0341-8162(03)00018-3

Wang, H., Takle, E. S., & Shen, J. (2001). Shelterbelts and windbreaks: Mathematical modeling and computer simulations of turbulent flows. *Annual Review of Fluid Mechanics, 33*(1), 549-586. doi: 10.1146/annurev.fluid.33.1.549

Wang, Q.-G., Kang, Y., Liu, H.-J., & Liu, S.-P. (2006). Method for measurement of canopy interception under sprinkler irrigation. *Journal of Irrigation and Drainage Engineering, 132*(2), 185-187. doi: 10.1061/(ASCE)0733-9437(2006)132:2(185)

Yazar, A. (1980). *Determination of evaporation and drift losses from sprinkler irrigation systems under various operating and climatic conditions*. University of Nebraska. Lincoln.

Yazar, A. (1984). Evaporation and drift losses from sprinkler irrigation systems under various operating conditions. *Agricultural Water Management, 8*(4), 439-449. doi: 10.1016/0378-3774(84)90070-2

Zazueta, F. S. (2011). Evaporation loss during sprinkler irrigation. *BUL290. Revised November 2011.* Gainsville, Florida: IFAS Extension, University of Florida. http://edis.ifas.ufl.edu/pdffiles/AE/AE04800.pdf.

Zhang, L., Zhang, X., Kang, S., & Liu, J. (2010). Spatial variation of climatology monthly crop reference evapotranspiration and sensitivity coefficients in Shiyang river basin of northwest China. *Agricultural Water Management, 97*(10), 1506-1516. doi: 10.1016/j.agwat.2010.05.004

APPENDIX A - R - CODE FOR PERFORMING MULTIPLE REGRESSION ANALYSIS USING R – STATISTICAL SOFTWARE

The multiple regression analysis of the evaporation loss data for each experiment was performed using R- statistical software by the following script. It should be noted that air temperature (T_a), vapour pressure deficit (e_s - e_a) in the R script are represented as temp and VPD respectively, while $\log_e(x)$ is represented by log (x) in line with R programming notation.

Defining terms: Temp = air temperature, RH = relative humidity, radiation = solar radiation

VPD = vapour pressure deficit, SEL = spray evaporation loss, S = spinner models,

R= rotator models, log= natural logarithm, log = natural logarithm/logarithm to base e

lm = linear model

```
#############################################################################
```

A.1. Script for the Spinner S3000 and Rotator R3000 data for model development using temperature, relative humidity, wind and solar radiation

```
data<-read.table(file.choose(),header=T)
attach(data)
names(data)

A1<-lm(log(SEL)~log(wind)+log(radiation)+log(Temp)+log(RH),data = data)
A2<-lm (log (SEL)~log(radiation)+log(Temp)+log(RH),data = .data)
A3<-lm (log (SEL) ~ log (wind) +log (Temp) +log (RH), data = data)
A4<-lm (log (SEL) ~log (wind) +log (radiation) +log (RH), data = data)
A5<-lm (log (SEL) ~log (wind) +log (radiation) +log (Temp), data = data)
A6<-lm (log (SEL) ~ (wind) +log (Temp) +log (RH), data = data)
A7<-lm (log (SEL) ~ (wind) + (Temp) +log (RH), data = data)
A8<-lm (log (SEL) ~ (wind) + (Temp) + (RH), data = data)

summary (A1)
par (mfrow=c(2,2))
plot (A1)
summary (A2)
par (mfrow=c(2,2))
plot (A2)
summary (A3)
par(mfrow=c(2,2))
plot (A3)
summary (A4)
par (mfrow=c(2,2))
plot (A4)
summary (A5)
par (mfrow=c(2,2))
```

```
plot (A5)

summary (A6)

par (mfrow=c(2,2))

plot (A6)

summary (A7)

par (mfrow=c(2,2))

plot (A7)

summary (A8)

par (mfrow=c(2,2))

plot (A8)
```

A.2. Script for the Spinner S3000 and RotatorR3000 for model development using vapour pressure, wind speed and solar radiation

```
data<-read.table(file.choose(),header=T)

attach(data)

names(data)


B1<-lm (log (SEL) ~log (wind) +log (radiation) +log (VPD), data =data)

B2<-lm (log (SEL) ~log (wind) +log (VPD), data=data)

B3<-lm (log (SEL) ~log (radiation) +log (VPD), data = data)

B4<-lm (log (SEL) ~log (wind) +log (radiation), data = data)

B5<-lm (log (SEL) ~ (wind) +log (VPD), data =data)

B6<-lm (log (SEL) ~ (wind) + (VPD), data = data)

B7<-lm (log (SEL) ~log (wind) + (VPD), data =data)

B8<-lm (log (SEL) ~ (wind) + (radiation) +log (VPD), data = data)


summary (B1)

par (mfrow=c(2,2))

plot (B1)

summary (B2)
```

```
par(mfrow=c(2,2))
plot(B2)
summary(B3)
par (mfrow=c(2,2))
plot (B3)
summary (B4)
par (mfrow=c(2,2))
plot (B4)
summary (B5)
par (mfrow=c(2,2))
plot (B5)
summary (B6)
par (mfrow=c(2,2))
plot (B6)
summary(B7)
par(mfrow=c(2,2))
plot(B7)
summary(B8)
par(mfrow=c(2,2))
plot(B8)
```

APPENDIX B - SUMMARY OF EQUATIONS

The development of spray evaporation models was presented in Section 4.2.4 (Chapter 4). This appendix provides a complete summary of models which were considered in the analysis in order to select the best fit model for each nozzle. Table B-1 gives a description of the variables and the their units as used in the analysis while Table B-2 provides the summary models when wind velocity, solar radiation, air temperature and relative humidity were considered as variables for both nozzles. The results for when wind velocity, vapour pressure deficit and solar radiation were considered are shown in Table B-3.

The results showed that elimination of solar radiation in the analysis caused little or no improvement in the model. Table B-2 and Table B-3 show that there was little effect on R^2 when the radiation variable was removed from the analysis. Equations (B-7), (B-8) and (B-24) for Rotator R3000 nozzle showed a slightly higher R^2 value when compared to the best fit models selected. Similarly, Equations (B-15), (B-16), (B-30) and (B-31) for Spinner S3000 nozzle also showed a higher R^2 value when compared to the best fit model selected. The reason for the rejection of these models was that the assessment of residues showed that the errors were not randomly distributed. Hence, the best SEL predictive equations are given by (B-6) and (B-14) for Rotator R3000 and spinner S3000 nozzle, respectively, when SEL is expressed as function of air temperature, relative humidity and wind speed. When SEL is expressed as function as vapour pressure deficit and wind velocity, the best fit models are given by Equations (B-21 and (B-29).

Table B-1: Description of variables

Variable number	Symbol	Description and Units
1	SEL	Spray evaporation loss (%)
2	u	Average wind velocity at 2 m (m/s)
3	T_a	Air temperature (^{0}C)
4	RH	Relative humidity (%)
5	$(e_s - e_a)$	Vapour pressure deficit (mbar)

Table B-2. The effect of removal of different variables on model accuracy considering solar radiation, air temperature, wind velocity and relative humidity

Sprinkler Nozzle	Model Equation	R^2	Equation No
Rotator R3000	$SEL = 0.701u^{0.418} I^{0.262} T_a^{0.976} RH^{-0.605}$	0.766	(B-1)
	$SEL = 0.149 I^{0.178} T_a^{2.013} RH^{-0.785}$	0.643	(B-2)
	$SEL = 47.917u^{0.520} I^{0.306} RH^{-1.030}$	0.743	(B-3)
	$SEL = 1.679 u^{0.386} T_a^{1.154} RH^{-0.584}$	0.741	(B-4)
	$SEL = 0.018u^{0.437} I^{0.256} T_a^{0.428}$	0.753	(B-5)
	$SEL = 1.027exp (0.253u) T_a^{0.825} RH^{-0.345}$	0.856	(B-6)
	$SEL = 4.368 exp (0.245u) exp(0.048 T_a) RH^{-0.328}$	0.8605	(B-7)
	$SEL = 1.821exp (0.248u) exp(0.046 T_a) exp(0.007RH)$	0.8605	(B-8)
Spinner R3000	$SEL = 0.526u^{0.578} I^{0.088} T_a^{1.30} RH^{-0.292}$	0.837	(B-9)
	$SEL = 0.106 I^{-0.021} T_a^{2.415} RH^{-0.726}$	0.564	(B-10)
	$SEL = 0.323u^{0.562} T_a^{1.291} RH^{-0.283}$	0.844	(B-11)
	$SEL = 23.03u^{0.680} I^{0.025} RH^{-0.448}$	0.775	(B-12)
	$SEL = 0.078u^{0.601} I^{-0.030} T_a^{1.448}$	0.832	(B-13)
	$SEL = 0.378 exp(0.286 u) T_a^{0.911} RH^{-0.149}$	0.860	(B-14)
	$SEL = 1.915 exp (0.278u) exp(0.052 T_a) RH^{-0.131}$	0.860	(B-15)
	$SEL = 1.252exp (0.282u) exp(0.052 T_a) exp(0.002RH)$	0.860	(B-16)

Table B-3. The effect of removal of different variables on model accuracy considering solar radiation, wind velocity and vapour pressure deficit.

Sprinkler Nozzle	Model Equation	R^2	Equation No
Rotator R3000	$SEL = 0.217u^{0.429} I^{0.273} (e_a - e_s)^{0.683}$	0.779	(B-17)
	$SEL = 0.889u^{0.404} (e_a - e_s)^{0.741}$	0.751	(B-18)
	$SEL = 0.135 I^{0.204} (e_a - e_s)^{1.204}$	0.639	(B-19)
	$SEL = 0.622u^{0.686} I^{0.345}$	0.667	(B-20)
	$SEL = 0.907\exp(0.256u) (e_a - e_s)^{0.508}$	0.863	(B-21)
	$SEL = 1.745\exp(0.249u) \exp[0.046(e_a - e_s)]$	0.863	(B-22)
	$SEL = 2.194u^{0.385}\exp[0.070(e_a - e_s)]$	0.773	(B-23)
	$SEL = 0.775\exp(0.251u) \exp(0.001I)(e_a - e_s)^{0.510}$	0.867	(B-24)
Spinner S3000	$SEL = 1.796u^{0.606} I^{-0.051} (e_a - e_s)^{0.542}$	0.835	(B-25)
	$SEL = 1.390u^{0.603} (e_a - e_s)^{0.530}$	0.832	(B-26)
	$SEL = 0.330 I^{-0.085} (e_a - e_s)^{0.1.117}$	0.516	(B-27)
	$SEL = 2.521u^{0.753} I^{0.102}$	0.753	(B-28)
	$SEL = 1.417\exp(0.299u) (e_a - e_s)^{0.327}$	0.854	(B-29)
	$SEL = 2.095\exp(0.280u) \exp[0.035(e_a - e_s)]$	0.869	(B-30)
	$SEL = 2.626u^{0.556}\exp[0.053(e_a - e_s)]$	0.861	(B-31)
	$SEL = 1.365\exp(0.298u) \exp(0.0004)(e_a - e_s)^{0.294}$	0.854	(B-32)

APPENDIX C - SOIL PHYSICAL PROPERTIES AND CROP PARAMETERS USED FOR MODELLING USING WaSim MODEL

For irrigation design and management, the water holding capacity of the soil, the effective crop rooting depth, and the maximum allowable depletion of the crop must be known. This appendix provides the representative values of soil physical properties including water holding capacity (Table C-1); and maximum effective rooting depths and management allowed depletion for selected fully-grown crops (Table C-2).

Table C-1. Representative physical properties of soils for selected textures.

Soil texture	Total pore space (% by vol)	Apparent specific gravity (A_s)	Field capacity FC_v (% by vol)	Permanent wilting point PWP_v (% by vol)	Available water AW (mm/m)
Sandy loam	(37 to 40) 39	(1.56 to 1.59) 1.58	(11 to 22) 16%	(3 to 12) 7%	(50 to 110) 80%
Sandy clay loam	(38 to 42) 41	(1.53 to 1.60) 1.57	(20 to 32) 26%	(13 to 19) 16%	(70 to 120) 100
Loam	(40 to 43) 42	(1.50 to 1.58) 1.55	(18 to 31) 25%	(7 to 16) 12%	(110 to 150) 130
Silt loam	(40 to 46) 43	(1.44 to 1.59) 1.52	(16 to 36) 29%	(3 to 16) 11%	(130 to 230) 180
Silt	(39 to 42) 40	1.55 to 1.61) 1.58	(25 to 32) 29%	(4 to 8) 6%	(210 to 250) 230
Silty clay loam	(45 to 50) 47	(1.33 to 1.47) 1.4	(34 to 40) 37%	(17 to 22) 20%	(160 to 200) 180
Clay loam	(42 to 47) 44	(1.41 to 1.53) 1.47	(30 to 37) 34%	(17 to 22) 20%	(130 to 160) 140
Clay	(44 to 56) 49	(1.19 to 1.44) 1.35	(36 to 47) 42%	(23 to 33) 28%	(130 to 150) 140

Note: Numbers are rounded; normal ranges are shown in parentheses.

(Saxton & Rawls, 2006)

Table C-2. General maximum effective rooting depths of fully-grown crops and management allowed depletion (MAD) levels for selected crops.

Crop	Rooting depth range (m)	MAD (%)
Alfalfa	1.0 - 2.0	55
Beans (Green)	0.5 - 0.7	45
Brocolli	0.6	40
Cotton	0.8 - 1.7	35
Grapes	1.0 - 2.0	35 - 45
Grass pasture	0.5 – 1.5	50
Potatoes	0.4 - 0.6	35
Peas	0.6 - 1.0	40
Pineapple	0.3 - 0.6	50
Tomatoes	0.4 – 0.8	40

The crop used for modelling in this study is pasture grass and the effective rooting depth and MAD used from Table C-2 is 0.70 m and 50%, respectively.